THE UNIVERSITY OF CHICAGO

FORELIMB SHAPE, DISPARITY, AND FUNCTIONAL MORPHOLOGY IN THE DEEP EVOLUTIONARY HISTORY OF SYNAPSIDA

A DISSERTATION SUBMITTED TO

THE FACULTY OF THE DIVISION OF THE BIOLOGICAL SCIENCES

AND THE PRITZKER SCHOOL OF MEDICINE

IN CANDIDACY FOR THE DEGREE OF

DOCTOR OF PHILOSOPHY

GRADUATE PROGRAM IN INTEGRATIVE BIOLOGY

BY

JACQUELINE K LUNGMUS

CHICAGO, ILLINOIS

DECEMBER 2020

To all the animals I've called family. You have never failed to fascinate me, inspire me, and love me. It has always been about you.

Max *(Canis l. familiaris)*
Shy *(Terrapene ornata)*
Speedy *(Terrapene ornata)*
Augie *(Canis l. familiaris)*
Sonic *(Atelerix albiventris)*
Dahli *(Equus f. caballus)*
Seymour *(Canis l. familiaris)*
Gunther *(Canis l. familaris)*
Juniper *(Canis l. familiaris)*

TABLE OF CONTENTS

LIST OF FIGURES

LIST OF TABLES

ACKNOWLEDGMENTS

Virtually no part of this dissertation would have been possible without the support and guidance of my two advisors, Dr. Zhe-Xi Luo and Dr. Kenneth Angielczyk. You have been so generous with your time and resources, and you make every project you collaborate on stronger and more interesting. Because of you I was able to see amazing fossils, learn cutting edge science, and travel all over the world. For this I cannot thank the both of you enough. I am also grateful to my committee members, who always made me feel like they were on my side. Dr. Mark Westneat and Dr. Michael Coates always knew the right question to ask, and responding to your comments throughout committee meetings has played a large role in advancing my ability to communicate my science strongly and succinctly, and undoubtedly prepared me for a long career of this. Dr. Graham Slater was a huge support through the whole process, but especially Chapter 4, which has proved to be one of my most challenging intellectual pursuits yet. He has also proven to be a good friend, always being kind to my dogs, and providing a wonderful daughter who is always ready to give Seymour the attention he truly deserves.

I would not be in science, or paleontology to begin with, without the unwavering support of mentors at my undergraduate institution. Dr. Christian Sidor (University of Washington) invited me into his lab space as a sophomore in college, let me stick around even when I was barely doing anything, and when the time came supported my application to the University of Chicago (his alma mater). In addition, Dr. Adam Huttenlocker (University of Southern California) truly gave me my start in paleontology. He has been one of my closest academic mentors since I met him almost a decade ago and is unquestionably the reason I have made my focus in Permian synapsids. I am so grateful you didn't get sick of me.

Before I fell in love with the fossils and the field work of paleontology, I fell in love with the scientific community. It is a small world, and there have been countless moments of support, kindness and friendship through the process. Much of this comes from my lab mates in the Luo-Angielczyk working group. Caroline Abbott, Isaac Maganelles, and Tristan Reineke – I'm sorry to be leaving so soon into your graduate careers, but I promise you're in the best hands. Post-doctoral researchers: Dr. Pia Viglietti, Dr. Stephanie Smith, Dr. Spencer Hellert (all currently at the Field Museum), you make up a powerhouse of women-in-science. Thank you for always having my back and doing the heavy lifting when I really needed it. Dr. Christian Kammerer, my honorary committee member, thank you for holding me to such a high standard and always being so kind. Previous teammates Dr. David Grossnickle and Dr. Julia Schultz, I miss you both and look back at brewery crawls and board games in lab as some of my happiest memories in graduate school. Dr. Brandon Peecook, it's been fun growing up with you.

I have great family and friends, both in academia and outside of it. My parents have never questioned my choice in career and have supported my endeavors practically in spite of it. Almost everything good about my personality comes from my brother and sister – they're funnier and better looking and kinder than me. My best friend Krista Giuntoli is the greatest thing that has ever happened to me and is my soul mate, in case she doesn't know it. My second mother Shannon Richie was always there when I needed to complain about everyone I just thanked, which was frankly a lot of times, so thank you for putting up with that.

There were several important funding sources, first the Women in Science Board at the Field Museum of Natural History, who funded a year of my graduate education. The work they do is phenomenal, and I am proud to get to be associated with them. Two National Science Foundation grants funded the rest of my time at the University of Chicago: (NSF DEB-

1754502)(NSF EAR-1714829). I also need to take the time to thank everyone who I worked alongside or got to hang out with at the Field Museum of Natural History. It's been a dream to work there. I am similarly thankful to the collections managers and teams from institutions all over the world who not only accommodated me, but also generally put up with me in my never end search for a larger sample size.

2020 has been, arguably, the strangest year of my life. Nothing looks the way I (or anyone else) expected. I wish I could hug each of you, especially everyone I've been in graduate school alongside the last six years (Katie, Ben, Natalia, Andrew, Tom, Tim, Mo, Kristina, and countless I'm forgetting), but we are currently resigned to small computer screens or waves from six-feet apart. I know that will eventually change though, so I can't wait to share beers and hugs on the conference circuit when things to back to normal.

ABSTRACT

Mammals and their closest fossil relatives use their shoulders and forelimbs for many functions, which is reflected by the great range of mammalian forelimb shapes. Little work has been done to quantify this diversity as it relates to deep mammalian evolutionary history. Using geometric morphometric techniques on the humerus and ulna, I sought to quantify morphometric disparity, functional diversity, and the phylogenetic influence of the two across the 300-million-year evolution of this clade. I found that forelimb shape diversity in the early mammalian lineage (Synapsida) began to increase about 270 million years ago, with the emergence of a group called Therapsida, and is accompanied by new forelimb functions. The functional diversification of therapsid forelimbs was curtailed by the Permo-Triassic mass extinction, but eventually continued as more mammal-like therapsids evolved new ecologies. The analyses presented in this dissertation characterize the deep time origin of a quintessential part of the mammalian body plan: evolutionarily labile forelimbs that can be deployed in a wide range of functional and ecological roles.

Continuing this research on the origins and diversification of synapsid forelimb structure, I undertook a critical assessment of the ecological comparability of mammals to their fossil forerunners. Three interrelated goals are addressed: (1) to estimate when in synapsid evolutionary history modern mammal morphologies become effective for predicting fossil ecologies; (2) to investigate examples of morphological convergence within our geometric morphometric framework; and (3) to compare the functional solutions of distinct synapsid radiations in light of their shared phylogenetic history. I found that mammal limb shapes are not analogous to fossil synapsids until very close to the origin of crown Mammalia. These results suggest that phylogenetic placement strongly influences how an organism can respond to

functional pressures, emphasizing that each synapsid radiation explored distinct areas of morphospace and arrived at functional solutions that reflected their separate ancestral morphologies.

Building upon this work, I quantified the influence of shared ancestry upon the macroevolution of synapsid forelimbs. Using a composite phylogenetic tree including 218 genera across 320 million years of synapsid evolution, I compared the phylogenetic signal and phenotypic rate change among forelimb metrics between phylogenetic groups and across anatomical forelimb elements. This work points to a critical but previously underappreciated feature of the synapsid forelimb: that individual forelimb elements are undergoing independent evolutionary pressures and responding to those pressures at different rates. The work presented here challenges the traditional narrative of synapsid forelimb evolution as clear progression towards increasingly mammalian morphologies, and instead reveals a broad diversification of forelimb shapes early in synapsid history. This mosaic evolution of the synapsid forelimb reveals the complexity of forelimb evolutionary history, highlights the importance of forelimb morphometry to functional interpretation, and presents an increasingly dynamic picture for the forelimb evolution of Mammalia's deepest fossil ancestors.

CHAPTER 1 INRODUCTION

Variation in morphology and function is a cornerstone of evolution by natural selection. Beyond the simple presence of variation, however, the patterns and degree of variation through space and time have macroevolutionary implications for the tempo and mode of clade evolution. The two metrics most often used to quantify these patterns are morphometric disparity and functional diversity. Morphometric disparity is defined as the variance among forms of anatomical elements within a group (Foote 1993) and critically, disparity has been shown to be vital for understanding the evolution of major clades (Figure 1.1). Through the quantification of morphology in combination with comprehensive analysis of phylogenetic organization through time, paleontological research has yielded insight into the evolutionary implications of these interrelated factors**.** Contextualizing morphological disparity in geological time and within specific clades can provide an effective tool for interpreting macroevolutionary processes acting through deep time (Foote 1997; Erwin 2007; Moyne and Neige 2007; Hughes, Gerber, and Wills 2013; Ruta, Angielczyk, et al. 2013; Knope et al. 2015; Jablonski 2017;).

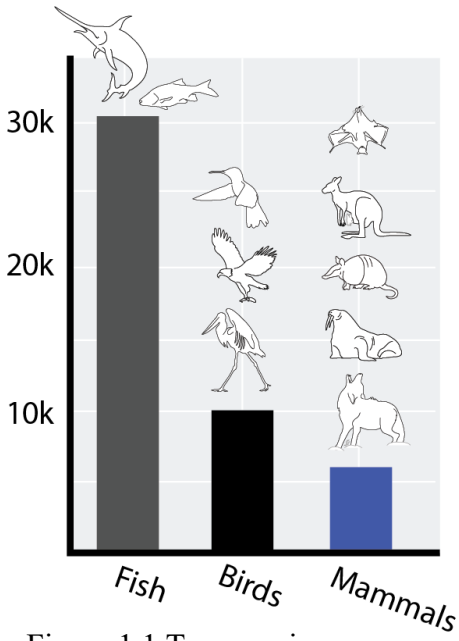

Figure 1.1 Taxonomic diversity of major vertebrate groups - Histogram showing species abundances (Y-axis) of three vertebrate groups, with examples of the diversity within each group. Note the form disparity of mammals despite their lesser taxonomic diversity.

The null hypothesis of morphological disparity through time is simply that it follows a Brownian motion pattern, increasing in proportion to species diversification and the amount

elapsed time. However, biological systems infrequently follow this strict pattern, effectively equivalent to genetic drift, and studying how the null model is broken can reveal important

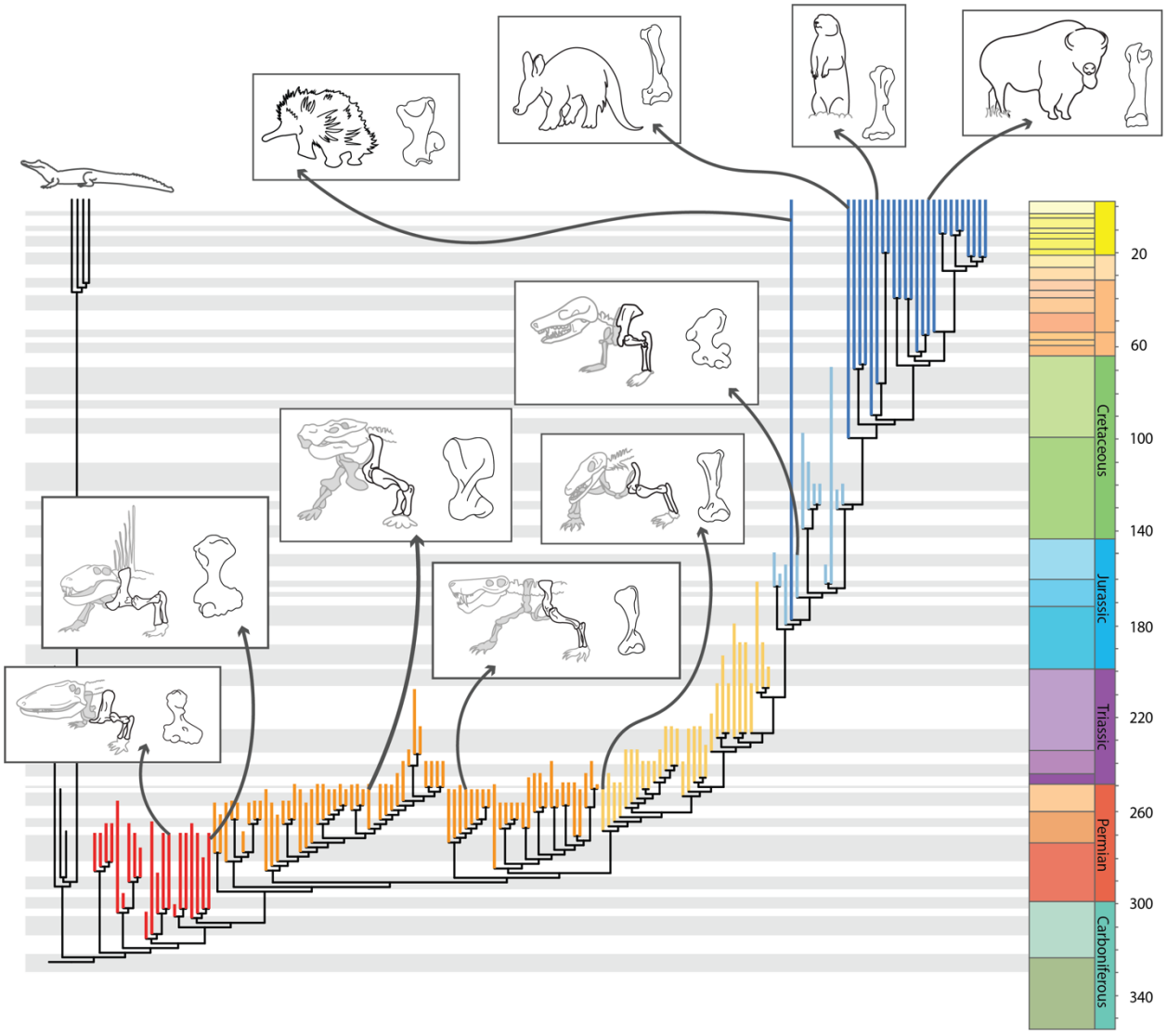

Figure 1.2 Cladogram and morphological examples of Synapsida – Composite phylogeny used in analyses throughout this dissertation, with examples of groups and associated humeral morphologies. Major grades are color-coded. Red: pelycosaur-grade synapsids; Orange: non-cynodontian therapsids; Yellow: pre-mammaliaform cynodonts; Light blue: non-Therian members of mammaliamorpha; Dark blue: Extant representatives of Mammalia. Specimen genus identifications going from the base of the tree crownward are as follows: *Ophiacodon, Dimetrodon, Aulacephalodon, Gorgonops, Procynosuchus, Fruitafossor, Tachyglossus* (Echidna), *Orycteropus* (Aardvark), *Geomys* (Pocket Gopher), *Bison* (Bison). Taxa defining beginnings and endings of defined groups can be viewed in Chapter 4.

insights. For example, when morphological disparity does not increase as phylogenetic diversity increases, it implies a constraint acting on the system preventing movement into new morphospace despite the general rise in taxa, which can then be further examined (Foote 2000; Erwin 2007). The interplay between skeletal morphology and ecology is termed an organism's ecomorphology (Barr 2018), and it is a lens for exploring functional diversity. The study of ecomorphology is important in understanding extinct species and ecosystems because it has predictive power. In organisms for which we have morphology but cannot directly observe ecology, as in fossil organisms, specific hypotheses can be tested by quantifying ecologically significant aspects of morphology in extant species for comparison.

An example of how the interaction of these factors can be illuminating can be illustrated using the clade Mammalia. The Mammalia are often noted for their expansive morphological disparity and functional diversity despite its lower species richness compared to other vertebrate groups, such as the actinopterygian fishes and birds (5,400 species of mammals versus ~30,000 species of actinopterygian fishes and just over 10,000 species of birds) (Wilson and Reeder 2005; Gill and Wright 2006) (Figure 1.1). However, mammals are the only extant representatives of the major amniote clade Synapsida, which has an evolutionary history and fossil record spanning over 300 million years. Additionally, fossil finds over the last two decades have shifted the scientific community's understanding of functional and ecology diversity through Synapsida's deep evolutionary history. This includes, for example, the discovery of swimming and gliding mammaliaforms in the Mesozoic (Ji et al. 2006; J. Meng et al. 2006), solidifying the presence of advanced ecological diversity outside of crown Mammalia. Less appreciated, however, is that researchers have long inferred the existence of distinct ecomorphologies as far back in synapsid evolution as the latest stages of the Paleozoic (Cox 1972; Kemp 1982; Fröbisch

and Reisz 2009; Kemp 2009; Cluver 1978; Nasterlack, Canoville, and Chinsamy 2012), indicating that the roots of mammalian ecomorphological disparity can be traced back to at least the Permian. However, within the very earliest members of the synapsid clade, the Early Permian pelycosaur-grade synapsids (pelycosaurs), group-wide morphological disparity is apparently low. Despite being one of the first major amniote radiations to include terrestrial large-bodied forms and instances of terrestrial herbivory (Carroll 1988; Sues and Reisz 1998; Reisz 2006; Hotton, Olson, and Beerbower 1997) the morphology of pelycosaurs is often considered functionally primitive (Watson 1917; Romer 1922; Romer and Price 1940; Jenkins 1973; Kemp 1982). The ecomorphological expansion of major transitions in forelimb anatomy associated with locomotor systems of synapsids across the Permian has not been extensively quantified, and this leaves a significant gap in our understanding of the morphological history of Synapsida.

The pectoral girdle and forelimbs are especially well suited to answer this type of question (Figure 1.2). This functional system's critical importance to quadruped locomotion, the lack of functional morphometric research conducted specifically on early synapsid forelimbs, and the observation that pectoral girdle evolution may have been heavily constrained (Beck 2004), make it a powerful system through which to study the acquisition of morphological disparity and functional diversity within this large group of amniotes. Additionally, many extant ecomorphologies can be observed and thus quantified through pectoral girdles. Examples of this include burrowing and running, both of which result in specific and quantifiable morphological changes to the shoulders and upper limbs (Hildebrand 1985; Hildebrand et al. 1985; Vizcaíno and Milne 2002; Sansalone et al. 2019). Finally, although the Mammalia are noteworthy for their ecological diversity, forelimb skeletal elements are homologous across Synapsida, making comparison through time highly amenable.

The pelycosaurs, more correctly referred to as ‘pelycosaur-grade’ synapsids, retain a primitive forelimb organization that they inherited from their stem-amniote ancestors. The forelimb is rooted upon a massively built scapulocoracoid that includes a highly distinctive glenoid articulation for the forelimb Described as “screw-shaped”, it is hypothesized to have limited the range of locomotor capabilities of these earliest synapsids and necessitated a sprawling posture with lateral undulation during locomotion. The requirements of lateral undulation, combined with their overall bulky skeletons likely played in further role in constraining the ecological diversity of these animals, preventing the evolution of more derived ecologies such as fossoriality, cursoriality, or arboreality. This forelimb morphology is in stark contrast to that of extant therian mammals, which undergo a dramatic reduction in the number of bones that comprise the pectoral girdle and the overall connectivity of the system, transitioning from a girdle that relies on closely aligned skeletal connections to one in which the shoulder and forelimb are entirely suspended in a muscular-sling. Phylogenetically intermediate forms between pelycosaurs and mammals are well described, and document progression towards the

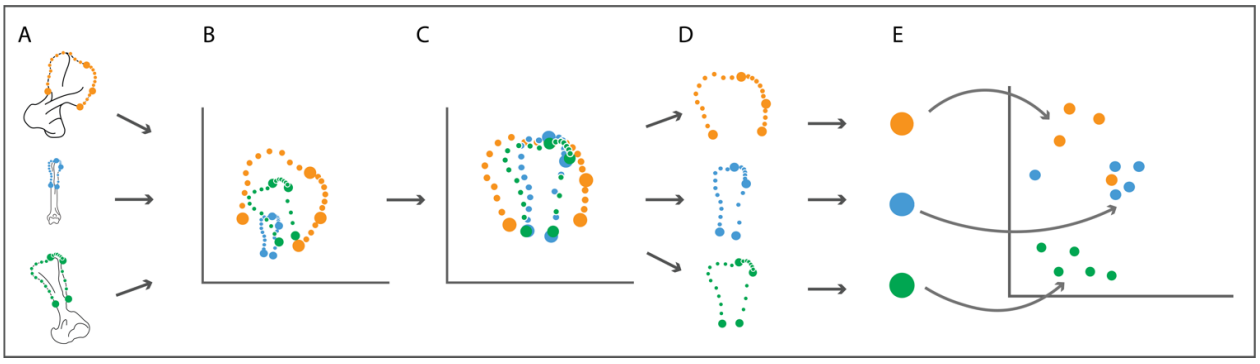

Figure 1.3 Geometric morphometric methodological pipeline – Example of geometric morphometric methodological pipeline. A) The shape of anatomically homologous elements are digitized through the placement of X-Y coordinate landmarks. B - C) Correction procedures scale and reorient coordinates, effectively leaving shape as the only variable. D) The spatial associations of the coordinates become individual data points that are subsequently, E) plotted in tangent space for comparison.

increasingly mobile and gracile mammalian form with its great diversity highly specialized locomotor ecologies.

Considering the scope of this transition, and its critical implications for mammalian evolution, deeper exploration of the acquisition of diverse ecologies in synapsid history is merited. Increased resolution, both phylogenetically and temporally, of the patterns of diversity in forelimb morphology and its association with ecological traits may elucidate moments of transition and innovation in the deep ancestors of mammals. This methodology has been used extensively in paleontological systems (M. Chen and Wilson 2015; Wilson 2013; Benevento, Benson, and Friedman 2019), including to confirm specific ecologies in Mesozoic mammaliaforms through direct comparison to mammalian ecomorphologies. However, these comparisons have only recently begun to be used in systems beyond the Mesozoic, deeper in synapsid evolutionary history. The noteworthy diversity of mammal ecologies and skeletal morphologies makes them tempting models for their fossil ancestors, yet the very depth of synapsid history makes particularly acute the question of whether crown-group mammals are instructive analogues for the earliest fossil synapsids (Jones et al. 2018; 2020; Lungmus and Angielczyk 2019).

To address these questions of early synapsid forelimb evolution and to make comparisons to extant mammalian forelimbs, I use the methodology of geometric morphometrics throughout this dissertation (Figure 1.3). At its most intuitive, geometric morphometrics is a way to statistically compare shapes, wherein shape is defined as "all the geometric information that remains once location, scale, and rotational effects are filtered out from the object" (Kendall 1977; Zelditch, Swiderski, and Sheets 2012). This approach allows for the variable of shape to be directly compared between specimens and across organisms that are otherwise vastly different.

Advances in this methodology over the last 30 years (Rohlf and Slice 1990; Rohlf 1999; Claude 2008; Zelditch, Swiderski, and Sheets 2012; Adams and Otárola-Castillo 2013) have dramatically increased the scale at which geometric morphometric comparison can be made and the overall applicability of this methodology. Combined with increases in computing and analytical power, geometric morphometrics is an effective method to address biological questions about anatomical morphology, and here I use it as the primary means of addressing macroevolutionary questions of synapsid history.

In this dissertation, I quantify the shape of the humerus and ulna across the deep evolutionary history of Synapsida to address three topics (Figure 1.2). First, I quantify the magnitude of morphological change across the two earliest radiations of Synapsida (pelycosaurs and Permian therapsids) and explore the timing of those changes in relation to ecological divergences. From there, I explore the use of modern mammals as ecological analogues for fossil synapsids in attempt to understand how accurately we can map changes in shape to explicit ecological developments. Lastly, using a large composite phylogeny covering all of the analyzed groups, I consider how changes in phenotype and phylogenetic signal relate to historically recognized macroevolutionary patterns in Synapsida. Specifically, I address how differences in the way synapsid morpho-functional changes are characterized can influence the broader understanding of forelimb evolution in these groups. In total, all three of the major research components of this dissertation found consistent patterns in the timing and character of morphological diversification, and perhaps most significantly, recovered robust evidence that different sections of the forelimb are evolving under separate and unique pressures. These findings support new interpretations of synapsid forelimb evolution as highly dynamic and

mosaic, instead of the historical perspective of synapsid forelimb evolution as a linear progression from ‘primitive’ forms towards increasingly ‘advanced’ and mammalian ones.

CHAPTER 2 ANTIQUITY OF FORELIMB ECOMORPHOLOGICAL DIVERSITY IN THE MAMMALIAN STEM LINEAGE (SYNAPSIDA)

Published as: Lungmus, Jacqueline K., and Kenneth D. Angielczyk. "Antiquity of forelimb ecomorphological diversity in the mammalian stem lineage (Synapsida)." *Proceedings of the National Academy of Sciences* 116, no. 14 (2019): 6903-6907.

2.1 ABSTRACT

Mammals and their closest fossil relatives are unique among tetrapods in expressing a high degree of pectoral girdle and forelimb functional diversity associated with fully pelagic, cursorial, subterranean, volant, and other lifestyles. However, the earliest members of the mammalian stem lineage, the "pelycosaur"-grade synapsids, present a far more limited range of morphologies and inferred functions. The more crownward nonmammaliaform therapsids display novel forelimb morphologies that have been linked to expanded functional diversity, suggesting that the roots of this quintessentially mammalian phenotype can be traced to the pelycosaur–therapsid transition in the Permian period. We quantified morphological disparity of the humerus in pelycosaur-grade synapsids and therapsids using geometric morphometrics. We found that disparity begins to increase concurrently with the emergence of Therapsida, and that it continues to rise until the Permo-Triassic mass extinction. Further, therapsid exploration of new regions of morphospace is correlated with the evolution of novel ecomorphologies, some of which are characterized by changes to overall limb morphology. This evolutionary pattern confirms that nonmammaliaform therapsid forelimbs underwent ecomorphological diversification throughout the Permian, with functional elaboration

initially being more strongly expressed in the proximal end of the humerus than the distal end. The role of the forelimbs in the functional diversification of therapsids foreshadows the deployment of forelimb morphofunctional diversity in the evolutionary radiation of mammals.

2.2 INTRODUCTION

Modern mammals have modified their shoulders and forelimbs for an unparalleled variety of functions. In contrast to the rest of Amniota, mammals have evolved highly distinctive forelimb shapes and functional specialization associated with burrowing, climbing, running, brachiating, flying, and swimming (Polly 2007; Luo 2015). An expansion in ecological diversity is well documented in the forelimbs of the fossil forerunners of mammals as far back as 164 Mya. This includes the discovery of swimming, gliding, and digging mammaliaforms in the Jurassic (Ji et al. 2006; J. Meng et al. 2006; Q.-J. Meng et al. 2017), demonstrating the presence of functionally derived ecological diversity outside of crown Mammalia. However, Synapsida, the clade that includes all living mammals and their fossil relatives, has a history extending back to over 315 Mya (Angielczyk and Kammerer 2018). Within the very earliest members of Synapsida, the Pennsylvanian and early Permian "pelycosaur"-grade synapsids (hereafter referred to as pelycosaurs), groupwide ecomorphological diversity across the pectoral girdle and forelimbs qualitatively appears to be very low. Despite comprising one of the first major amniote radiations (Carroll 1988), including the earliest large-bodied terrestrial forms (Kemp 2005), some of the first instances of tetrapod herbivory (Angielczyk and Kammerer 2018), and a substantial taxonomic diversity, the forelimb morphological disparity of pelycosaurs is surprisingly limited (Watson 1917; Romer 1922; Romer and Price 1940). Pelycosaurs are characterized by robust, widely sprawling (abducted) forelimbs, and all members of the grade possess a screw-shaped scapular glenoid and humeral head indicative of a highly restricted

range of motion (Romer 1922; Hopson 2015). This can be contrasted with the phenotype of the nonmammaliaform therapsids (here- after therapsids), the more crownward synapsids that replaced pelycosaurs as the dominant tetrapods in the middle Permian (approximately 275 Mya). Permian therapsids include more gracile large- and small-bodied predators (Sues 1986; Kemp 1978; Huttenlocker and Sidor 2016), highly specialized scratch-digging burrowers (Cluver 1978; Nasterlack, Canoville, and Chinsamy 2012; Kammerer, Bandyopadhyay, and Ray 2016), and arboreal herbivores (Fröbisch and Reisz 2009). Important shifts in therapsid limb morphology have been linked to inferred changes in locomotion, posture, and gait (Jenkins 1971a; 1973; Lai, Biewener, and Pierce 2018). Multiple hypotheses on the timing and staging of this morphological transition during the Permian period have been posited (Angielczyk and Kammerer 2018; Kemp 2006), but questions remain on the magnitude of morphological change and how that may relate to ecological and phylogenetic diversification patterns within Synapsida.

Considering the importance of forelimb disparity to the evolutionary radiation of Mammalia, the juxtaposition between the extant representatives of Synapsida (mammals) and the very earliest synapsids is striking. However, little work has been done to pinpoint the temporal and phylogenetic first appearance of increased forelimb disparity in a quantitative framework, or to explore this characteristic's role in synapsid macroevolution. Here, we quantified the morphological disparity of synapsid humeri in the two earliest evolutionary radiations of Synapsida, starting in the Pennsylvanian with pelycosaurs and continuing through the Permian and into the Triassic with therapsids. Be- cause pelycosaurs and therapsids are temporally successive major synapsid radiations, they are well suited for comparisons of ecomorphological disparity through time. Studies of other aspects of morphological disparity have been conducted on Permian synapsid groups (Ruta, Angielczyk, et al. 2013; Ruta, Botha-Brink, et al. 2013; Romano 2017), but little work has addressed the magnitude of morphological

changes between pelycosaurs and therapsids in the context of the important functional and ecological transitions observed across this interval. Our analyses characterize the origin of a canonical aspect of the derived synapsid bauplan: evolutionarily labile forelimbs that can be deployed in a wide range of functional and ecological roles.

2.3 METHODS

2.3.1 Taxonomic Sampling

Non-mammalian synapsids are the stem lineage of the mammalian crown-group. As such the two subgroups of synapsids examined in this study (pelycosaurs and therapsids) are paraphyletic assemblages. Pelycosaurs comprise the grade of synapsids on the stem of Therapsida. Therapsida is a monophyletic clade that includes stem-lineage non-mammalian therapsids and mammals. Our work focuses on the paraphyletic assemblage of nonmammaliaform therapsids from the Permian and Triassic periods, exclusive of mammals and their close relatives (mammaliaforms). We consider this approach justified because pelycosaurs and therapsids are two important, temporally-successive evolutionary radiations of synapsids. Our focus on pelycosaurs and therapsids is comparable to analyses of non-avian dinosaurs exclusive of birds. All specimens were categorized to the genus level. Pelycosaur and therapsid taxa were grouped for analysis using the current consensus view of pelycosaur and therapsid phylogeny. The distal humerus sample comprised 284 specimens representing every major clade from the temporal range of this study except Biarmosuchia. Mean shapes were calculated for 73 genera (18 pelycosaurs, 55 therapsids). The proximal humerus sample comprised 309 specimens, with the same taxonomic sampling as the distal end analysis. Mean proximal shapes were calculated for 73 genera (19 pelycosaurs, 54 therapsids). The total time range of

this study spanned from 305 Mya (Pennsylvanian) to 235 Mya (Middle Triassic), representing three separate geological periods and nearly all of pelycosaur and noncynodontian therapsid history (Angielczyk and Kammerer 2018; Ruta, Botha-Brink, et al. 2013; Z.-Q. Chen and Benton 2012). A full list of the sampled genera is provided in the Appendix II. The "pelycosaur" clade Eothyrididae is represented by one distal humerus referable to the *Baldwinonus trux (*MCZ1650). This single distal humerus contributes to the total disparity values and the within-group treatments for the times bins in which it is present (305 & 300 mya), but does not allow a separate treatment of eothyridid disparity. The distal end of a single specimen of *Ruthenosaurus russellorum* (MNHN.F.MCL-1) was digitized during data collection, but was not included in the final analyses because of the uncertainty surrounding its age (Reisz et al. 2011). However, the specimen is noteworthy in having an unusual distal humerus shape and would likely increase pelycosaur distal humerus disparity if it's time bin could be accurately assigned.

2.3.2 Temporal Sampling

Genus stratigraphic ranges were compiled from the Paleobiology Database (PBDB), and occurrences were binned as presence/absence data across 5-My time intervals. We conducted a generalized distancing analysis in R (Lloyd 2008) to check whether taxonomic sampling was correlated with measured trends in disparity and found no correlation between taxonomic sampling and disparity values across all of the analyzed time bins (Table 2.1). A detailed description of the sample, including specimen numbers and stratigraphic ranges, is presented in Appendix II and Appendix IV-VI.

Time range data for the specimens were designated at the species level for those specimens that had confident species identifications. Specimens that could only be identified at a higher taxonomic level were given bin placements for the entire time range of the most precise

identification possible (e.g., each time bin in which a genus occurs). Specimens that could not be identified to a genus were excluded from the analysis. The singular exception is a gorgonopsian humerus from a historic and well-studied forelimb (Cambridge University Museum of Zoology No. T.883). This specimen was given a stratigraphic bin assignment that represent the range of possible ages for Gorgonopsia. Bin placement is defined as a time range, with "presence" being designated if the taxon that the specimen represents was present at any point during the 5-million-year time span. Pelycosaurs and therapsids overlapped temporally during their evolutionary history, and that overlap occurs in two time bins in the analysis (270 and 265 Mya).

Table 2.1 Full Procrustes variance values for each time bin

Time Bin	Pelycosaur		Therapsid	
	Proximal	Distal	Proximal	Distal
305 mya	0.005113621	0.004017046		
300 mya	0.004070158	0.001291970		
295	0.004131235	0.001291970		
290	0.003902196	0.003456816		
285	0.004451662	0.004536993		
280	0.005199914	0.005631861		
275	0.006574254	0.005572765	0.004988890	
270	0.006300588	0.008591300	0.011434922	
265			0.009116469	0.005364114
260			0.013204671	0.007642401
255			0.01458609	0.008900727
252			0.010047123	0.009942058
245			0.013507737	0.010449260
240			0.01266810	0.008314050
235			0.009441241	0.005277366

2.3.3 Phylogenetic Signal

There is no comprehensive phylogeny of non-mammalian synapsids that includes all of the taxa examined in this analysis. To investigate possible phylogenetic effects on the disparity signal we built a composite phylogeny by hand using a variety of literature sources for relationships within and among subclades as follows: pelycosaurs: (Berman et al. 2014), (Brocklehurst 2015); relationships among major therapsid clades: (Sidor and Hopson 1998); Dinocephalia: (Rubidge and van den Heever1997); Anomodontia: (Kammerer and Angielczyk

2009); Therocephalia: (Huttenlocker and Smith 2017); Cynodontia:(Ruta, Botha-Brink, et al. 2013), (Van den Brandt and Abdala 2018), (Pavanatto et al. 2016). Stratigraphic ranges for the included taxa were collected from the PBDB, and a time tree was produced in R using the Claddis package (Lloyd 2015) using minimum branch length. We then conducted a multivariate phylogenetic least squares regression using mean genus shapes, treating centroid size as a covariate, and the time tree in Geomorph (Adams et al. 2016). Results showed no significant influence of phylogeny on mean shape (proximal Pagel's $\lambda = 0.3807071$, $p = 0.445$; distal Pagel's $\lambda = 0.2887207$, $p = 0.429$). Tree topology used for the analysis can be viewed in Figure 2.1 and Figure 2.2. A generalized distancing analysis was conducted to confirm that the disparity pattern was not being driven by a bias in the number of groups from bin to bin. Results using both Spearman's rho and Kendall's tau show that sample size is not correlated with the disparity (p values – distal = 0.8651, 0.9647; proximal = 0.1447, 0.1949).

Phylogenetic evidence implies a long therapsid ghost lineage that is not included in our analyses (Angielczyk and Kammerer 2018). The pelycosaur clade Sphenacodontidae is widely considered to be the sister group of Therapsida (Angielczyk and Kammerer 2018; Kemp 2012), and the Pennsylvanian first appearance of Sphenacodontidae implies that therapsids must have diverged by that time. However, there are no known Pennsylvanian therapsid fossils, and the only potential early Permian record of Therapsida is controversial and consists only of cranial material (Laurin and Reisz 1990; Liu, Rubidge, and Li 2009; 2010). This implies that therapsids could have had a long and undocumented period of time to accumulate the forelimb disparity the group displays when it first appears in our sample. However, the absence of Permo-Carboniferous therapsids does not allow us to determine whether therapsids initially were characterized by a pelycosaur-like low level of humeral disparity that gradually increased across

this time interval, or if disparity rapidly increased near their definitive first appearance in the fossil record in the middle Permian, or at a different time in their history (e.g., a rapid increase shortly after their divergence from sphenacodontids). Regardless of timing, the high disparity coincident with the emergence of Therapsida in our dataset is clearly related to critical differences in forelimb morphology and inferred function compared to pelycosaurs. As discussed, the appearance of novel morpho-functional types is a hallmark of therapsid evolution from the middle Permian onwards, and is observable across much of the therapsid body plan. Determining whether this property of therapsids is the result of changes in selection pressures, developmental mechanisms, other factors that occurred in the middle Permian, or is the culmination of evolutionary changes that had been accumulating "off-stage" since the Pennsylvanian, will require the discovery of Permo-Carboniferous therapsid fossils. Likewise, attempts to infer rates and models of evolution during the early history of therapsids using currently available fossils and phylogenetic data is suspect because the results would be unconstrained by fossil data for the therapsid lineage (see (Mitchell 2015) for a comparable example in birds)

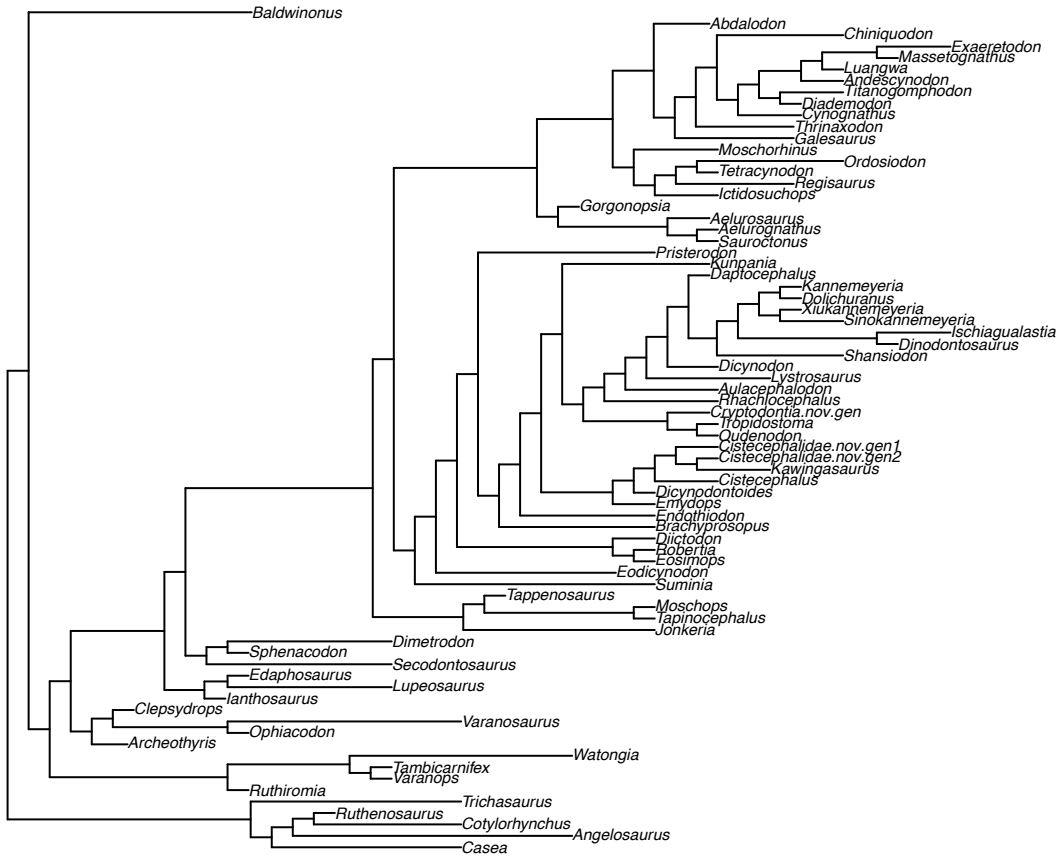

Figure 2.1 Phylogeny of proximal humeral sample - Phylogeny used to test for phylogenetic signal in proximal humeral morphology. Details of tree construction are in Appendix II.

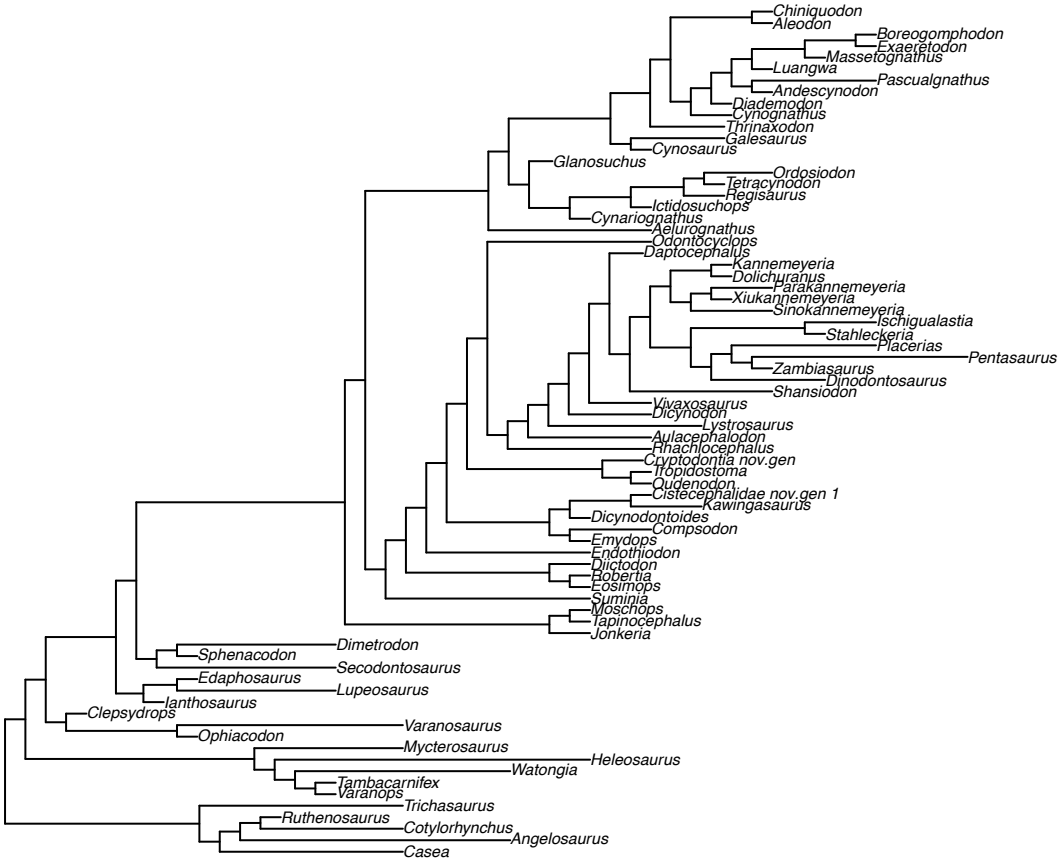

Figure 2.2 Phylogeny of distal humeral sample - Phylogeny used to test for phylogenetic signal in proximal humeral morphology. Details of tree construction are in Appendix II.

2.3.4 Geometric Morphometrics and Disparity Analysis

Shape outline data were acquired through 2D landmark-based geometric morphometrics, using photographs taken by the authors and a small number of high-quality illustrations from the published literature (Table 2.2). The geometric morphometric analysis of the humerus was split into distal and proximal end shapes. Because the proximal and distal ends of the humerus are offset in most pelycosaurs and many therapsids, and the degree of offset frequently is affected by taphonomic distortion, splitting the analysis into distal and proximal portions allows for the full 2D shape of both functional surfaces to be measured accurately. All analyses were conducted on

left humeri; in cases where the only available element was a right humerus, the element was mirrored across its proximal–distal axis for analysis.

The landmarks and semilandmarks were digitized and scale recorded using tpsDIG2ws (Rohlf 2010). Landmark and curve positions are shown in Figure 2.6B, and descriptions of landmark placements are presented in Table 2.3. The landmarks represent consistently recognizable extrema on the outlines of the humerus because there are no usable internal landmarks on either end of the humerus across this evolutionary interval. The proximal humerus was analyzed in posteroventral view, emphasizing the perspective that maximized the total width of the proximal end. This view permits the posterior side of the humeral head to be viewed, as well as the entire delto- pectoral crest in a way that captures the curvature of the deltopectoral crest along the long axis of the humerus. The distal humerus was analyzed in dorsal view, although all analyzed morphology is visible in either dorsal or ventral view.

Analyses were split between the two ends of the humerus because of the dramatic degree of long axis twisting in many pelycosaur and therapsid humeri. This twisting prevents a single two-dimensional view from capturing details of both articulation surfaces. Moreover, the degree of twisting is frequently affected by taphonomic deformation (i.e., it can be reduced or exaggerated depending on the direction in which a specimen experienced compression), potentially biasing three-dimensional data that could theoretically capture the entire humeral shape. The approach of splitting the humerus into two functional ends had the added benefit of maximizing sample size because it allowed the inclusion of humeri in which one end was intact but the other was damaged or missing. Finally, separate consideration of the shapes of the two sections of the humerus contributed to the unique finding that the proximal end of the humerus represents a disproportionate amount of therapsid humeral disparity.

A Procrustes ANOVA was used to assess the covariation between shape coordinates and

log centroid size, with residual randomization (summary and significance in Table 2.4). The results of the analysis revealed that size was a significant predictor of shape for both humeral ends. Because of this, the centroid size of each specimen (or genus in the case of mean shapes) was treated as a known covariate during the regression analysis. Data were visualized with a principal components analysis, and an expanded set of PC axes are presented in Figure 2.4 and 2.5, along with an associated scree plot of variance captured by each PC (Figure 2.6).

All disparity values reported and plotted in Figure 2.3 and Table 2.1 were measured as Procrustes variance directly upon the multivariate geometric morphometric data. Procrustes variance is the sum of the diagonal elements of the covariance matrix of a defined group, divided by the number of occurrences within that group (Adams et al. 2016; Rohlf 2010; Zelditch, Swiderski, and Sheets 2012). Research comparing the effects of sampling on various disparity metrics shows that variance-based metrics are relatively immune to biases caused by small sample size (Wills, Briggs, and Fortey 1994; Brusatte et al. 2012). Regardless, the total-group disparity values were additionally analyzed to understand the amount of error present in the results. The sample of genera present during each time bin were randomly resampled with replacement to the same sample size as the true dataset in that given time bin, this new simulated sample subsequently underwent a morphological disparity analysis in the 'R' Geomorph package. This random resampling and conducting of a new disparity analysis was conducted 1,000 times for each time bin, and the variation in those results were used to calculate the standard deviation of each time bin.

A phylogenetic least squared (PGLS) analysis was run to check for phylogenetic signal in the shape data, based on a composite phylogeny built off of published literature on sampled groups (). Pagel's lambda (λ) was calculated from the co- variance matrix produced by the PGLS. The results

were not significant (proximal: $\lambda = 0.1753$, $P = 0.6305$; distal: $\lambda = 0.1761$, $P = 0.5095$) (Table 2.4).

The Permo-Triassic mass extinction is hypothesized to have taken place 252.24 Mya (Burgess, Muirhead, and Bowring 2017). The Permo-Triassic Mass Extinction event is designated as a time bin at 252 Mya, and represents the fauna immediately post-extinction, capturing both survivors and new taxa in the immediate disaster fauna. Given the severity of the extinction event, the finding that distal humeral disparity does not decrease in this time interval is counterintuitive. Detailed analysis conducted upon the individual specimens present across the interval revealed that the clearing of morphospace resulting from the extinction occurred primarily in the intermediate areas of morphospace, whereas the survivors are derived groups that occupy the periphery of morphospace (such as Therocephalia). Combined with the overall decrease in sample size across the extinction, this results in the average distance from the total group mean increasing in the distal end of the humerus. Results show an expected effect of the mass extinction event for proximal humeral morphology, with decreases across the extinction interval. Following this, disparity values imply a diversification in limb disparity as both ends of the humerus increase beyond pre-extinction levels of morphological disparity (Figure 2.3).

Table 2.2 – Illustrations and associated publications used in Chapter 2 analyses

Citation	Specimen number	Specimen ID
(Reisz and Berman 1986)	KUVP 69035	*Ianthasaurus hardestii*
(Spindler, Scott, and Reisz 2015)	KUVP 133735	*Ianthodon schultzei*
(Botha-Brink and Modesto 2009)	SAM-PK-K8305	*Heleosaurus scholtzi*
(Reisz, Wilson, and Scott 1997)	OMNH 52368	*Mycterosaurus* sp.
(Berman et al. 2014)	MNG 10596	*Tambicarnifex unguifalcatus*
(Campione and Reisz 2010)	TMM 43628-1	*Varanops brevirostris*
(Reisz and Laurin 2004)	UCMP 143478	*Watongia meieri*
(Jenkins 1971a)	NMB C.2693	?*Cynognathus* sp.
(Jenkins 1971a)	SAM-PK-K1395	*Thrinaxodon liorhinus*
(Gregory and Broom 1926)	N/A	*Moschops* sp.
(Angielczyk and Rubidge 2013)	NHMUK 23345	*Eosimops newtoni*
(Cox 1972)	GPIT K55	*Kawingasaurus fossilis*
(King 1981)	SAM-PK-11885	*Robertia broomiana*
(Kemp 1982)	CMZ T883	Indet. Gorgonopsian
(Colbert and Broom 1948)	AMNH 2240	*Lycaenops ornatus*
(Fourie and Rubidge 2009)	SAM-PK-K7809	*Glanosuchus macrops*
(Fourie and Rubidge 2007)	BP/1/3973	*Regisaurus* sp
(Botha-Brink and Modesto 2011)	NMQR 3605	*Olivierosuchus parringtoni*

Table 2.3 Placement of landmarks on proximal and distal humerus

Humeral end	Landmark #	Placement
Proximal morphology	1	Proximal lateral end of diaphysis
	2	Medial edge of humeral head
	3	Ventral-most extent of deltopectoral rest
	4	Distal-most extent of deltopectoral crest
Distal morphology	1	Anterior distal end of diaphysis
	2	Middle of entepicondyle
	3	Anterior edge of ulnar condyle
	4	Posterior edge of ulnar condyle
	5	Distal edge of ectepicondyle
	6	Middle of ectepicondyle
	7	Proximal edge of ectepicondyle
	8	Posterior distal end of diaphysis

Table 2.4 Summary and Significance of Procrustes ANOVA

		Df	SS	F	Z	P value
Proximal	log(size)	1	0.13428	10.187	3.6551	0.009901
	Total	71	0.93588			
Distal	log(size)	1	0.03089	3.161	2.3782	0.0198
	Total	71	0.69376			

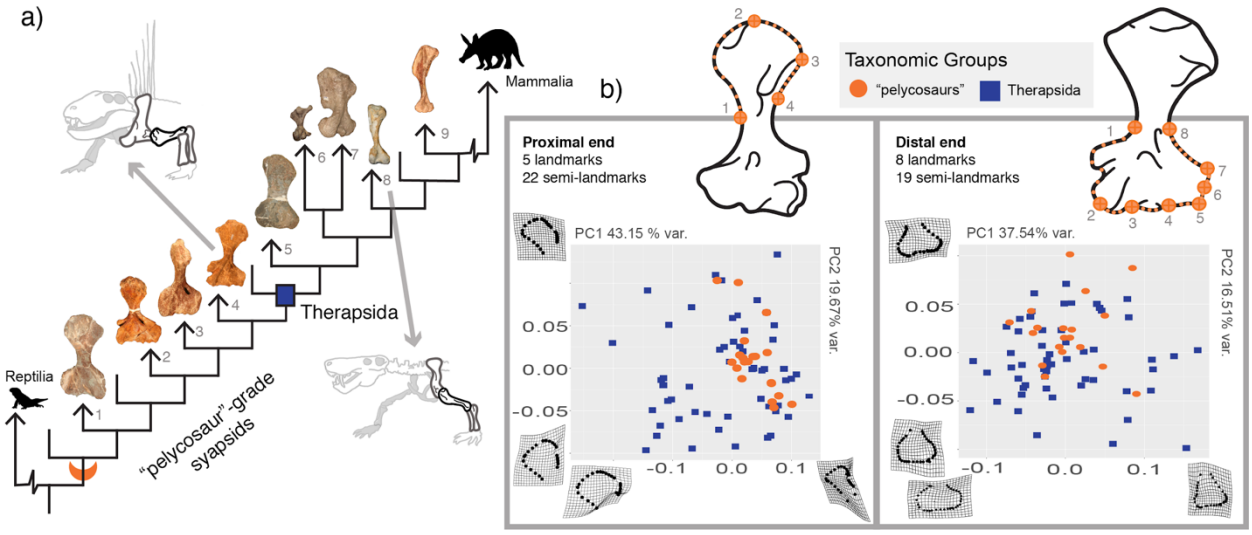

Figure 2.3 Contrasting forelimb disparity in the rise of Therapsida - Simplified cladogram of Synapsida showing humeral diversity and morphospace distribution of major studied clades. A) pelycosaurs (orange semi-circle) comprise the first major radiation following the split from Sauropsida. Sample humeri from four pelycosaur clades display morphological conservatism (1 –*Cotylorhynchus hancocki*, 2 –*Ophiacodon retroversus*, 3 –*Edaphosaurus sp*, 4 –*Dimetrodon limbatus*). Pelycosaurs were replaced by therapsids (blue square) in the middle Permian. Five sample humeri display the morphological disparity of therapsids. (5 –*Jonkeria sp*, 6 – *Cistecephalus microrhinus*, 7 –*Ischigualastia jenseni*, 8 – Gorgonopsia, 9 –*Massetognathus pascuali*). B) Principal component plots of the humeral datasets, with percent variance captured by each axis and warp grids displaying morphological change along these axes. Landmark and semi-landmark placement is shown to the right of the associated morphospaces.

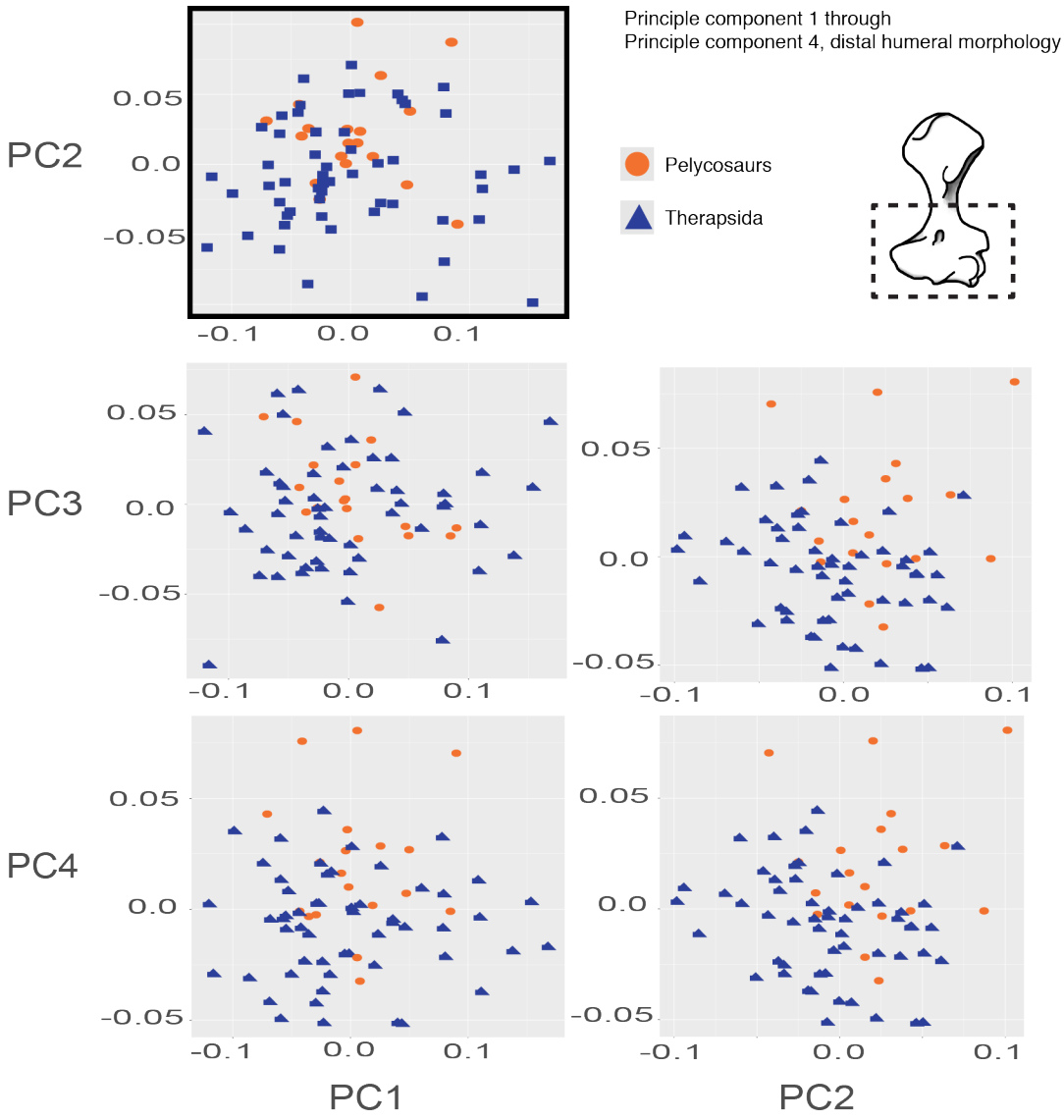

Figure 2.4 Distal end morphospaces of PC1 through PC4 - Colored by clade: orange circles are "pelycosaurs" and blue triangles are therapsids. Black box highlights the plot reported in the Figure 2.3.

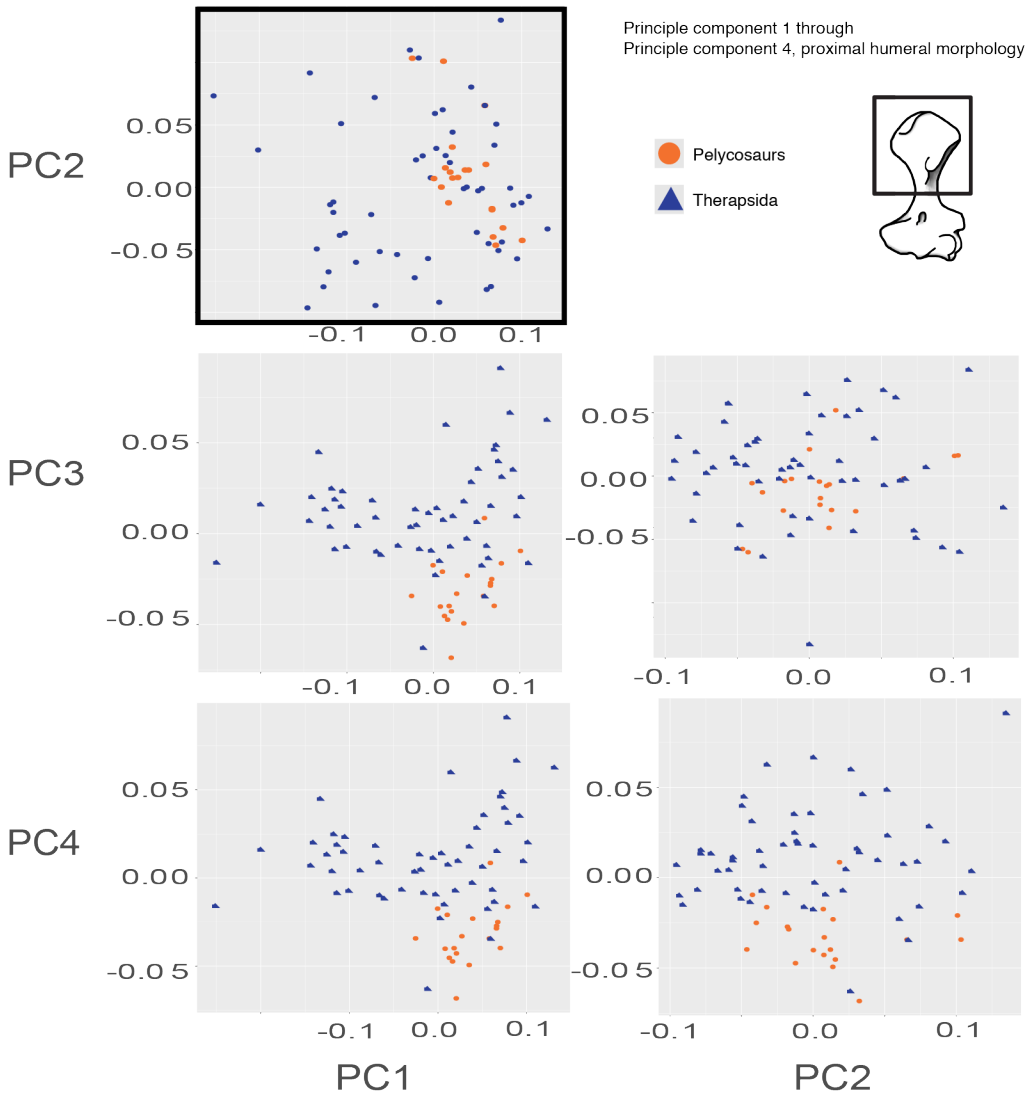

Figure 2.5 Proximal humeral principal components plots - Proximal end morphospaces of PC1 through PC4. Colored by clade: orange circles are “pelycosaurs” and blue triangles are therapsids. Black box highlights the plot reported in the Figure 2.3.

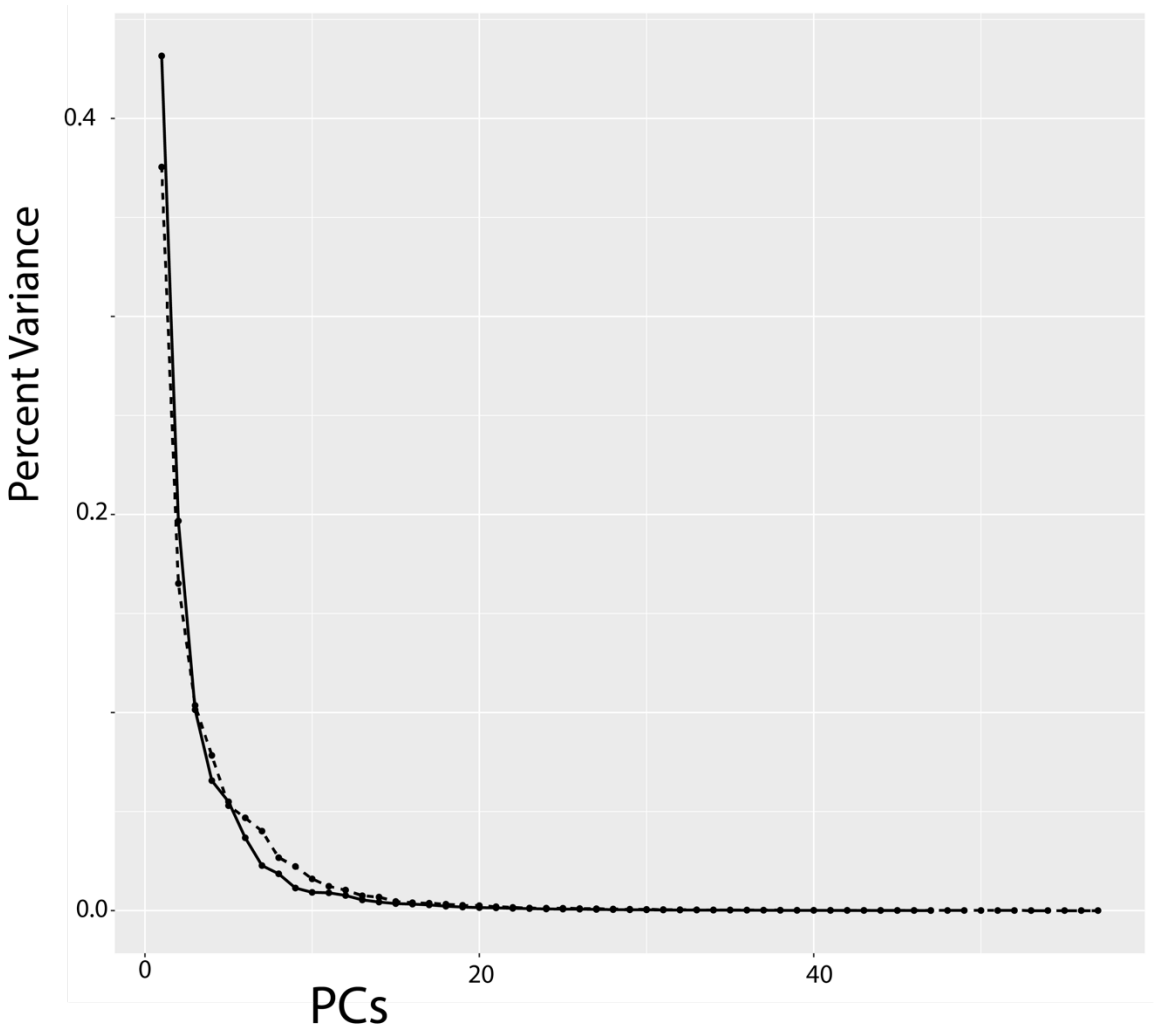

Figure 2.6 Skree plot of variances for Chapter 2 analyses - Skree plot showing percent variance of principle components axes for distal (dashed line) and proximal (solid line) ends.

2.4 RESULTS

2.4.1 Principal Components Analysis

Shape data were acquired through 2D landmark-based geometric morphometrics. Landmark placements are visualized in Figure 2.3B. Landmarks and semilandmarks were collected separately for the distal and proximal ends of the humerus. Mean proximal and distal humeral shapes were calculated for each sampled genus and used in subsequent analyses. For singletons or genera that did not have

multiple sampled representatives, the single sampled individual was used as the representative for the genus. The full sample list is presented in Appendix II. A principal components analysis was conducted to compare pelycosaur and therapsid humeral shape spaces (Figure 2.3B). For both the distal and proximal humerus, therapsids occupy a larger volume of morphospace than pelycosaurs; this is particularly pronounced for the proximal humerus. However, there is considerable overlap in the regions of morphospace occupied by pelycosaurs and therapsids. This implies that the evolution of therapsids was not accompanied by a whole-sale change in humerus shape. Instead, some therapsids began to explore new areas on the periphery of synapsid morphospace that likely correspond to novel ecologies and locomotor modes.

2.4.2 Disparity

Procrustes variance across the entire humerus is low during the early stages of the pelycosaur-dominated Permian. Variance levels of the distal and proximal ends only vary slightly between 305 and 275 Mya, with proximal humerus disparity being notably low from 300 to 295 Mya (Figure 2.7A). Pelycosaur variance is highest during the later stages of their evolutionary history, specifically within the 275 Mya time bin for the proximal end (0.0065) and at 270 Mya for the distal end (0.0085). Although sampling does not correlate with the variance results through time (Figure 2.7B and C), the presence of unusual pelycosaur taxa played a role in the heightened variance values during the latest stages of pelycosaur sampling. Specifically, the taxonomic and morphological diversification of Caseidae, a derived and enigmatic clade of large-bodied herbivorous pelycosaurs, drives the pelycosaur disparity increase starting at 285 Mya.

Therapsids emerge in the sample during the 270- and 265-Mya time bins for the proximal and distal humerus, respectively. It is at this point in the time series that total disparity for both parts of the

humerus begins to increase to variance levels that are higher than the range seen through the majority of the early synapsid sample. It is also during these time bins that the distal and proximal ends begin to express increasingly different values of disparity, though the overall pattern of increase continues to hold. Specifically, with the exception of the time bin representing the Permo- Triassic mass extinction, proximal disparity contains a disproportionate amount of the total humeral variance, and proximal values remain higher throughout the remainder of the time bins.

Overall, therapsids have greater Procrustes variance than pelycosaurs in both the distal and proximal ends of the humerus, across the majority of sampled time bins. Within therapsids, the proximal end of the humerus displays more variance than the distal end across all sampled time bins, and the magnitude of the difference between the proximal and distal variance values fluctuates only slightly through time. Therapsid proximal humerus variance was highest in the time bin just after the Permo- Triassic mass extinction (placed at 252 Mya instead of 250 Mya, following the 252.24-Mya age of the Permo-Triassic boundary) (Burgess, Muirhead, and Bowring 2017) (proximal = 0.014). Excluding the time bins that have noteworthy departures from the overall pattern (300–295, and 252 Mya) pelycosaur proximal humeri account for 50.49% of humeral variance on average, whereas in therapsids the proximal humerus accounts for 61.55% of humeral variance on average. Proximal variance remains high through the 240-Mya bin, but decreases following this maximum and returns to pre-extinction values in the Middle Triassic (235 Mya). Counter to the proximal trend, distal humeral disparity increases across the extinction interval. Analyses revealed that this disparity increase is caused by the removal of intermediate morphologies during the extinction.

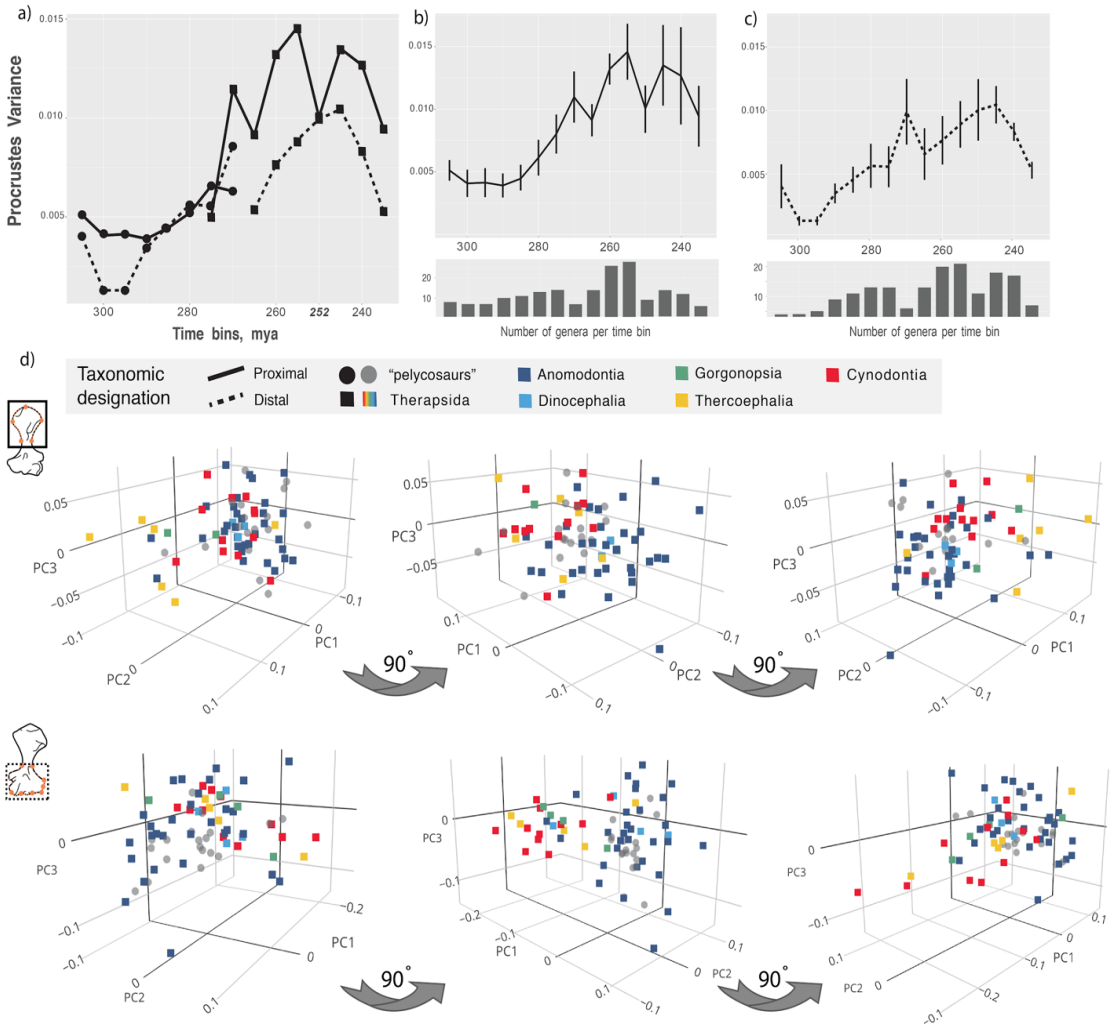

Figure 2.7 Disparity of pelycosaurs and therapsids through time with associated therapsid morphospace distributions - A) Total Procrustes variance through time split by synapsid radiation. The lines linked by circles represent pelycosaurs; therapsids are represented by squares. B-C) The total-group disparity pattern through time including error-bars for each sampled time bin. The histograms below shows total genera sampled across each end of the humerus per time bin for the proximal end (B) and distal end (C). D) 3D morphospace (PC1vPC2vPC3) for the proximal end and the distal end. When viewed in three dimensions therapsid exploration of previously unoccupied morphospace is evident. Colored squares represent therapsids; grey circles represent pelycosaurs. Each plot is rotated 90 degrees counter-clockwise from the one immediately left. Areas of morphospace that are unoccupied by pelycosaur specimens are instead occupied by groups representing novel therapsid ecomorphologies, such as cynodonts (yellow) and anomodonts (blue).

2.5 DISCUSSION

Our results show that the rapid increase in humeral disparity beginning in the mid-Permian is coincident with the emergence of therapsids (Figure 2.7A). Although the earliest therapsids are known from before 265 Mya (arguably as early as 275 Mya)(Laurin and Reisz 1990; Liu, Rubidge, and Li 2009; 2010) many of the oldest and phylogenetically most basal therapsids either have no known forelimb material or could not be sampled for this project due to rarity. As therapsids diversify taxonomically through the Permian, disparity of both ends of the humerus continues to increase to levels much higher than those ever achieved by pelycosaurs. This result supports the distinctiveness of therapsid humeral morphology and variance relative to those of pelycosaurs. Therapsida is hypothesized to have split from its pelycosaur sister group (Sphenacodontidae) in the Pennsylvanian (Angielczyk and Kammerer 2018). In the earliest time bins including therapsids (275–265 Mya), phylogenetically basal clades (primarily Dinocephalia) dominate the therapsid sample. The similar levels of disparity between pelycosaurs and therapsids in these bins, and the position of the dinocephalians in morphospace, reinforce the perspective of dinocephalians as morphologically "primitive" branches of Therapsida that had not diverged from the ancestral morphotype to the degree seen in later taxa. The low early therapsid variance levels in our sample could indicate a gradual accumulation of morphological disparity during their earlier history, which is unsampled in the known fossil record. Alternatively, the therapsid bauplan, including heightened forelimb disparity, might have evolved rapidly in the middle Permian, as suggested by a more literal reading of our data, with dinocephalians simply preserving an early stage in this process. Variance increases continuously from the middle Permian onwards, corroborating the hypothesis that therapsids underwent morphological diversification throughout the remainder of the Permian. The finding that variance decreased in the 252-Mya time bin represents the effect of the Permo-Triassic mass extinction, the largest extinction in Earth history (Chen and Benton 2012),

although the details of this decline differed between the proximal and distal ends of the humerus. The therapsid disparity-through-time pattern corresponds with their notably greater total morphospace occupation than pelycosaurs (Figures 2.3B and 2.7D). Critically, some of this novel humeral morphospace is associated with the first experiments by therapsid clades with ecologies that have no counterparts among pelycosaurs. Figure 2.7D shows that when considered in three dimensions the peripheral areas of morphospace uniquely occupied by therapsids correspond to taxa that have been hypothesized to represent the first occurrences of various ecotypes among nonmammalian synapsids. Examples include fossorial cistecephalid dicynodonts (represented by the color blue), small-bodied faunivores such as therocephalians and cynodonts (red and yellow, respectively), and the gracile, midsized predatory gorgonopsians (green).

Pelycosaur total group disparity varies less across the two ends of the humerus than in Therapsida. This association in values presumably reflects the functionally restrictive morphology of the humeral joint surfaces of pelycosaurs (Hopson 2015; Jenkins 1973a), and the role the humerus played in stabilizing the pelycosaur body (Watson 1917; Jenkins 1973a). The complex and mechanically costly gait of pelycosaurs likely limited the morphofunctional diversification of the upper limb. In contrast, therapsid disparity is characterized by a separation of shape variance in the distal and the proximal ends of the humerus, with proximal humeral disparity disproportionately heightened in comparison with the distal humerus. Importantly, the pattern of increasing morphological disparity is most strongly expressed in the vicinity of the proximal articulation (gleno-humeral joint). Pelycosaurs and therapsids possess distinctly different pectoral girdle morphotypes. Pelycosaur gleno-humeral articulations are screw shaped, antero-posteriorly long but dorsoventrally narrow with a spiraling joint surface, and are characterized by a precise fit between the humeral and pectoral joint surfaces that limits range of motion (Watson 1917; Romer and Price 1940). In contrast, the therapsid gleno-humeral

joint is characterized by smooth, convex surfaces that present few bony limits on joint mobility (Broom 1911; Gregory and Broom 1926; Colbert and Broom 1948). Therefore, the therapsid rise in ecomorphological disparity is not accompanied by an increasingly complex humeral form but by simplification, in particular of the humeral head. Coupled with the simplification of the glenoid and scapulocoracoid complex in therapsids, the changes in humeral morphology facilitated in- novation in forelimb function by increasing locomotor capabilities. Specifically, these findings support the hypothesis that the re- organization of the pectoral girdle and forelimb played a key role in the diversification of therapsids by increasing forelimb range of motion (Jenkins 1971a; Cluver 1978; Jenkins and Weijs 1979; Fröbisch and Reisz 2009; Lai, Biewener, and Pierce 2018). Freeing the forelimb from the constraints of limited mobility was a critical first step that allowed therapsids to explore new ecologies, foreshadowing further simplification of the pectoral girdle and ecological diversification of the forelimb later in mammaliaform evolution. Mammalian evolution is characterized by the heightened functional diversity of the forelimb, and the earliest roots of this macroevolutionary pattern lie in the Middle Permian emergence of therapsids.

CHAPTER 3 PHYLOGENY, FUNCTION, AND ECOLOGY IN THE DEEP EVOLUTIONARY HISTORY OF THE MAMMALIAN FORELIMB

3.1 ABSTRACT

Mammals are the only living members of the larger clade Synapsida, which has a fossil record spanning 320Ma. Despite the fact that much of the ecological diversity of mammals has been considered in light of limb morphology, the ecological comparability of mammals to their fossil forerunners has not been critically assessed. Because of the wide use of limb morphology in testing ecomorphological hypothesis about extinct tetrapods, we sought: (1) to estimate when in synapsid history modern mammals become analogs for predicting fossil ecologies; (2) to document examples of morphological convergence; and (3) to compare the functional solutions of distinct synapsid radiations. We quantitatively compared the forelimb shapes of the multiple fossil synapsid radiations to a broad sample of extant Mammalia representing a variety of divergent locomotor ecologies. Our results indicate that each synapsid radiation explored different areas of morphospace and arrived at functional solutions that reflected their distinctive ancestral morphologies. This work counters the narrative of non-mammalian synapsid forelimb evolution as a linear progression towards more mammalian morphologies. Instead, a disparate array of early-evolving shapes subsequently contracted towards more mammal-like forms.

3.2 INTRODUCTION

Morphological comparisons between extant and extinct animals are fundamental to inferences about the locomotor strategies and ecologies of fossil taxa. When consistent ecomorphological relationships are identified in extant taxa, hypotheses can be tested about

organisms for which ecology cannot be observed directly. The conceptual foundation of ecomorphology is the overlap between ecology and morphology (Wainwright 1991; Barr 2018), but the interplay of both factors with the details of function and phylogenetic history is also of critical importance because it implies that similarity in shape may not guarantee similarity in function (and vice versa). To consider these issues more deeply, we conducted a 2D geometric morphometric analysis of forelimb shape in the clade Synapsida with three interrelated goals: (1) to estimate when in synapsid phylogenetic history modern mammals become useful analogs for predicting ecologies of extinct taxa; (2) to investigate individual examples of morphological convergence within this conceptual framework; and (3) to determine if members of the distinct evolutionary radiations of synapsids evolved comparable functional solutions to shared ecological problems.

Synapsida, the amniote clade that includes all living mammals and their extinct ancestors, spans an estimated 320 million years of evolutionary history (Benton et al. 2015; Mann et al. 2020), three major mass extinctions, and several consecutive adaptive radiations (Hopson 1994; Kemp 2005; Close et al. 2015; Angielczyk and Kammerer 2018; Grossnickle, Smith and Wilson 2019). Highly specialized morphologies can be observed among the Mesozoic mammaliaforms (Ji et al. 2006; J. Meng et al. 2006; Q.-J. Meng et al. 2015), with other probable examples dating to at least the Permian (Cox 1972; Cluver 1978; Fröbisch and Reisz 2009; Spindler et al. 2018). The high ecomorphological disparity of mammals makes them tempting models for their fossil ancestors, yet the very depth of synapsid history makes particularly acute the question of whether crown-group mammals are instructive analogues for early members of Synapsida (Lungmus and Angielczyk 2019; Jones et al. 2020;). Studies comparing fossil synapsids directly to crown mammals have focused primarily on the closest non-mammalian fossil relatives of extant

Mammalia from the mid to late Mesozoic. Research on teeth (Gill et al. 2014; Chen, Strömberg, and Wilson 2019;), jaws (Luo et al. 2017; Grossnickle 2017; 2019), and forelimb metrics (Q.-J. Meng et al. 2015) has demonstrated that Jurassic and Cretaceous mammaliaforms are broadly comparable to many extant groups. However, these studies are restricted in their phylogenetic scope and are limited in their applicability to aspects of ecology and function such as locomotion, which are influenced primarily by the appendicular skeleton.

Here we undertake a detailed comparison of forelimb morphology between a sample of extant Mammalia and a large dataset of fossil non-mammalian synapsids spanning most of the group's geologic history. To test whether phylogenetic history determines available functional solutions, as well as the utility of ecomorphological approaches, we utilize shape analysis of the humerus and the ulna. Many extant ecomorphologies, such as digging or efficient long-distance locomotion (cursoriality), can be identified and quantified through forelimb shape even when constituent bones are considered in isolation (Hildebrand 1985; Hildebrand et al. 1985; Vizcaíno and Milne 2002; Kilbourne 2017; Kilbourne and Hutchinson 2019). We conducted a 2D geometric morphometric analysis comparing extant mammals to specimens representing four major evolutionary radiations from the earliest members of Synapsida ('pelycosaurs') through to the evolutionary origin of Eutheria. Our quantification of humeral and ulnar shape outlines facilitates direct comparisons across the wide temporal, phylogenetic, and morphological disparity encompassed by our dataset. We found that throughout the long and diverse history of Synapsida, the clade never repeatedly evolved characteristic morphologies to accommodate specific ecological needs. Instead, phylogenetic position is a predictor of forelimb shape, even in ecologically specialized taxa. Further, we show the use of mammalian forelimb shapes to predict the ecomorphology of extinct synapsids is not viable until the origin of mammaliaforms.

3.3 METHODS

3.3.1 Taxonomic Sampling

We conducted geometric morphometric analyses on proximal and distal humeri and proximal ulnae. Our taxon sample comprises five radiations within Synapsida: (1) the Pennsylvanian and early Permian "pelycosaur"-grade synapsids (hereafter pelycosaurs), (2) the middle Permian through Late Triassic non-cynodont therapsids (therapsids), (3) non-mammaliamorph members of Cynodontia (cynodonts), (4) mammaliaforms, here defined as all taxa from the base of Mammaliamorpha to the base of crown Eutheria, and (5) extant representatives of Mammalia. We use these paraphyletic grades as our units of comparison because they are temporally- and morphologically-distinct radiations of synapsids, analogous to the more familiar radiations dinosaurs and birds. The mammal sample includes the monotreme *Tachyglossus* and members of the four major clades of Eutheria, but excludes Marsupialia because of a lack of relevant specimens.

Taxon sampling prioritized groups that we hypothesized would best represent extinct ecomorphologies, and specifically excluded groups for which there is no evidence of extinct analogues (e.g., volant, fully pelagic, and bipedal mammals, although gliding mammaliaforms have been described (J. Meng et al. 2006; Q.-J. Meng et al. 2017)). Our ecomorphological categories are: fully fossorial, semi-fossorial, generalist, unguligrade, cursorial and arboreal. A detailed description of the taxon sample and ecomorphological categorizations can be viewed in Appendix III. We also included a small sample of extant and extinct reptiles and amphibians to assess the similarity of early synapsids to potential outgroups. In total, the sample is comprised of 1870 individual specimens representing 218 genera.

3.3.2 Geometric Morphometric Analyses

We digitized landmarks and semi-landmarks, and recorded scale, on photographs taken by the authors and a number of high-quality published images (Colbert and Broom 1948 Jenkins 1971a; Cox 1972; Jenkins and Parrington 1976; Holmes 1977; Kemp 1982, 1986; Jenkins and Schaff 1988; Sumida 1989; Rougier 1993; Berman et al. 2000; Horovitz 2003; Reisz and Laurin 2004; Luo and Wible 2005; Liu, Soares, and Reichel 2008; Martin 2005; J. Meng et al. 2006; Oliveira 2006; Abdala 2007; Hurum and Kielan-Jaworowska 2008; Campione and Reisz 2010; Reisz et al. 2011; Martin 2013; Berman et al. 2014; Q.-J. Meng et al. 2015; Brocklehurst et al. 2016; Pavanatto et al. 2016; Kammerer 2018; Kammerer and Masyutin 2018; Liu, Schneider, and Olsen 2017; Jäger, Luo, and Martin 2019; Sulej and Niedźwiedzki 2019; Guignard, Martinelli, and Soares 2019), using tpsDIG2ws (Rohlf 2010). Type II landmark and semilandmark numbering is as follows: proximal humerus - 4 landmarks, 19 semilandmarks; distal humerus - 8 landmarks, 26 semilandmarks; proximal ulna - 5 landmarks, 22 semilandmarks (Figure 3.1). The landmarks represent consistently recognizable extrema on the outlines of the humerus and ulna because there are no usable internal landmarks across the breadth of morphological disparity and diversity of preservation styles present in our sample. We analyzed the proximal humerus in posteroventral view, emphasizing the perspective that maximized the total width of the proximal end and provided a view of the delto-pectoral crest (Figure 3.1). In the extant sample, we used anterior view for the proximal humerus because this perspective includes the deltoid tuberosity, making it a functionally analogous viewpoint. We analyzed the distal humerus in dorsal view, although all relevant morphology is visible in either

dorsal or ventral view. Our analysis of the ulna focused solely on the proximal end and the shape of the olecranon process.

The Geomorph package (Adams et al. 2016) in R was used for all processing of geometric morphometric data. Ggplot2 (Wickham 2016) was used in R for visualizations and all figures unless otherwise stated. The Psych package (Revelle 2011) was used for base summary statistics where appropriate. Raw landmarks and semilandmarks were read into R in TPS format with the semilandmark formations read in as curves. Our analysis utilized mean shapes for each genus. We averaged all specimen shapes for a given genus using the function 'mshape' in Geomorph, which uses the previously aligned coordinates to estimate a mean shape. For singletons, the single specimen itself represented the mean shape of that genus. We subjected the set of genus means to an additional general Procrustes alignment for all subsequent statistical analyses.

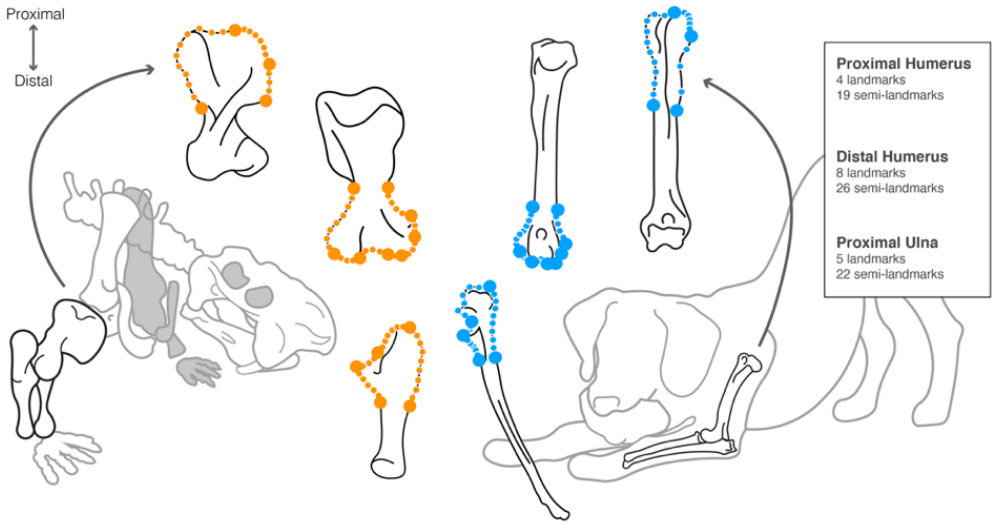

Figure 3.1 Landmark configuration for Chapter 3 analysis - Schematic of landmark configurations shown on the forelimb elements of a representative fossil synapsid (the therapsid *Sinokannemeyeria*; left) and an extant mammal (*Canis*; right). Proximal humeri were analyzed from a perspective that allowed the deltopectoral crest (deltoid tuberosity in mammals) to be digitized. Due to posture changes across Synapsida, this is posteroventral view for the fossil sample and anterior view for the mammals.

Singletons (genera for which we only had a single specimen) were digitized alongside the rest of the specimens but were separated prior to analysis from the rest of the sample to facilitate mean shape computations. The landmarks were not originally aligned to the principal axes to prevent incongruence between the singletons and larger dataset. Semilandmarks were aligned by bending energy and not by Procrustes distance. Considering the large size of the dataset, the phylogenetic breadth of the fossil sample, and the inclusion of extant mammals, using Procrustes distance as the metric for sliding added an additional level of noise that made comparing the disparate groups more difficult. Using bending energy as the method for spacing semilandmarks increased the overall comparability of the analyses to one another across the sample.

The classifiers were read into R as .csv files and included the categorizations of group, family, and genus, as well and two numbering schemes to track the order of the specimens in the TPS files. For the larger dataset that excludes singleton taxa, a mean shape was created for each genus present in the sample. For singletons, the single specimen itself represented the mean shape of that genus. This introduces the possibility of errors associated with taphonomy, distortion or human digitization error. However, many of the singleton specimens represent genera for which there is only a single known individual or are otherwise exceedingly rare. We decided any error introduced could be considered during landmark processing, and that the inclusion of these exceptional taxa was worth the small amount of error they may introduce.

Sampling of extant mammals was guided by a combination of ecological designation, phylogenetic breadth, and availability of specimens. Species were binned into a series of categories reflecting their locomotor ecologies: graviportal/unguligrade (rough categorization of very large herbivorous terrestrial mammals; see Appendix III), semifossorial, fossorial, arboreal, cursorial, generalist/terrestrial, and ‘outgroup’ (extant and extinct reptiles and extinct

amphibians). Members of the mammalian group Marsupialia were not included primarily because of lack of access to a large sample of specimens in the collections we used. Genera that were well-represented in collections, such as *Didelphis*, typically were generalist terrestrial species, a category that was already represented by the Eutherian mammals in the dataset. The group Rhinocerotidae is a family designation, not a genus designation like the rest of the mammalian sample, again reflecting the small sample of Rhinos available in most collections. The mean shape is a combination of three genera: *Rhinoceros* (Indian rhinos), *Diceros* (black rhinos), and *Ceratotherium* (white rhinos).

The extant coordinate data was imported and subjected to a protocol that exactly matched the analyses of the extinct sample. As with the extinct sample, the coordinates were subdivided by genus, and mean genus shape coordinates were generated and subsequently concatenated together. In contrast to the extinct sample, there were no singletons in the extant dataset. Following the generation of mean shapes for the extant sample, the data were combined into a new array that included all of the previously analyzed and grouped extinct data. A new classifier file was created for the combined analyses that included all the taxa together. This new dataset subsequently underwent an additional round of generalized Procrustes analysis to align the extinct and extant specimens.

We recognize that many ecomorphological categories are broadly defined, and our goal was to capture notable ecomorphologies based on the primary locomotor type of the organism. Ecological designation was based on a broad understanding of a taxon's locomotory habits and sought to recognize specialized ecological uses of the forelimbs. For example, the semi-fossorial mammals in this dataset can be equally well described as being simply terrestrial, but received

the categorization of semi-fossorial because digging plays a critical role in their life-history (usually through denning behavior or insectivorous foraging).

3.3.3 Phylogenetic Trees

We analyzed each functional unit (proximal humerus, distal humerus, proximal ulna) in a phylogenetic framework. We constructed a composite phylogeny for each functional unit that encompassed the unit's taxonomic sample (Figures 3.2-3.4). Because there is no single phylogeny that includes all of taxa present in this study, our composite trees are based on published phylogenetic analyses (Luo, Kielan-Jaworowska, and Cifelli 2002; Müller and Reisz 2006; Bonaparte 2008; Kammerer et al. 2008; Archibald and Averianov 2006; Gaetano and Rougier 2011; Kammerer 2011; Liu and Abdala 2014; Q.-J. Meng et al. 2015; Martinelli, Soares, and Schwanke 2016; Angielczyk and Kammerer 2017; Angielczyk, Hancox, and Nabavizadeh 2017; Kammerer and Masyutin 2018; Grunert, Brocklehurst, and Fröbisch 2019; Rodrigues et al. 2019; Huttenlocker et al. 2018; Abdala et al. 2019).

The trees were built manually in the program TreeGraph (Stöver and Müller 2010). To time calibrate the trees, first occurrence dates and last occurrence dates were gathered from the Paleobiology Database for each fossil taxon. For the mammal sample, divergence dates were used in place of first occurrence dates for the two diverging genera. The topology of the mammal tree and estimated divergence dates were drawn from (Upham, Esselstyn, and Jetz 2019). The tree was then analyzed under a minimum branch length model to create the full topology and time scaled with the package Claddis (Lloyd 2015).

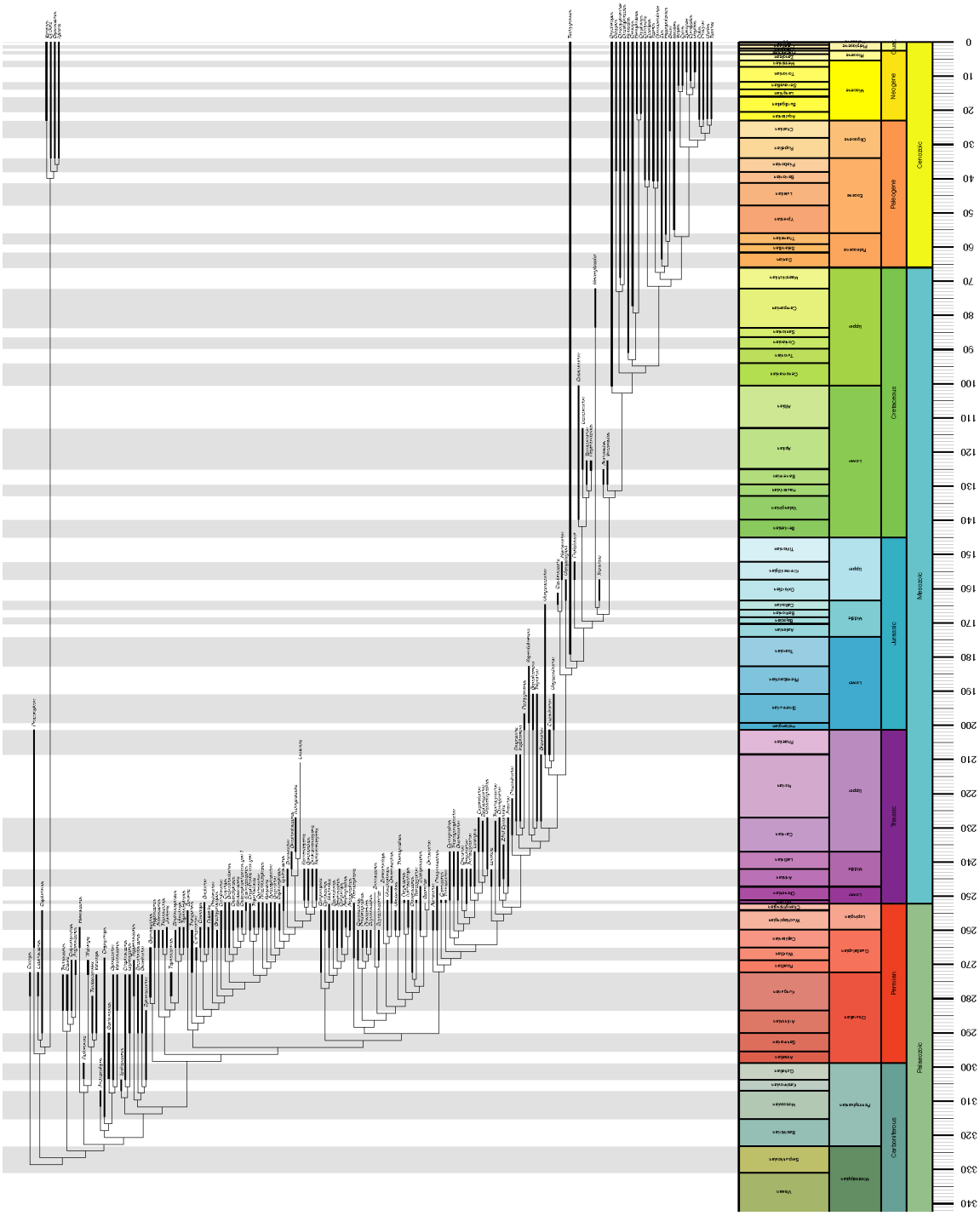

Figure 3.2 Phylogeny for proximal humerus analysis - The composite trees used for the phylogenetic analysis of the proximal humerus. Thicker bars represent the time ranges of the taxa. Details on taxonomic designation and occurrence dates can be found in Appendix IV.

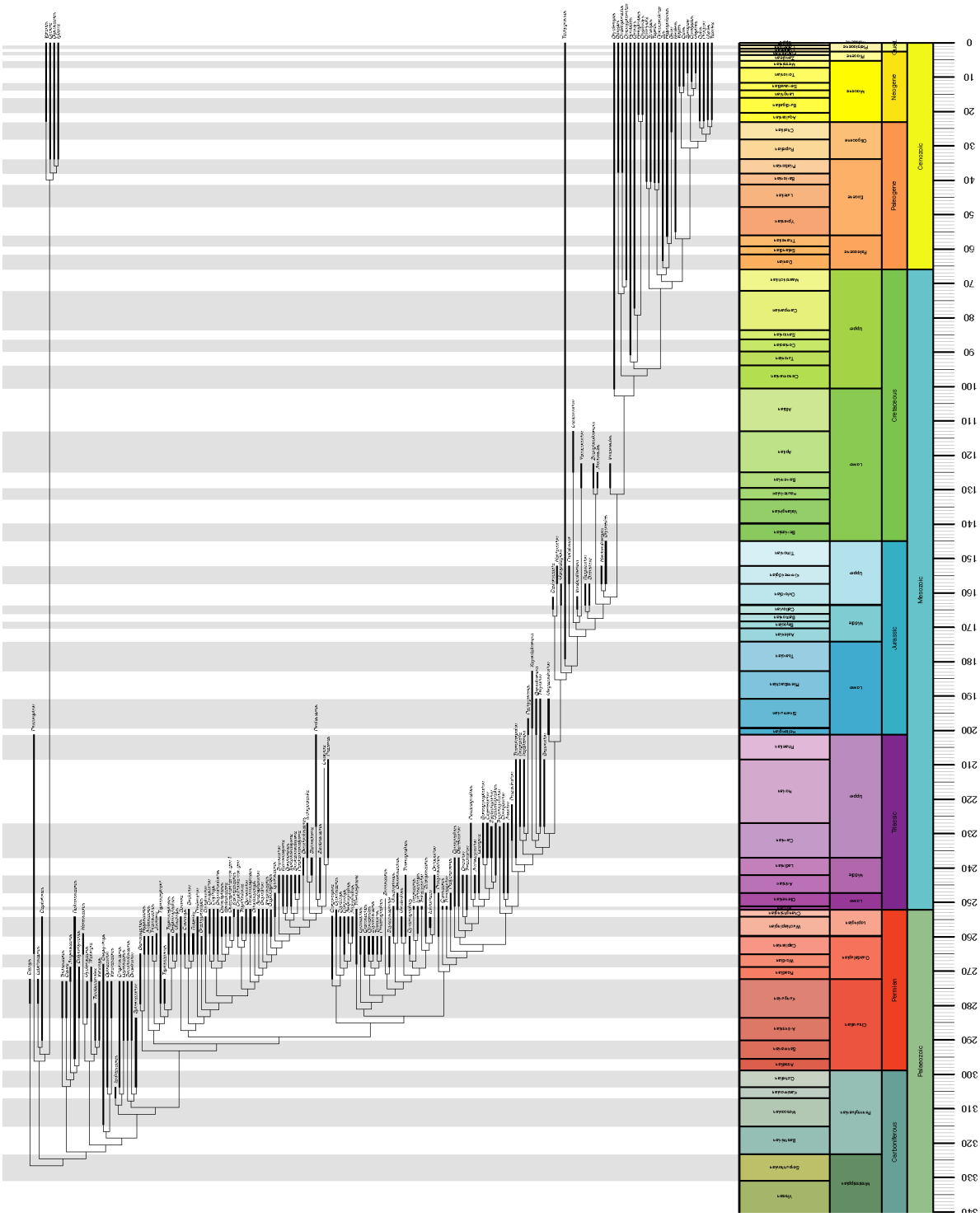

Figure 3.3 Phylogeny for distal humerus analysis - The composite trees used for the phylogenetic analysis of the distal humerus. Thicker bars represent the time ranges of the taxa. Details on taxonomic designation and occurrence dates can be found in Appendix V.

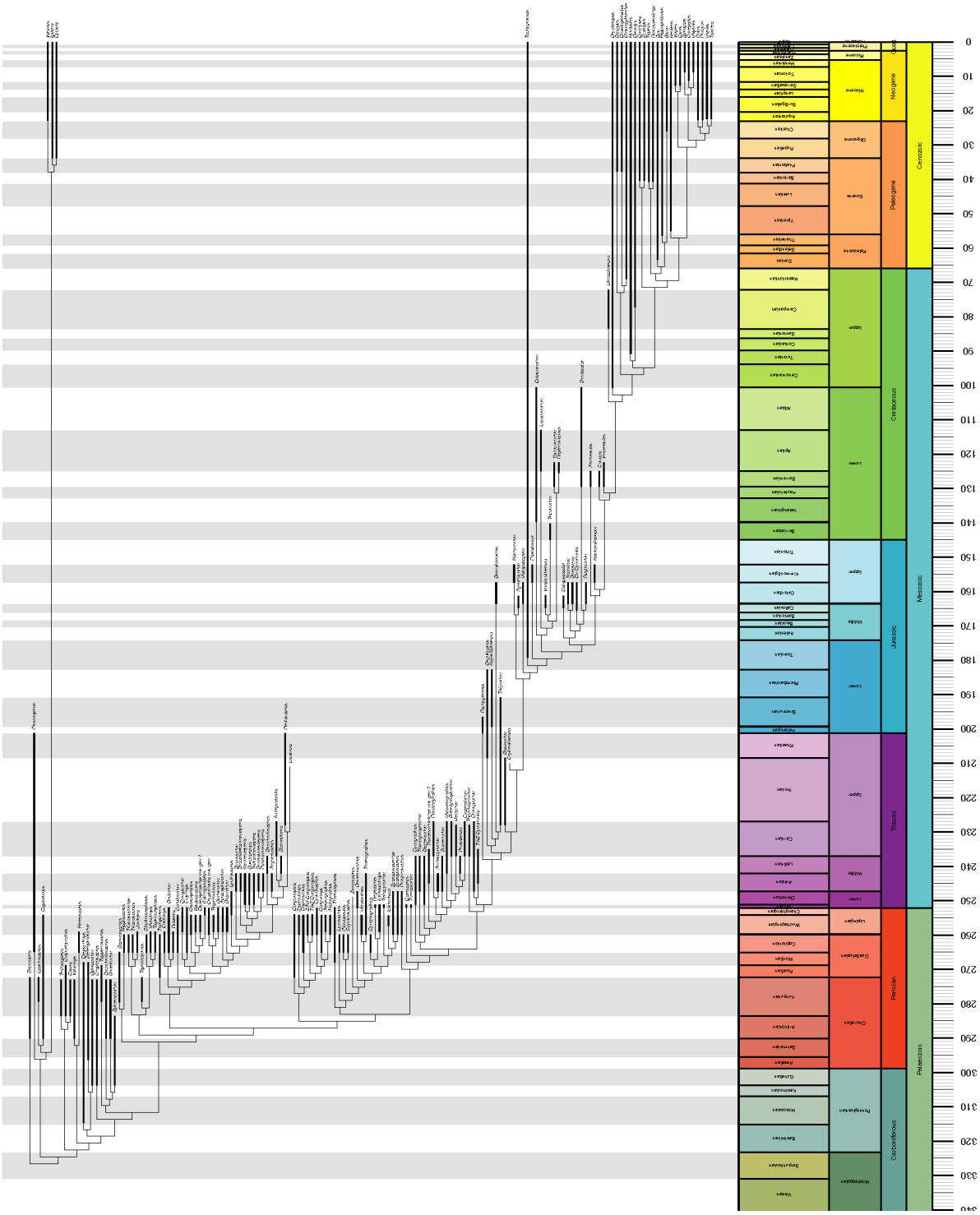

Figure 3.4 Phylogeny for ulna analysis - The composite trees used for the phylogenetic analysis of the ulna. Thicker bars represent the time ranges of the taxa. Details on taxonomic designation and occurrence dates can be found in Appendix VI.

3.3.4 Procrustes and Patristic Distances

Our primary method for comparing shape disparity among taxa was Procrustes distance (Gower 1975). We calculated Procrustes distance between each fossil genus and the mean of all mammalian shapes (i.e., the mean position of mammalian morphospace). Phylogenetic signal, measured here as the 'Kmult' statistic of (Adams 2014)(Table 3.1), shows that phylogeny influences taxonomic groups and all functional units to differing degrees. To address how strongly similarity in shape is dictated by phylogenetic relatedness, we regressed Procrustes distance against patristic distance, quantifying the relationship between phylogenetic position and morphospace location. We calculated patristic distance as the sum of branch lengths in units of time to the node of the first-diverging member of Eutheria in our sample, providing a measure of the phylogenetic proximity of each fossil genus to Eutheria. We estimated confidence intervals using a general linear model and conducted correlation tests in R (Wickham 2016)(Table 3.2).

Table 3.1 - Measured values for each group by divided by functional unit.

Functional Unit	K_{mult} by functional unit	K_{mult} by group	K	p	Procrustes Distance	Patristic Distance
Proximal	K = 0.59 p = 0.001	Pelycosaur	0.5418	0.886	0.3461295	361.1095
		Therapsid	0.6401	0.001	0.3086466	334.2062
		Cynodont	0.6822	0.179	0.2314723	281.8526
		Mammaliaform	0.4371	0.23	0.2424533	211.864
Distal	K = 0.301 p = 0.001	Pelycosaur	0.6442	0.725	0.1663678	362.5437
		Therapsid	0.671	0.001	0.1716007	324.2812
		Cynodont	0.6218	0.439	0.1483741	281.0444
		Mammaliaform	0.521	0.365	0.1880116	194.8573
Ulna	K = 0.4271 p = 0.001	Pelycosaur	0.8795	0.028	0.3233453	363.3654
		Therapsid	0.6901	0.002	0.3525188	322.4351
		Cynodont	0.9222	0.019	0.2862565	288.4625
		Mammaliaform	0.2832	0.963	0.1918486	201.2909

Functional Unit	Pearson Product-Moment Correlation	Kendall's Tau	Spearman's Rho
Distal humerus	p-value = 0.7748	p-value = 0.007814	p-value = 0.006755
	t = 0.28667 df =132	z = 2.66	S = 307584
Proximal humerus	p-value = 1.705e-05	p-value = 7.105e-09	p-value = 2.666e-10
	t = 4.4683 df = 129	z = 5.7884	S = 181091
Ulna	p-value = 1.301e-06	p-value = 0.0022	p-value = 0.002566
	t = 5.0972 df = 120	z = 3.0618	S = 220708

Table 3.2 - Correlation statistics for Procrustes distance and patristic distance (Figure 3.9) by functional unit.

3.4 RESULTS

3.4.1 Morphospace Occupation

Proximal humerus: The first five PCs capture nearly 90% of the variance in proximal morphology (PC1 - 53.53%; PC2 - 13.09%; PC3 - 10.89%; PC4 - 6.1%; PC5 - 5.1%). The group-level morphospace occupation for proximal morphology is differentiated, with more distantly-related groups being farther apart. For example, Mammalia has a clearly defined morphospace (Figure 3.5 and 3.6), and with the exception of a few noteworthy taxa (*Tachyglossus*, members of the family Talpidae), it does not overlap with the morphospace of its most distant relatives, the pelycosaurs. Therapsids occupy a large area of morphospace, and overlap every other group to at least to some degree. Cynodontia and Mammaliaforms take

smaller areas of morphospace along PC1 and PC2, but their mean positions are closer to mammalian morphospace. The two genera in Talpidae both fall far outside of the rest of mammalian morphospace, near the outer edges of morphospace in general. The mammaliaform genus *Fruitafossor* falls in a unique and otherwise completely unoccupied region, and dramatically increases the dimensions of mammaliaform morphospace.

Shape change along principal component 1 is dictated by the morphology of the delto-pectoral crest (or the deltoid tuberosity in the case of Mammalia). Mammals primarily possess high PC1 values, and this shape is characterized as gracile and elongate. The delto-pectoral crest in this case expands well down the length of the humeral shaft, sometimes fading into the

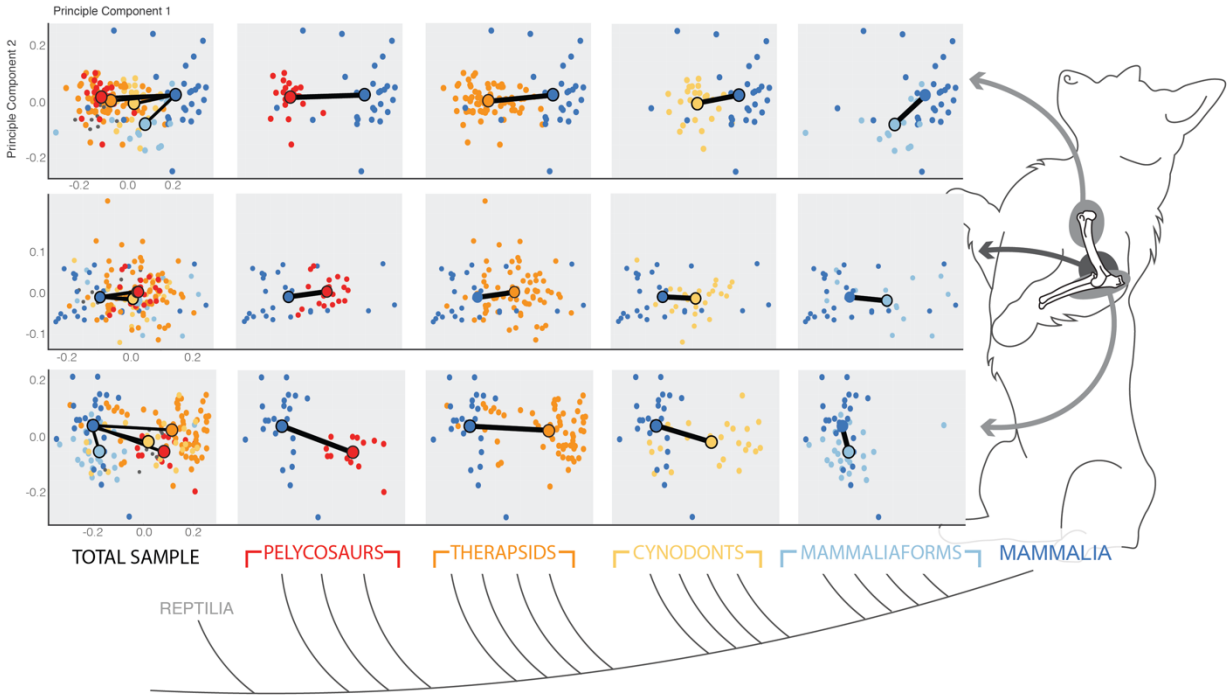

Figure 3.5 Principal component plots of shape data for the proximal humerus, distal humerus, and proximal ulna - Principle component plots of shape data for the proximal humerus (top row), distal humerus (middle), and proximal ulna (bottom). The full dataset (far left column) is followed by plots highlighting comparisons between mammals and each of the major synapsid radiations. Larger dots represent the mean position of a group's morphospace. Black lines visualize the magnitude and direction of differences between mean shapes.

humeral shaft as opposed to possessing a clear, sharply-pointed or angular end. Lower PC1 values correspond to pelycosaurian morphology and the majority (though not totality) of therapsid morphology. In these cases, the delto-pectoral crest is highly concave, and the terminal point of the DP crest falls more proximally along the humeral shaft. Considered in terms of landmark placement, this means that landmark 4 (the last landmark along the DP crest) is positioned proximal to landmark 1 (the first landmark, positioned along the humeral shaft on the posterior side of the short axis of the humerus). Additionally, this means that the placements of landmark 3 and 4 vary in relation to one another. Landmark 3, which defines the widest expanse of the deltopectoral crest (the most medial-ventral point along its edge) is much closer to landmark 4 in cases of low PC1 values and is sometimes close to being directly lateral to landmark 3. In cases of high PC1 values, landmarks 3 and 4 are more in line with one another and also spread more widely apart from one another.

PC2 deals with the shape of the dorsolateral edge of the proximal humerus (the side opposite to the delto-pectoral crest), the space and shape between landmarks 1 and 2. At low values, the outline defined by the semilandmarks between these two landmarks is relatively straight and continuous, with only a small dip associated with muscle attachment. For high values, however, the dorsal side of proximal humerus expands outward from the humerus here, creating a distinct process. This morphology is shared by talpid moles and cistecephalid dicynodonts, and is one of several instances of convergence between these groups (Cluver 1978). A secondary aspect of variation along PC2 again concerns the morphology of the deltopectoral crest. In this case it has to do with the "roundness" of the crest's shape and the distal expanse of the crest along the humeral shaft.

PC3 shape space continues the strong differentiation between clades, and morphological variation along this axis also pertains to the deltopectoral crest, primarily the placement of landmark 3, which defines the ventral-most expanse of the crest. In the case of high values, the distal point of the deltopectoral crest is in line with landmark 3, creating a straight and highly "square" deltopectoral crest. With low values, the distal-most point of the deltopectoral crest, defined by landmark 4, dives quickly back in line with the humeral shaft creating an almost convex line.

There are several taxa with noteworthy positions in morphospace that play an outsized role in defining the volume of their clade's morphospace, especially along PC1 and PC2. There are five mammalian taxa: the family Rhinocerotidae, the genus *Scalopus*, the genus *Condylura*, the genus *Hylobates* (lowest mammalian PC2 score), and the genus *Tachyglossus*. The positions of Rhinocerotidae, the talpid moles, and *Tachyglossus* are highlighted in the Figure 3.10. Rhinocerotidae falls in what would be considered a more therapsid area of morphospace. The genera in Talpidae both fall far outside of the rest of mammalian morphospace and occupy the outer edges of morphospace in general. *Hylobates* also falls in its own area of morphospace, possessing a unique combination of high PC1 scores and low PC2 scores. Additionally, the mammaliaform genus *Fruitafossor* falls in a unique and otherwise completely unoccupied area of morphospace. This dramatically increases the dimensions of mammaliaform morphospace overall and impacts the subsequent analyses of mammaliaform shape space.

The proximal humerus articulates with the glenoid of the scapula or scapulocorocoid, forming the complex and dynamic shoulder joint. We hypothesize that biomechanical and morphological constraints, largely stemming from a given species' ancestral shoulder girdle construction, limit the potential for members of different synapsid radiations to evolve highly

convergent shapes even when the species have similar ecologies. The underlying architecture of a morphologically 'primitive' forelimb and shoulder of a burrowing mammaliaform or a large-bodied anomodont channeled humeral shape evolution towards specific shapes that are not comparable to that of an extant mammal, even if their hypothetical ecologies are similar. This explains why rare examples of ecomorphological convergence across synapsid radiations can be pinpointed, but for the most part each radiation explored its own region of morphospace.

Distal humerus: The first five principal components (PCs) (Figure 3.7) capture over 80% of the variance in the dataset (PC1 - 48.61%; PC2 - 12.22%; PC3 – 10.75%; PC4 - 6.83%; PC5 -

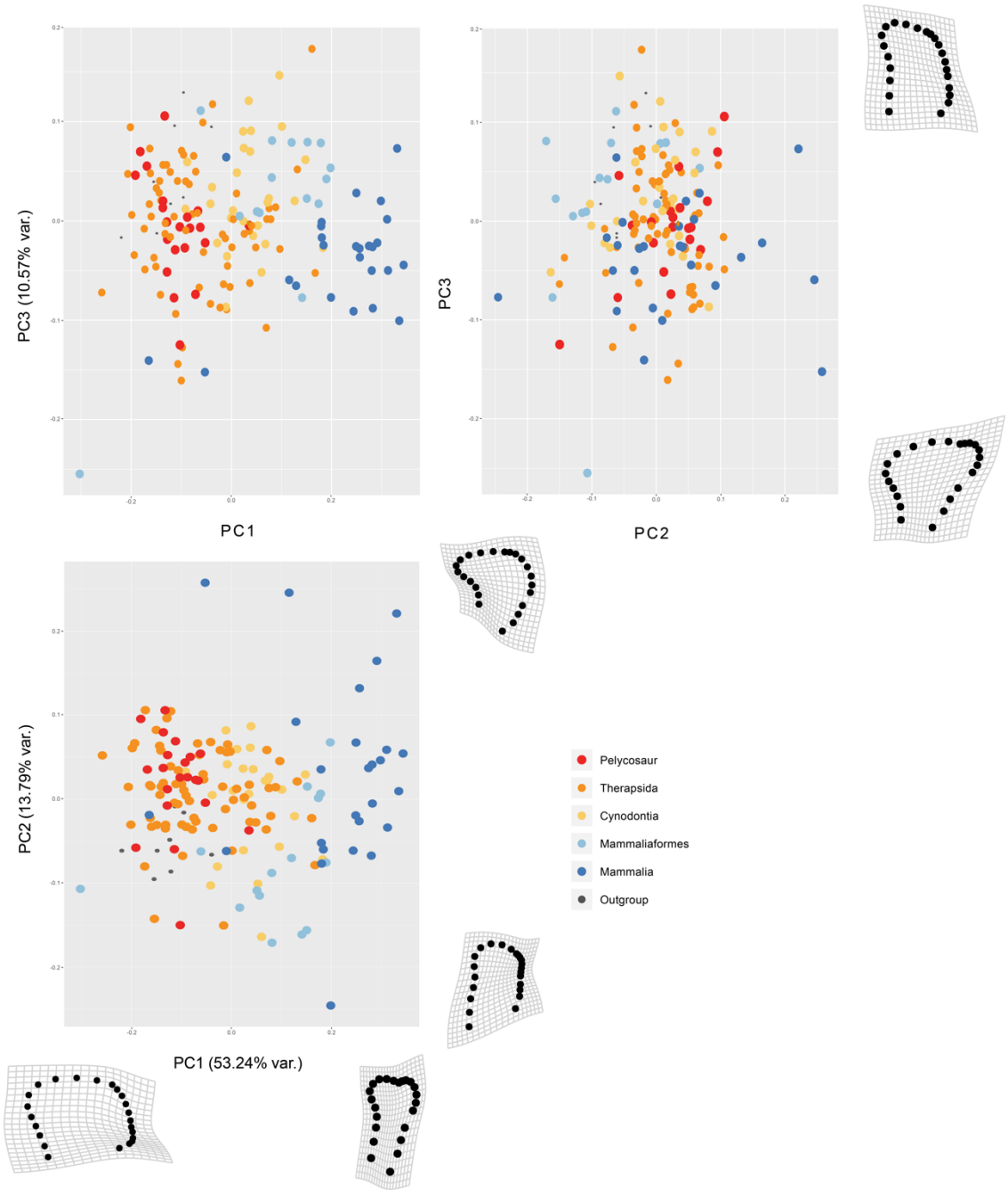

Figure 3.6 Proximal humeral principal components plots - Principal component plots 1 through 3 for the proximal humerus. Warp grids represent the shape change extremes along the x and y axes. Full percent variance for the first 5 PCs can be found in the Morphospace descriptions section of S1.

4.82%). There is significant overlap among all the fossil and extant groups on PC1 and PC2, providing no obvious means by which to differentiate group-specific areas of morphospace or classify areas of morphospace based on a given mammalian morphology.

The shape change along principal component 1 is defined by the breadth of the ectepicondyle and entepicondyle along the lateral axis of the distal humerus. Higher PC1 scores correspond to elongate and slightly flaring condyles on both ends, whereas low scores correspond to a noticeably more gracile shape where the condyles are proportionally more in line with the humeral shaft. The differences in these shapes primarily are expressed through the differing placements of landmarks 2 through 7. In the case of high PC1 scores, these landmarks are stretched out along the short axis of the humerus, while the opposite is true in the case of low PC1 scores, in which these landmarks are all closer together.

Shape variation along principal component 2 primarily concerns the shape and size of the entepicondyle. High PC2 scores correspond to an entepicondyle that is less elongate and more expansive along the long axis on the humerus (i.e., broader proximo-distally). In contrast, low PC2 scores represent an entepicondyle shape that can be described as “pointed”, with the the most distal-posterior expanse of the condyle expanding away from the humeral midline and coming to a rounded process at its tip. This creates a concave, u-shaped edge leading from the posterior line of the humeral shaft down to the entepicondyle, in contrast to the convex entepicondylar shape associated with high PC2 scores. This is primarily reflected as changes in the placement of landmarks 6, 7 and 8, and specifically how close they are to one another. In the case of high PC2 scores, landmarks 6 and 7 are far away from one another with 7 and 8 closer to

one another. Conversely, in low PC2 scores the opposite is true, with 6 and 7 being very close to one another.

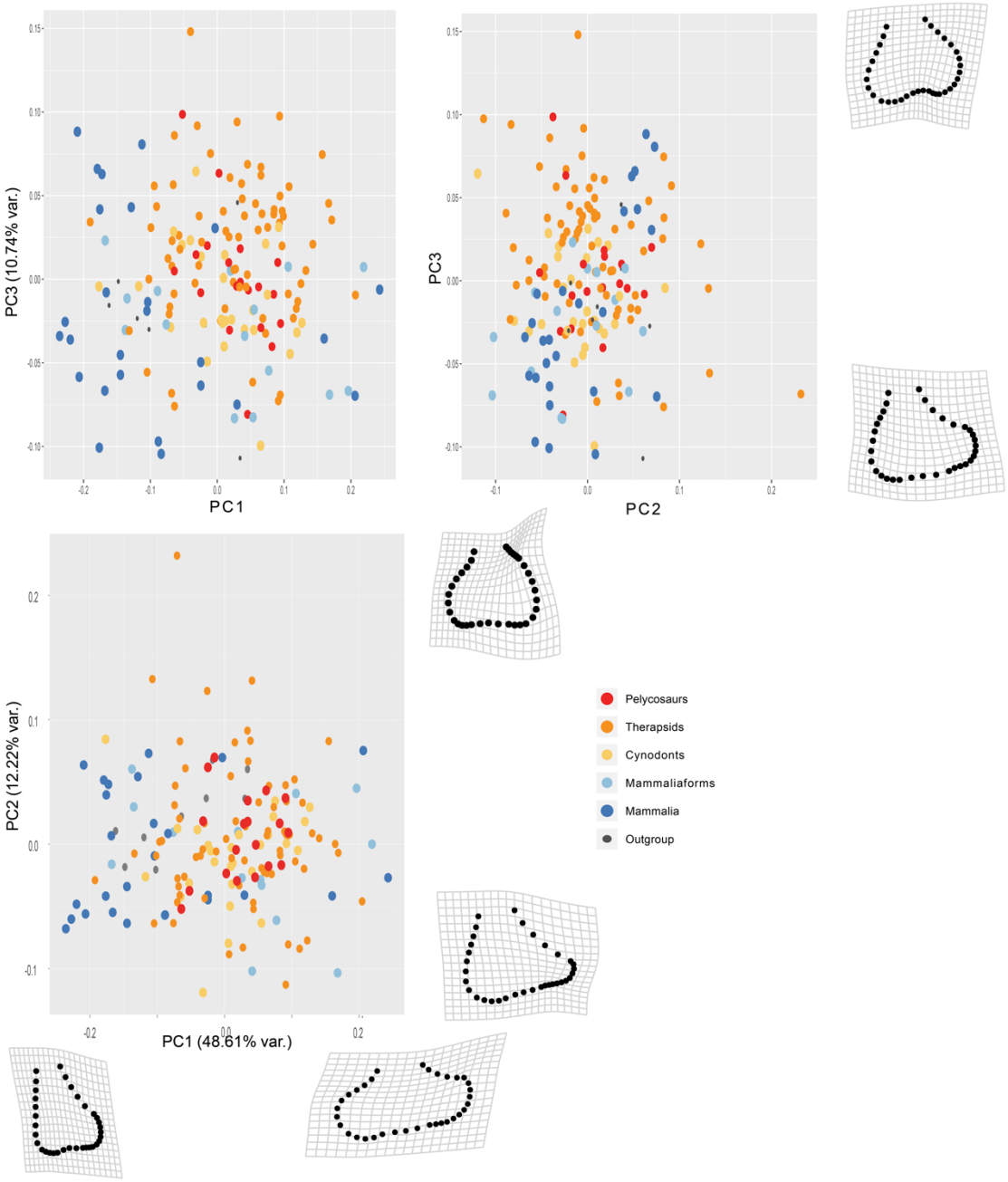

Figure 3.7 Distal humeral principal components plots - Principal component plots 1 through 3 for the distal humerus. Warp grids represent the shape change extremes along the x and y axes. Full percent variance for the first 5 PCs can be found in the Morphospace descriptions section of S1.

Shape variation along PC3 is broadly similar to that of PC2, but is less pronounced. In the case of high PC3 scores, the entepicondyle is still large, but is overall more rounded and represents a continuous convex edge, expressed through a more even spacing between landmarks 6, 7, and 8 along the posterior expanse of this condyle. Similarly, low PC3 scores express a clear entepicondylar projection, but it is less pronounced than in PC2, while still being much more strongly defined than the ectepicondyle.

Ulna: The first five principal component axes capture over 90% of the variance in ulnar morphology (PC1 - 65.58%; PC2 - 14.52%; PC3 - 5.69%; PC4 - 4.31; PC5 - 2.6%) (Figure 3.8). Some group-level distinctions are present in ulnar morphospace, but an additional level of differentiation occurs as a strong demarcation between two primary ulnar morphologies that transcend taxonomic identification. Pelycosaurs and outgroup (reptile and amphibian) taxa have high PC1 scores, whereas all mammals and mammaliaforms (excluding *Fruitafossor*) are characterized by low PC1 scores. Therapsids and cynodonts are spread across PC1, with some possessing more phylogenetically 'basal' shapes (high PC1 scores) whereas others fall closer to extant mammalian shape space (low PC 1 scores). For therapsids this differentiation is driven by the presence of enlarged olecranon processes in small burrowing dicynodonts and large Triassic dicynodonts.

Variation along PC1 includes the length and width of the olecranon process, and it unsurprisingly makes up the majority of total variation in ulnar morphology. High values along PC1 correspond to olecranon processes that are stout, with the distal portion of the lunar notch being offset from the proximal portion of the notch and representing the widest point of the entire ulna. The articular surface is weakly concave and gradually slopes into the olecranon

process. This morphology could be accurately described as reptilian, pelycosaurian, or therapsid, although it does not singularly characterize therapsid morphology. Low PC1 values correspond to more mammalian morphologies, as well as those of Triassic large-bodied dicynodonts. This morphology is characterized almost entirely by a thin but highly elongate olecranon process and a more mammalian semi-lunar notch as it is classically understood. The articular surface is highly U-shaped and concave. The distal and proximal edges of the semi-lunar notch, defined by landmarks 2, 3, and the semilandmarks between landmarks 3 and 4, are strongly aligned with one another. The shape of the olecranon process is rounded and the widest part of the ulna is often in the middle of the olecranon process, above the articular surface.

The variation along PC2 primarily concerns the length of the olecranon process. In this case, enlarged olecranon processes are present on both ends of the axis, but the overall length, curvature and width of the olecranon varies along with the shape of the articular surface. In the case of high PC2 scores, the olecranon process is long and wide, but the semi-lunar notch is still slightly offset, with the distal portion of the notch offset laterally. For low PC2 scores the olecranon is short and stout, but there is still a distinct semi-lunar notch.

PC3 does not constitute a large portion of overall variance (5.69%) and primarily reflects the unique morphologies of several distinct extant mammalian taxa such as the large ungulates *Bison* and the family Rhinocerotidae. In this case, the proximal portion of the semi-lunar notch expands laterally beyond the expanse of distal portion of the notch, creating a distinct "over-hang" to the articular surface that is present in many large bodied unguligrade mammals, but is uncommon in the extinct taxa. This ulna shape appears to evolve in situations where powerful movements at the elbow and a reduced risk of dislocation are necessary. In the case of large bodied animals, this presumably corresponds to the pressure to move large and heavy bodies

while minimizing the risk of dislocation at the ulnar joint. In the case of the moles, the size and shape of the olecranon is also being driven by the pressures of a unique locomotor style, though in this case the large muscle attachments pertain to moving substrate while burrowing.

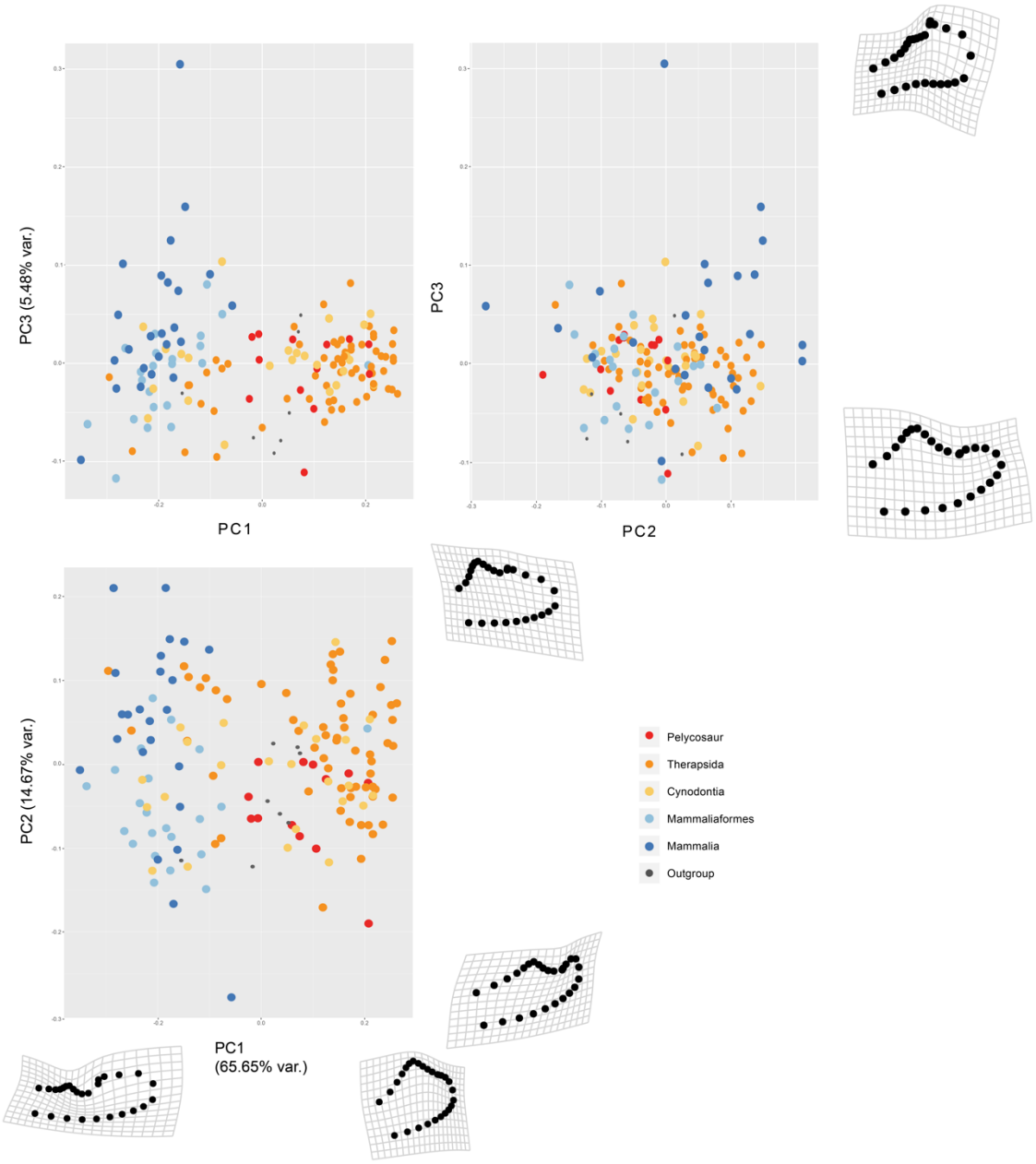

Figure 3.8 Ulna principal components plots - Principal component plots 1 through 3 for the proximal humerus. Warp grids represent the shape change extremes along the x and y axes. Full percent variance for the first 5 PCs can be found in the Morphospace descriptions section of S1.

3.4.2 Phylogenetic Signal, Procrustes Distance, and Patristic Distance

Kmult was less than 1 for each functional region, regardless of whether it was calculated for our full phylogenies or for portions of the tree corresponding to our taxonomic subgroups (Table 3.1). Despite its relatively low values, permutation tests showed that Kmult was always significantly greater than zero at the scale of the whole phylogeny. However, only the Kmult values for therapsids were significantly different than zero for all three functional regions. Values for the other subgroups typically were not significantly different than zero except for the ulna dataset. Of the three functional areas, distal humerus Procrustes distance is the most similar across the groups (Figure 3.9). The plot of Procrustes distance versus patristic distance provides additional evidence that there is little group-specific differentiation of the distal end, with most groups occupying similar ranges of Procrustes distance values.

Procrustes distances for the proximal humerus conform to a more predictable phylogenetic pattern. The outgroup has the highest values and is farthest away from mammalian morphospace (Figures 3.5). Each subsequent phylogenetic group expresses lower average Procrustes distance to crown Mammalia. As for the distal humerus, therapsids and mammaliaforms have the highest ranges of distances. Therapsids have relatively even occupation of their full range, but the wide range in mammaliaforms is primarily driven by *Fruitafosser*, which has a unique, highly derived morphology that differs strongly from the mammal-like forms of the other mammaliamorphs.

Ulnar Procrustes distances show a pattern in which there is an increasing restriction of morphologies moving towards mammals, with a few noteworthy taxa providing individual exceptions. The groups that are the most phylogenetically distant from extant Mammalia have

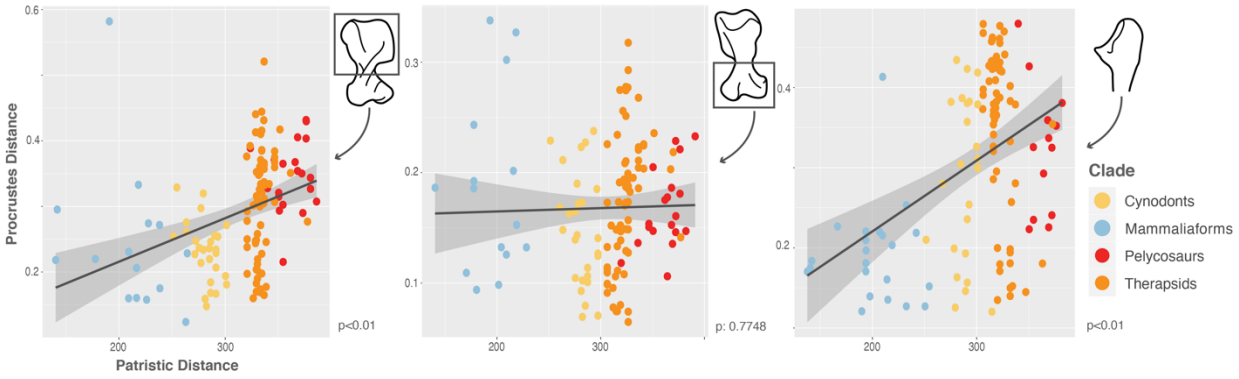

Figure 3.9 Procrustes distance versus patristic distance correlations - Linear regressions of Procrustes distance against patristic distance. Regressions are significant for the proximal humerus (left) and the proximal ulna (right). Shaded area represents 95% confidence interval. Range along the y-axis can be conceptualized as the disparity of shapes within the group. When compared to phylogenetic distance, instances can be observed where a fossil genus is more similar in shape to mammals than would be expected given its phylogenetic relatedness (Procrustes distance below the regression line) and vice versa.

the highest Procrustes distances on average, but therapsids and cynodonts include a mixture of both morphologically-disparate and mammal-like morphologies (Figure 3.9). Most of this disparity is lost in mammaliaforms, which are much more uniform in their possession of mammal-like shapes.

The correlations between Procrustes distances and patristic distance are consistent across the various correlation tests (Table 3.2). For distal humerus morphology, there is no correlation between patristic distance and Procrustes distance. This supports the interpretation of the morphospace plots in which there were no meaningful groupings or trends towards a mammalian morphology for the distal end. The proximal humerus shows a much stronger correlation than the distal end and is highly significant. The ulnar results are similar to the proximal humerus and are also highly significant.

Of the three functional areas, distal humerus Procrustes distance is the most similar between the groups. Indeed, the lowest value for Procrustes distance is actually for the outgroup,

providing more evidence that the group-specific differentiation of the distal end is not significant. In turn, this apparent conservatism supports the argument that distal humerus shape is unlikely to have strong ecomorphological or phylogenetic value. Of the fossil groups, cynodonts and mammaliaforms have lower values and therefore are closer to the mammalian mean shape than pelycosaurs and therapsids. Mammaliaforms and therapsids have the widest ranges of values, which is consistent with the overall larger volumes of morphospace occupied by the groups.

Proximal humerus and proximal ulna Procrustes distances conform to a more predictable phylogenetic pattern. The outgroup clade has the highest values and is thus the farthest away from mammalian morphospace on average (Table 3.1). Each subsequent group that is more closely related to crown Mammalia also expresses lower Procrustes values. For the proximal end as in the distal end, therapsids and mammaliaforms have the highest ranges. In the case of mammaliaforms, this range is mostly the result of a few divergent taxa such as *Fruitafossor.* For the ulna there is more disparity than in the humerus for all groups, with a notable contraction taking place in mammaliaforms. This implies a potentially rapid transition towards mammalian morphologies, with all mammaliaform ulnae being much more similar to mammals than would be expected given their phylogenetic distance (the exception being *Fruitafossor*, which is disproportionately dissimilar). For distal humeral morphology, there is no correlation between patristic distance and Procrustes distance (Table 3.2), reflecting the lack of meaningful groupings or trends towards a mammalian morphology in the PCA plots. The proximal humerus shows a much stronger correlation than the distal end (Table 3.2). This corroborates the observation that the closer a given taxon is to Mammalia phylogenetically, the closer it is on average in morphospace (Table 3.1).

3.5 DISCUSSION

It is tempting to view synapsid forelimb evolution as a simple trend towards increasingly mammal-like morphologies, particularly because discussions of the topic often focus on a relatively small number of exemplar taxa (Kemp 1980; 1982; Hopson 2015). However, the distribution of synapsid taxa in morphospace is more consistent with the major synapsid groups exploring particular regions of morphospace than with a continuous shift towards more mammal-like shapes. This finding is corroborated when morphological similarity to mammals, measured as Procrustes distance, is considered alongside the phylogenetic context of patristic distance. Although there is a significant correlation between Procrustes distance and patristic distance for the proximal humerus and ulna, consideration of the plots in Figure 3.9 reveals the complexity underlying this apparent trend. In both cases, the earliest synapsids (the pelycosaurs) are both morphologically disparate from mammals and relatively conservative in their morphology. With the origin of therapsids, morphological disparity expands both towards and away from more mammalian morphologies (expressed as an increase in the range of Procrustes distances). For the ulna, the high range of shapes is initially maintained early in cynodont history, but this disparity is culled in more crownwards cynodonts such that only relatively mammal-like shapes remain in these taxa and in mammaliaforms. For the proximal humerus this cut occurs earlier, with the cynodont-mammaliaform range of variation being established at the base of cynodonts. The pattern for the distal humerus is similar in having an initial increase in disparity going from pelycosaurs to therapsids but lacks the subsequent contraction towards more mammalian shapes. Therefore, instead of a simple trend towards more mammal-like forelimb shapes across synapsid

history, forelimb evolution may be better characterized as an initial diversification into a broad array of shapes that was then winnowed in subsequent radiations.

This pattern may also help to explain the pattern of phylogenetic signal in our data. Interpretation of phylogenetic signal is complex because a variety of evolutionary processes can result in high or low values (Revell, Harmon, and Collar 2008; Kamilar and Cooper 2013). However, stochastic peak shifts, in which stable selection is disrupted by occasional small to moderate shifts in fitness peak location, are known to produce values of Blomberg's K similar to our Kmult values (Revell, Harmon, and Collar 2008). Previous researchers have suggested that a number of significant shifts in the musculoskeletal organization of the forelimb occurred over the course of synapsid evolutionary history, typically locating these changes near the base of therapsids, cynodonts, and mammals (Romer 1922; Jenkins 1973; Jenkins and Weijs 1979; Kemp 2005). It is easy to see how such reorganizations could relocate any adaptive peaks, thus accounting for the low phylogenetic signal in some groups and the expansions and contractions of morphological disparity observed in our dataset. Further investigation of the functional disparity of these hypothesized grades of organization and the topographies of their adaptive landscapes is necessary to fully test this hypothesis.

3.5.1 Are Extant Synapsids Analogues for Fossil Synapsids?

In order for extant mammals to be considered appropriate analogs for fossil synapsids, fossil and extant species must overlap in morphospace in a relatively precise, ecologically- and functionally-structured way. Given the range of functions encapsulated by a complex structure like the forelimb, similar morphologies can arise from simple biomechanical pressures, such as increasing mechanical advantage across a joint, while not signaling an accurate similarity in

functional usage (see 3.5.2 *Functional Convergence versus Morphological Convergence* below). Therefore, not only must fossil and extant taxa overlap in morphospace, specific areas of morphospace must correspond to a narrow range of functional ecologies. The results of our analyses demonstrate that these assumptions break down when making comparisons between fossil non-mammalian synapsids and extant mammals.

For example, there is relatively little overlap in proximal humerus morphology between our fossil and extant taxa. Although each successive synapsid group more closely approaches mammal morphospace, even the mammaliaforms are located at the periphery of the core region occupied by extant mammals (Figure 3.5). Because of this, extant mammals are likely to be imprecise functional analogs for synapsid limb function in general, let alone for identifying specific functional ecologies. The opposite problem exists for the distal humerus, where the non-mammalian synapsid groups extensively overlap each other and extant mammals in morphospace. This pattern suggests that distal humerus function has been relatively conserved through synapsid history, and such conservatism implies that ecologically-specific morphotypes are less likely to repeatedly evolve. The ulna dataset shows perhaps the greatest promise for identifying specific ecological analogs given that select therapsids and cynodonts, and many mammaliaforms, fall well within the core of mammalian morphospace. However, the overall distribution of taxa suggests that the restriction of ulna morphologies to a consistently mammal-like form (and by extension function) was exclusive to mammaliaforms. Taken together, our results indicate that most eutherians are unlikely to be good functional and ecological analogues for non-mammalian synapsids, even for taxa that are closely related to mammals.

3.5.2 Functional Convergence Versus Morphological Convergence

Although the results of our analysis suggest that the extant mammals in our dataset have humeral and ulnar shapes that are very different from the majority of non-mammalian synapsids, there are some instances where ecomorphological convergence is evident. For example, fossorial eutherians have some of the lowest PC1 scores for mammals (Figure 3.10) and fossil synapsids for which we have a priori evidence for fossoriality (Nasterlack, Canoville, and Chinsamy 2012; Laaß 2015) also have low PC1 scores for their groups. The broad and square proximal humeri of the therapsid genera *Kawingasaurus* and *Cistecephalus*, and the mammaliaform *Fruitafossor* (Figure 3.10), resemble those of the lipotyphlan moles *Scalopus* and *Condylura*. Interestingly these fossil taxa also show considerable similarity to the mammalian genus *Tachyglossus*, which is the mammal with the lowest PC1 score in our dataset. *Tachyglossus* possesses a powerfully

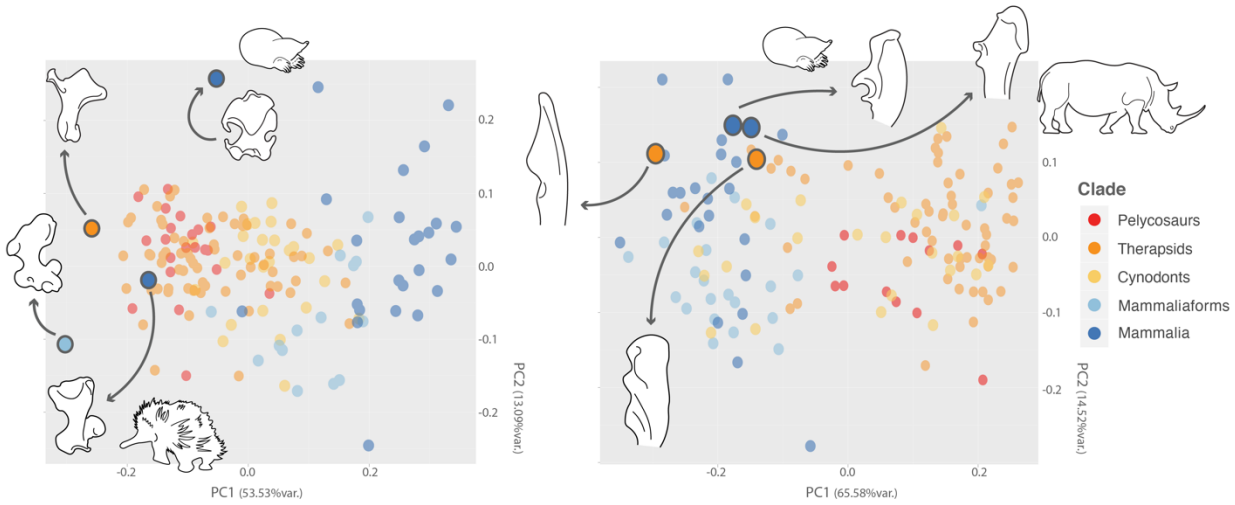

Figure 3.10 Examples of morphological and functional convergence - Plot of principal components 1 and 2 for the proximal humerus (left) and ulna (right) with highlighted examples of ecological convergence and shape convergence. For the proximal humerus, the fossil genera *Kawingasaurus* (therapsid) and Fruitafossor (mammaliaform) converge with the mammals *Tachyglossus* and *Scalopus* at the lower end of PC1, supporting the hypothesis that these taxa were powerful substrate movers. The ulna plot shows an example where shape is convergent despite incongruence in ecology. The burrowers *Scalopus* (Mammalia) and *Kawingasaurus* (Therapsida) group with the large terrestrial Rhinocerotidae (Mammalia) and *Ischigualastia* (Therapsida).

built shoulder girdle and forelimb utilized for digging as well as breaking open fallen logs and anthills when foraging for insects (Augee, Gooden, and Musser 2006; Jenkins 1970), raising the possibility of a similarly mixed functional ecology in cistecephalids and *Fruitafossor*. More broadly, *Tachyglossus* also has been suggested to share functional characteristics at the shoulder joint with pelycosaurs (Regnault and Pierce 2018) and its position within pelycosaur proximal humerus morphospace corroborates this hypothesis.

There are also cases where convergence in shape and some aspects of function do not reflect shared ecologies. For example, an elongate olecranon process of the ulna with a small, tightly defined semi-lunar notch is characteristic of large cursorial mammals and several large-bodied anomodonts such as *Lisowicia* and *Sinokannemeyeria* (Figure 3.10). However, because our analysis considers shape independent of size, animals like rhinos, hippos, and bison also group with burrowing mammals and the hypothesized burrowing therapsids. All of these animals are under strong selective pressure for highly muscular, tightly integrated articulations at the elbow that emphasize movement along a single plane to prevent joint dislocation, but for different ecological reasons (resisting strong forces associated with digging versus large body size). This results in a noteworthy similarity in morphometrically defined shapes, driven by the mechanics of the skeleton without ecological convergence and emphasizes the breakdown that can happen when attempting to reconstruct fossil ecology, on the basis of morphometrics alone. Though these structures follow predictable patterns of physical function, extending those to an organism's ecology can result in incorrect ecomorphological comparisons.

3.5.3 Diversity of Functional Solutions in Synapsida

Given the highly predictable ways in which shape changes in response to mechanical demands, we might assume that common selective pressures associated with a capacity for burrowing, running, or other highly derived locomotor ecologies will drive a similarity in morphological responses. However, this assumption fails to consider the way in which an organism's phylogenetic placement restricts the functional solutions available to it. The more distantly related two organisms are, the more difficult it will be for them to evolve precisely matching solutions to shared ecological pressures because their evolutionary starting points are likely to be morphologically disparate.

Our study supports this hypothesis because fossil synapsid groups occupy and explore mostly independent regions of morphospace (Figure 3.5). This implies that each of the main radiations derived its own solutions to functional problems, reflecting their different ancestral forelimb morphologies. For example, therapsids occupy a wide range of morphospace, including areas that are unexplored by other groups (e.g., ulna shape in Figure 3.8). As part of this diversification they arrived at functional solutions that do not have direct counterparts among extant mammals. The specialized digging dicynodont *Kawingasaurus* shows some similarities to modern diggers, but its combination of humeral and ulnar morphologies is unique and related to its derivation from a more generalized therapsid ancestor (Figures 3.5 and 3.10). Therefore, although some broad functional comparisons are possible (e.g., a large in-lever will be present when strength at the elbow is necessary), exact functional convergence between fossil synapsids and mammals should not be expected.

3.6 CONCLUSION

In this study, we investigated three complementary questions: (1) whether extant mammals are ecomorphological analogues for their fossil ancestors; (2) if there are examples of ecomorphological convergence among the various synapsid radiations; and (3) whether functional solutions are influenced by phylogenetic relatedness. We found that members of past synapsid radiations tend to occupy distinct areas of morphospace that are separated from modern mammals. The Mesozoic mammaliaforms tend to approach crown mammals most closely, but even there the similarity is imperfect. Therefore, modern mammals are unlikely to be accurate ecomorphological analogs for most non-mammalian synapsids. There is a limited degree of convergence associated with extreme ecologies such as burrowing, but the effects of physical constraints also lead to morphological convergence in ecologically disparate taxa. Moreover, the functional solutions arrived at by the different radiations reflected their particular ancestral morphologies. This work counters the narrative of synapsid forelimb evolution as a linear progression towards more mammalian morphologies. Instead, an initial wide diversification of humerus and ulna shapes subsequently contracted towards mammal-like shapes to varying degrees.

CHAPTER 4 MAJOR TRANSITIONS AND MOSAIC EVOLUTION OF THE SYNAPSID FORELIMB

4.1 ABSTRACT

The synapsid pectoral girdle and forelimb have undergone dramatic change across their evolutionary histories that went hand-in-hand with increasing morphological variance and ecological diversification. Many hypotheses have been posited surrounding the timing, placement, and importance of these changes. Importantly, these have historically been built within a framework of single exemplar taxa often used as proxies for much larger diverse groups of animals. Without both a large quantitative dataset and a foundational phylogeny, rigorous testing of the accuracy of these hypotheses has not been fully possible. Relying on the robust phylogenies developed in recent decades for various synapsid clades I have built a dataset upon which these questions can be rigorously tested, as well as suggested a novel breakdown of synapsid evolutionary history comprised of five paraphyletic radiations. I tested two macroevolutionary metrics: phylogenetic signal and rate of phenotypic change (evolutionary rate). I hypothesize that the increasing lability of the system would result in sequential increases in evolutionary rate as the forelimb is given increasing opportunity to evolve novel forms. Using the metrics of phylogenetic signal and phenotypic rate change in conjunction with one another, I compare and contrast synapsid forelimb evolution in variously historically hypothesized ways. When considered together, these metrics can signal the presence of previously hypothesized morpho-functional transitions and provide a framework to interrogate these historically held expectations for synapsid forelimb change.

4.2 INTRODUCTION

The forelimb morphology of therian mammals is unique within the synapsid lineage and is the result of a major reorganization of the ancestral form over the course of 300 million years of evolutionary history (Kemp 1982; 2005; Hopson and Barghusen 1986; Angielczyk and Kammerer 2018). The first major radiation of Synapsida, the Pennsylvanian and Permian 'pelycosaur-grade' synapsids represent the primitive morphological condition for the clade. The pelycosaur forelimb is characterized by a massively built scapulocoracoid that includes a highly distinctive glenoid articulation for the forelimb (Figure 4.1). Described as "screw-shaped", the glenoid is hypothesized to have necessitated a sprawling posture with lateral undulation during locomotion and limited the range of locomotor capabilities of these earliest synapsids (Jenkins

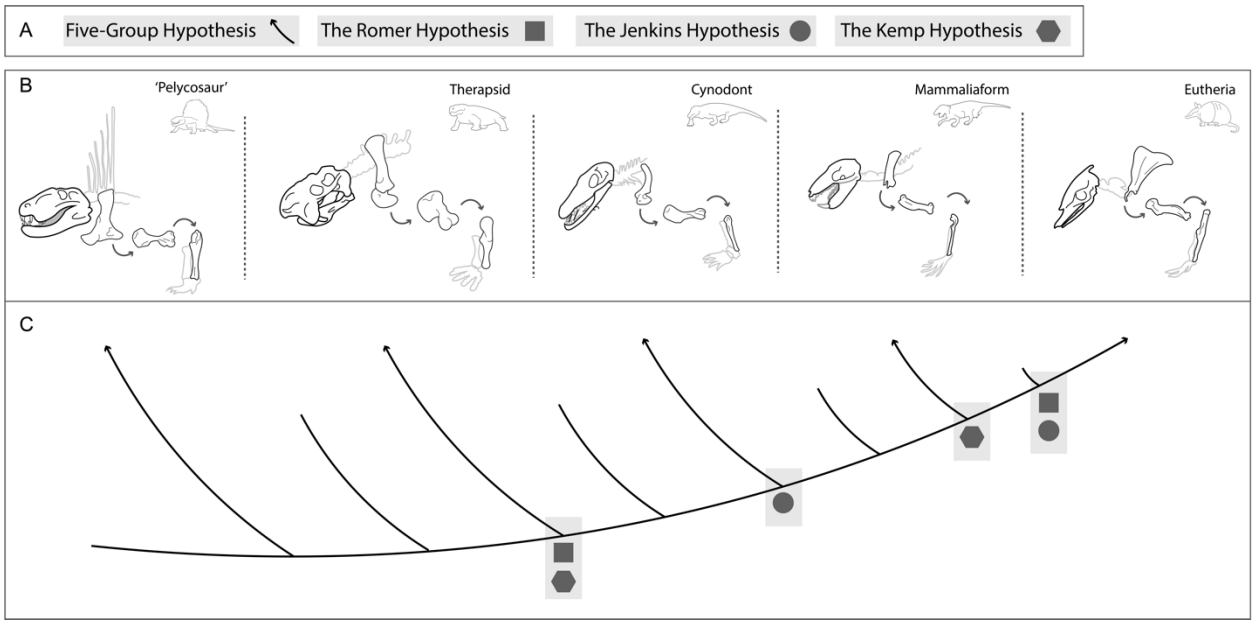

Figure 4.1 Study groups and historical perspectives on morpho-functional transitions - Breakdown of the four hypotheses under consideration in this study. A) Symbols relating to each hypothesis. B) The five considered paraphyletic clades that are part of the 'Five-Group Hypothesis', showing configuration of the elements in question. Arrows show points of articulation between the pectoral girdle, the humerus, and the ulna. C) Cladogram showing the placement of each above group, with change in symbol placement representing positioning of hypothesized morpho-functional transitions.

1971b; Hopson 2015). This is in stark contrast to the forelimb of extant therian mammals, which not only present a dramatic reduction in the number of bones that comprise the pectoral girdle, but also the development of a ball-and-socket glenoid articulation and a reduced connectivity of the system. The therian shoulder relies heavily on connective tissues to maintain articulation during locomotion with the scapular blade nested inside what is often termed a muscular-sling. This is in strong contrast to the plesiomorphic condition of early synapsids, in which shoulder articulation relied much more heavily on direct skeletal connections that in turn constrained the overall range of motion in the upper limb. The overall mobility of the mammalian shoulder has been argued to be a biomechanical innovation that facilitated the evolution of the highly diverse and specialized locomotor ecologies of Mammalia (Jenkins and Weijs 1979; Jenkins 1974; Sereno 2006), and therefore represents a critical aspect of the synapsid evolutionary story.

Comparison of the pelycosaur and therian morphotypes highlights the dramatic morphological changes that took place in the synapsid forelimb, and multiple hypotheses on the pacing of these major transformations have been proposed. Specifically, consideration of when - phylogenetically and temporally - major transitions in the synapsid forelimb occurred has been of long-standing interest (Romer 1922; Jenkins 1970; Kemp 1982), and the detailed fossil record of Synapsida has provided ample material upon which to consider and critique the proposed macroevolutionary changes. Despite the transition from the sprawling posture of the first synapsids to the fully upright posture of extant synapsids (especially Theria) being a exemplary evolutionary transition, little quantitative work has been done that incorporates the full diversity and morphological disparity of fossil synapsids in a way that allows for macroevolutionary comparison in a phylogenetic context. Here I focus on the morphology of two forelimb elements – the humerus and the ulna – to interrogate the key role these elements played in the broader

evolutionary changes of posture, morphometric disparity, and ecological diversification in synapsid evolutionary history.

4.2.1 Perspectives on Synapsid Forelimb Evolution

Historical hypotheses about the phases of synapsid forelimb evolution are based on functional interpretations of changes in the forelimb and pectoral girdle (e.g., Romer 1922; Jenkins 1970; Kemp 1982). These hypotheses attempted to pinpoint critical moments of change along the evolutionary trajectory to the therian forelimb by comparing forelimb morphology and function in a small number of exemplar taxa that were assumed to be representative of broad functional grades of organization (Kammerer 2014). Within these taxa, differences in robustness of the limb elements, rigidity of the glenoid articulation, and overall stance of the pectoral limb played large roles in delineating hypothesized moments of innovation in synapsid forelimb evolution. One of the earliest considerations of synapsid forelimb reorganization was by Romer (the 'Romer Hypothesis')(Romer 1922), who proposed two major evolutionary transitions, the first at the base of Therapsida, and the second at the base of crown-Mammalia (Figure 4.1C). Within this framing there are three major synapsid forelimb morpho-functional types: (1) the basal pelycosaur morphology of robust and highly sprawling forelimbs (Figure 4.1A); (2) the early therapsid and cynodont morphology, where the pectoral girdle still maintains its plesiomorphic composition and connectedness, but the reduction of size has allowed the evolution of a more gracile system and a different joint apparatus; and (3) the further reduced and highly mobile shoulders of therian mammals (Figure 4.1), with the early diverging members of Monotremata representing the primitive condition from which mammals, the living therians, their near phylogenetic, relatives evolved.

A second hypothesis on the placement of these transitions was developed by Jenkins (the 'Jenkins Hypothesis')(Jenkins 1971a; 1973). Under this model, there are still two major transitions, but the first one takes place at the base of Cynodontia (Figure 4.1C), and the second takes place within crown Mammalia, effectively excluding Monotremata and several groups of mammaliaforms from the third morphotype. In contrast to Romer, Jenkins argued that the first (1) forelimb morphotype is represented by both pelycosaurs and early therapsids, with (2) cynodonts and the earliest diverging mammals (now known as mammaliaforms) representing the second morphotype, and the final (3) transition being to a full therian morphotype in crown mammals, after the divergence of monotremes.

A third historic hypothesis on synapsid forelimb transitions was developed by Kemp (the 'Kemp Hypothesis')(Kemp 1982) and was more congruent with Romer's original thoughts than with Jenkins'. Here, the first transition (1) is placed at the base of therapsids, suggesting a pelycosaur morphotype that is separate from the rest of Synapsida (Figure 4.1C). This contrasts with Jenkins' interpretation that pelycosaurs and the more primitive therapsids had similar shoulder girdle and forelimb structures. The pelycosaur-therapsid transition is followed by a second transition at the origin of Eucynodontia, thus splitting the rest of Synapsida into a (2) Permian therapsid and early cynodontian morphotype, and (3) a true Eucynodontian morphology that includes the rest of synapsid evolutionary lineage.

Underlying these three major hypotheses are differences in opinion on what constitutes a critical change in the overall organization of the synapsid pectoral girdle and forelimb. In the absence of modern phylogenetic comparative methods for quantitative analysis of shape and functional disparity in a large number of taxa, a small number of taxa were considered in detail and used to summarize the hypothetical evolutionary transitions to mammals. In these historical

studies (e.g., Romer 1922; Jenkins 1970), differences in joint surfaces, such as size and shape of the glenoid articulation, were the key characters for categorizing these major transitions because the joint was interpreted to have a major functional role in posture and range of motion (Romer 1922; Colbert 1948; Sues 1986; Hopson 2015). Considering this, much discussion has centered on how the glenoid joint affected locomotion, and how that may have constrained or facilitated functional and ecological diversification at different points along the synapsid lineage. However, a considerable moprhological disparity exists within each of the historically-hypothesized functional grades, and now it is feasible to quantify this disparity. My detailed consideration of this disparity can now provide a test of the effectiveness of the historical hypotheses at characterizing overall patterns of synapsid forelimb evolution.

In my previous work, I have categorized Synapsida in a way that better emphasizes its remarkable disparity and have sought a classification scheme that provides a more biologically meaningful lens through which to consider forelimb evolution. Synapsid history can be characterized as a series of successive radiations leading up to extant Mammalia. This perspective of Synapsida as a sequence of radiations is different from the historical perspectives on the forelimb that rely much more heavily on a functionally-based groupings. My characterization of the diversification of forelimb is more consistent with current understanding of macroevolutionary patterns of synapsids as a whole (Angielczyk and Kammerer 2018). Relying on the robust phylogenies developed in recent decades for various synapsid clades (Benson 2012; Liu and Abdala 2014; Brocklehurst et al. 2016; Huttenlocker and Sidor 2016; Kammerer 2019; Kammerer and Masyutin 2018; Huttenlocker et al. 2018), I have described Synapsida as being comprised of five paraphyletic radiations: (1) the Pennsylvanian and early Permian “pelycosaur”-grade synapsids (hereafter pelycosaurs), (2) the middle Permian through

Triassic non-cynodont therapsids (therapsids), (3) non-mammaliamorph members of Cynodontia (cynodonts), (4) mammaliaforms, here defined as all extinct taxa from the base of Mammaliamorpha to the base of crown Eutheria, and (5) extant representatives of Mammalia. This novel framework for considering forelimb evolution is hereafter referred to as the 'Five-Group Hypothesis', and it provides a more phylogenetically-focused alternative to the historical functional hypotheses based on exemplary taxa.

4.2.2 Phylogenetic Signal and Evolutionary Rate

In this study, I use phylogenetic comparative methods to test for changes in macroevolutionary dynamics in synapsid forelimb evolution. Specifically, this study uses a multivariate version of Blomberg's K (K_{mult}; (Adams 2014)) to quantify phylogenetic signal across a composite phylogeny in the context of the four hypothetical frameworks: the Five-Group Hypothesis (Figure 4.1), the Romer Hypothesis (Romer 1922), the Jenkins Hypothesis (Jenkins 1970), and the Kemp Hypothesis (Kemp 1982). The expectation is that the anatomical

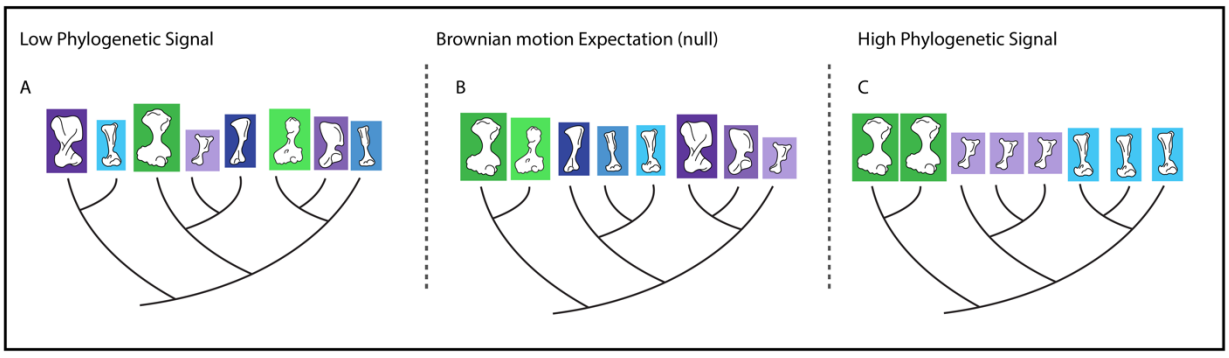

Figure 4.2 Hypotheses of phylogenetic signal - Visualization of the theoretical scenarios described. Low phylogenetic signal (A) in which taxa resemble one another less than would be anticipated given their relatedness. High phylogenetic signal (C), in which taxa resemble each other more than would be expected given their relatedness. The null expectation is Brownian motion (B), in which resemblance between taxa is proportional to time since their divergence.

and functional changes represented by these transitions will alter the macroevolutionary dynamics of the synapsid forelimb, resulting in different levels of phylogenetic signal (measured by K_{mult}) in taxa before and after the functional shifts (Figure 4.2). K_{mult} is particularly suited for comparing across datasets because the metric is a proportion, grounded on a Brownian motion expectation of divergence (Figure 4.2B). K values close to 1 represent the Brownian motion expectation, specifically that organisms are as similar as would be expected given their phylogenetic relatedness (Figure 4.2B)(Revell 2010; Revell, Harmon, and Collar 2008). Values lower than one mean that organisms are less similar than would be expected, and conversely values above one suggest an excess of similarity given relatedness.

Changes in phylogenetic signal can imply important macroevolutionary patterns, similar to metrics like morphological disparity (Chapter 2)(Hughes, Gerber, and Wills 2013; Slater 2013; Slater and Harmon 2013; Hopkins and Smith 2015). One way to conceptualize phylogenetic signal as it relates to geometric morphometric data is through the consistency of shape based on phylogeny. For example, if organisms are diversifying under a Brownian motion model, more closely related animals will be more morphologically similar and more distantly related ones less so, in proportion to how recently the organisms diverged from one another. Low phylogenetic signal indicates that an organism's morphologies may not be a reliable indicator of the organism's placement on a tree, for example as a result of extensive convergent evolution (Figure 4.2A). The exact opposite is true for very high phylogenetic signal, where most of morphological variation occurs between major clades, but morphology is conserved w these major clades (Figure 4.2C). Here, high similarity in shape might indicate a potential constraint on ability of the taxa within a major clade to diverge from each other, or a very recent divergence event. Given these and other scenarios (e.g. Revell et al. 2008), abrupt changes in phylogenetic

signal associated with the hypothesized functional transitions in synapsid forelimbs can inform us about whether and how the functional transitions influenced diversification dynamics in the clade. This is particularly important because expansions in morphological and ecological diversity are thought to coincide with the hypothesized transitions between major synapsid morpho-functional types in the historical studies (Romer 1922; Jenkins 1970; Kemp 1982).

Critically, however, processes like diversification or constraint can be manifested in a system in multiple ways, necessitating a combination of metrics to narrow down the number of possibilities. Constraint is of particular interest here because historical studies of the synapsid forelimbs argued that it likely played a role in synapsid evolutionary history. Namely, the loss of constraint through time has been thought to characterize major transformations along the synapsid lineage and throughout the synapsid body plan, even though this has not often been explicitly tested in the work of the authors considered here. Work by Revell et al. (Revell, Harmon, and Collar 2008) has shown that, for example, the strength of a process such as stabilizing selection can influence phylogenetic signal, with strong selection creating low phylogenetic signal due to a lack of structure in the variance across groups. Further, in the case of constraint being caused by a bounded-morphospace scenario, they observed that phylogenetic signal was high when evolutionary rates were low, but signal decreased as evolutionary rate increased. Importantly, as rate increased, signal was observed to decrease as well, and it changed the way constraint was manifested in the system.

Considering this, the expectation is that I will observe an evolutionary rate and phylogenetic signal combination that is consistent with constraint early in synapsid history (Table 4.1). As synapsids evolve, the metric combination will transition away from one typical of constraint and potentially towards a combination that typifies Brownian motion or

convergence, for example. This scenario most closely matches the historical perspective of synapsid forelimb evolutionary history, wherein the morphology of the pectoral girdle and upper limb placed physical limitations on the evolvability of the forelimb. The earliest synapsids, the pelycosaurs, had the most extreme limitations with a more limited range of motion. Their tightly articulated joints and heavily sprawling posture preventing the evolution of highly derived locomotor modes or ecological diversity. As described above, through evolutionary time the synapsid upper body becomes observationally more gracile, and there is both an overall increase in the amount of morphospace occupied (Chapter 2) and an increase in the number of advanced ecologies present (Chapter 3). Considering all of this, I expect that the metrics of evolutionary rate and phylogenetic signal will change in correspondence to decreasing constraint through time, or to the breakdown of a constraint of the bounded-morphospace style, across each of the major transitions in synapsid evolutionary.

Given how K_{mult} is measured, an additional aspect of this metric is the way it describes how morphological variance is partitioned within groups versus between them. One thing a high K value implies is that with each divergence event organisms move away from their previous relatives in morphospace, and this creates a partitioning of variance. $K < 1$ corresponds to variance being within clades and $K > 1$ corresponding to variance being spread amongst or between the clades. As such, for trees with K values above 1.0, the diversity would be concentrated on monophyletic clades, with each clade having its unique diversity pattern, but not like its sister clades (Figure 4.2B). Considering this, K_{mult} can characterize interesting aspects of how clades are diversifying, such as whether changes are focused amongst closely related organisms or spread largely between them.

As new morpho-functional types evolve, I hypothesize that overall constraint on the system breaks down and this can coincide with the large morphological changes taking place. I hypothesize that the increasing lability of the system through time (culminating in Mammalia) will result in sequential increases in evolutionary rate as the forelimb is given increasing opportunity to evolve novel forms. Given expectations on how phylogenetic signal is spread amongst or between groups, the consideration of rate in combination with phylogenetic signal helps in identifying plausible evolutionary scenarios (Table 4.1), and may also help address the question of whether particular group partitions deserve to be considered inflections points in synapsid limb evolution. Using the metrics of phylogenetic signal and phenotypic rate change, I compare and contrast functional hypotheses in the context of phylogeny to investigate whether the hypothesized functional shifts results in changes in diversification dynamics.

Table 4.1- Example outcomes of combined phylogenetic signal and evolutionary rate patterns, with of focus on those hypothesized to be primarily occurring across synapsid evolutionary history

Level of phylogenetic signal	Rate of phenotypic change	Type of change in values	Potential evolutionary process
<1.0	Low	Constant	Constraint
	High	Increasing	Release from constraint
<1.0	High	Constant	Convergence
		Decreasing	Constraint
1.0	Low	Constant	Brownian motion
>1.0	Low	Increasing	Constraint
>1.0	High	Constant	Radiation

4.3 METHODS

4.3.1 Taxonomic Sample and Geometric Morphometrics

Overall taxonomic sample and geometric morphometric methodology are identical to that of Chapter 3. In brief, I conducted geometric morphometric analyses on proximal and distal humeri and proximal ulnae. The taxonomic sample is comprised of extinct synapsids starting in the Carboniferous (~320 mya) and continuing to the end of the Cretaceous (66 mya). Additionally, a selection of extant mammals, primarily Eutherians but including the monotreme taxa *Tachyglossus*, was sampled to represent extant Mammalia (full taxonomic breakdown in Appendix III). In total, the sample includes 1,870 individual specimens representing 218 genera.

I processed the coordinate data and conducted geometric morphometric analyses with the Geomorph R package (Adams et al. 2016). The analysis utilized mean shapes for each genus. I averaged all specimen shapes for a given genus using the function 'mshape' in Geomorph, which uses the previously aligned coordinates to estimate a mean shape. For singletons, the single specimen itself represented the mean shape of that genus. I subjected the set of genus means to an additional general Procrustes alignment for all subsequent statistical analyses.

4.3.2 Phylogenetic Trees

I analyzed each functional unit (proximal humerus, distal humerus, proximal ulna) in a phylogenetic framework. I constructed a composite phylogeny for each functional unit that encompassed the unit's taxonomic sample. Because there is no single phylogeny that includes all of the taxa present in this study, the composite trees are based on published phylogenetic analyses (Luo, Kielan-Jaworowska, and Cifelli 2002; Bonaparte 2008; Kammerer et al. 2008;

Gaetano and Rougier 2011; Kammerer 2011; Archibald and Averianov 2006; Liu and Abdala 2014; Q.-J. Meng et al. 2015; Martinelli, Soares, and Schwanke 2016; Angielczyk, Hancox, and Nabavizadeh 2017; Kammerer and Masyutin 2018; Grunert, Brocklehurst, and Fröbisch 2019; Rodrigues et al. 2019; Huttenlocker et al. 2018; Abdala et al. 2019; Müller and Reisz 2006; Angielczyk and Kammerer 2017). First taxa and last taxa defining the beginnings and ends of groupings for phylogenetic analyses can be viewed in Table 4.2 and Table 4.3. I scaled the time trees using first and last occurrence dates from the Paleobiology Database and the Claddis package in R (Lloyd 2015). Divergence dates for extant taxa were based on (Upham, Esselstyn, and Jetz 2019) with last occurrence dates set to zero to represent the present. I subdivided the full tree for each functional unit into sub-trees consistent with each of the four hypotheses being tested (Figure 4.1). This created five sub-trees for the Five-clade Hypothesis, and three different sub-trees for the three historical hypotheses. Analyses were run both upon the full trees for each functional unit, and the hypothesis-specific sub-trees.

As discussed in Chapter 3, no single cladistic analysis has been attempted that includes all genera in this sample. Because of this, the composite tree inherently varies in its statistical support between groups and across analyses. Further, some phylogenetic trees that were used came from publications that pre-date matrix-based cladistic analyses, and therefore do not have associated support values at nodes or taxa of interest. All of this was considered during construction of the composite tree with the focus being to include only the most consistently resolved relationships. It is worth noting that the overall topology of the synapsid phylogeny, as it relates to the placement of the five major radiations of the Five Group Hypothesis, for example, has been shown to be incredibly stable through many different phylogenetic analyses over the last few decades. Variability exists in recovered relationships and branch support within

the major clades but not nearly as much between them. Given this, overall support for genus-level branch positions varies heavily but is currently unavoidable. The composite tree used for these analyses is based on recent references (above) that reflect the current thinking on synapsid phylogenetics.

Table 4.2 – First taxa and last taxa delimitating each functional group for the three historical hypotheses. For details on full group representation, compare this table to Figures 3.2-3.4.

Functional Unit	First taxon/ Last taxon	First taxon/ Last taxon	First taxon/ Last taxon
Proximal	Group 1	Group 2	Group 3
Romer Hypothesis	*Trichasuaurs/ Dimetrodon*	*Hipposaurus/ Maiopatagium*	*Tachyglossus/ Conepatus*
Jenkins Hypothesis	*Trichasaurus/ Bauriidae*	*Abdalodon/ Fruitafossor*	*Gobiconodon/ Conepatus*
Kemp Hypothesis	*Trichasauru/ Dimetrodons*	*Hipposaurus/ Thrinaxodon*	*Cynognathus/ Conepatus*
Distal			
Romer Hyp.	*Trichasaurus/ Dimetrodon*	*Hipposaurus/ Maiopatagium*	*Tachyglossus/ Conepatus*
Jenkins Hyp.	*Trichasaurus/ Ictidodraco*	*Prochynosuchus/ Fruitafossor*	*Liaoconodon/ Conepatus*
Kemp Hyp.	*Trichasaurus/ Dimetrodon*	*Hipposaurus/ Platycraniellus*	*Cynognathus/ Conepatus*
Ulna			
Romer Hyp.	*Trichasaurus/ Dimetrodon*	*Hipposaurus/ Maiopatagium*	*Tachyglossus/ Conepatus*
Jenkins Hyp.	*Trichasaurus/ Ictidodraco*	*Procynosuchus/ Fruitafossor*	*Gobiconodon/ Conepatus*
Kemp Hyp.	*Trichasaurus/ Dimetrodon*	*Hipposaurus/ Thrinaxodon*	*Cynognathus/ Conepatus*

Table 4.3 First taxa and last taxa that define the synapsid radiation for the Five Group Hypothesis. For full group representation, compare this table to Figures 3.2-3.4 or view the taxonomic designations of each sampled genus in Appendices D – F.

Functional Unit	First taxon/ Last taxon	First taxon/ Last taxon	First taxon/ Last taxon	First taxon/ Last taxon	First taxon/ Last taxon
Five Group Hypothesis	Group 1	Group 2	Group 3	Group 4	Group 5
Proximal	*Trichasaurus/ Dimetrodon*	*Hipposaurus/ Buariidae*	*Abdalodon/ Brasilodon*	*Morganucodon/ Vincelestes*	*Tachyglossus/ Conepauts*
Distal	*Trichasaurus/ Dimetrodon*	*Hipposaurus/ Ictidodraco*	*Procynosuchus/ Brasilodon*	*Megazostrodon/ Vincelestes*	*Tachyglossus/ Conepatus*
Ulna	*Trichasaurus/ Dimetrodon*	*Hipposaurus/ Ictidodraco*	*Procynosuchus/ Brasilodon*	*Erythrotherium/ Ukhaatherium*	*Tachyglossus/ Conepauts*

4.3.3 Phylogenetic Signal

Phylogenetic signal was measured as the 'K_{mult}' statistic of (Adams, 2014). K_{mult} is an adaptation of 'Blomberg's K' (Blomberg, Garland Jr, and Ives 2003) that is suitable for highly multivariate data, such as geometric morphometric analyses. As with Bloomberg's K, K_{mult} is centered on a value of 1.0, with $K_{mult} < 1$ implying that taxa are less similar than expected by Brownian motion (low phylogenetic signal). $K_{mult} > 1$ suggests a higher phylogenetic signal, where specimens are more similar than would be expected by Brownian motion. Phylogenetic signal was calculated for all groups and the full trees using the Geomorph package (Adams et al. 2016) in R.

4.3.4 Evolutionary Rate

Tests of evolutionary rate were conducted directly upon the aligned geometric morphometric data, and utilized the compare.evol.rates function from the Geomorph package in R (Adams et al. 2016). This distance-based metric calculates the accumulation of variance along the branches of the phylogenetic tree, with the expected variation of the geometric morphometric data estimated under a Brownian Motion model of evolution. The rate metric is expressed as the ratio between the observed value and the expected Brownian motion value. Rate was calculated for each individual genus, with group level or clade level rates being determined through analysis of the genus-level data. Each group-specific evolutionary rate was then compared through pairwise t-testing to check for significant differences between groups, as defined for each of the four hypotheses.

4.4 RESULTS

All results can be viewed in Table 4.4 and are visualized in Figures 4.4 - 4.6.

Table 4.4 - Observed values of K_{mult} (phylogenetic signal) and group-average rates of phenotypic change (evolutionary rate) for each of the four hypotheses, further subdivided by group.

	Five-Group Hypothesis				Romer		Jenkins		Kemp	
Functional Unit		K_{mult}	Avg. rate	**Group**	K_{mult}	Avg. Rate	K_{mult}	Avg. Rate	K_{mult}	Avg. Rate
Proximal Humerus	Pelycosaurs	0.5418	1.42e-5							
	Therapsids	0.6401	1.66e-5	**1**	0.5418	1.31e-5	0.5348	1.67e-5	0.5418	1.31e-5
	Cynodonts	0.6822	1.37e-5	**2**	0.5928	1.67e-5	0.6003	1.45e-5	0.6453	1.75e-5
	Mammaliaforms	0.4371	3.27e-5	**3**	0.9292	1.93e-5	0.7506	1.93e-5	0.4383	1.73e-5
	Mammals	0.8845	1.2e-5							
Distal Humerus	Pelycosaurs	0.6442	6.92e-6							
	Therapsids	0.671	9.80e-6	**1**	0.6442	5.79e-6	0.3036	9.54e-6	0.6442	5.79e-6
	Cynodonts	0.6218	7.72e-6	**2**	0.5688	9.98e-6	0.4429	8.72e-6	0.6631	1.04e-5
	Mammaliaforms	0.521	1.46e-5	**3**	0.6415	7.74e-6	0.2643	7.74e-6	0.3264	8.06e-6
	Mammals	1.0226	5.72e-6							
Ulna	Pelycosaurs	0.8795	1.35e-5							
	Therapsids	0.6901	2.00e-5	**1**	0.8795	7.47e-6	0.484	1.94e-5	0.8795	7.47e-6
	Cynodonts	0.9222	1.69e-5	**2**	0.6388	2.27e-6	0.6484	2.45e-5	0.6841	2.21e-5
	Mammaliaforms	0.2932	2.57e-5	**3**	0.4684	1.22e-6	0.4882	1.18e-5	0.5381	1.68e-5
	Mammals	0.6678	1.08e-5							

4.4.1 Phylogenetic and Morpho-functional Hypotheses

Proximal humerus

Five-Group Hypothesis - K_{mult} values vary considerably from group to group. K_{mult} is highest in mammals, suggesting a shift towards among clade variation in mammals compared to the fossil groups. Mammaliaforms have the lowest K_{mult} values, followed by therapsids and cynodonts. From the base of the phylogeny at pelycosaurs, building up towards mammals, phylogenetic signal increases incrementally at each group transition, with the exception of at mammaliaforms.

Romer Hypothesis - K_{mult} is very close to 1.0 for the third group, which includes all crown mammals. The other two groups have K_{mult} values substantially lower than the third group, and K_{mult} values increase across the tree.

Jenkins Hypothesis - K_{mult} values for crown mammals are the same as that of the Romer Hypothesis (reflecting the fact that the membership of this group is the same as in Romer's

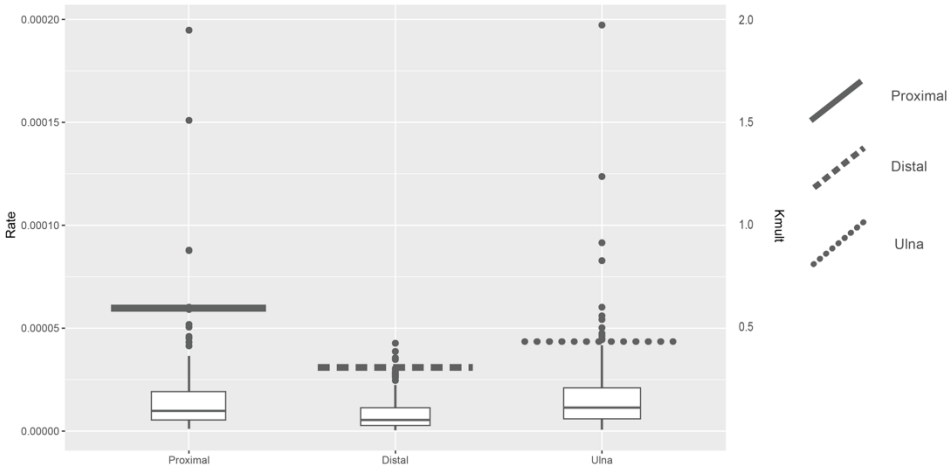

Figure 4.3 Evolutionary rates and phylogenetic signal for all functional units - Phenotypic rate change (left Y axis) and phylogenetic signal (K_{mult}, right Y axis) broken down by functional unit measured across the entire phylogeny of each unit. Rate is represented by the boxplots, which was measured for each individual genus (dots). Solid horizontal lines represent the observed K_{mult} value.

hypothesis), but the phylogenetic signal for group 2 is higher and group 1 is lower, likely due to the inclusion of therapsids (which have low K_{mult} values) in the first morphotype. Overall, there is a pattern of increasing phylogenetic signal with each subsequent group, suggesting increasing signal through time in this phylogenetic framework. This further suggests a transition in variance partitioning, wherein in there is more between group variation, than within group variation.

Kemp Hypothesis - K_{mult} is midrange and varies less between the groups. The highest K_{mult} values are in the second group, represented by Permian therapsids and pre-eucynodontian cynodonts, whereas the most crownward part of the tree (group 3) has the lowest K_{mult} values.

Distal humerus

Five-Group Hypothesis - K_{mult} values are higher on average than for the proximal humerus. This counter-intuitive result suggests that when considered within a given sub-group, placement on the tree is in fact more predictive of shape, and it is only within the context of total synapsid phylogenetic history that K_{mult} is low. The mammalian sample, specifically, has the highest value with K_{mult} above 1.

Romer Hypothesis – All K_{mult} values are less than one. The values of group 1 and group 3 are almost identical, with group 2 having a slightly lower value.

Jenkins Hypothesis – K_{mult} values are the lowest on average for this hypothesis. In contrast to the Romer Hypothesis, group 2 has the highest K_{mult} value in the Jenkins Hypothesis. Further, a reduction in K values are observed with group 3, which is represented just by Mammalia here. This runs counter to some of the other findings in which Mammalia has stronger phylogenetic

signal and more variation is concentrated between major groups (i.e. between Mammalia and Mammaliaforms) than within the groups.

Kemp Hypothesis - All K_{mult} values are less than one. Both group 1 and 2 have higher values, with a dramatic drop in K_{mult} occurring in group 3, which in this hypothesis includes mammaliaforms and mammals.

Ulna

Five Group Hypothesis - Mammaliaforms have the lowest values, with cynodonts having the highest. This, thus, represents a potentially important change, where overall phylogenetic signal is switching at the transition to a mammaliaform morphology.

Romer Hypothesis – All K_{mult} values are less than 1. Phylogenetic signal is highest in the earliest group and decreases in a step-wise pattern through time, being lowest in group.

Jenkins Hypothesis - All K_{mult} values are less than 1. Group 1 has a lower K value than in the other hypotheses, most likely caused by the inclusion of therapsids in group 1, unlike in the other two hypotheses.

Kemp Hypothesis - All K_{mult} values are less than 1. Phylogenetic signal is highest in the earliest group and decreases through time. The similarity of the Romer Hypothesis and the Kemp Hypothesis is being driven by the very low phylogenetic signal of mammaliaforms, whose placement is the only thing the Romer Hypothesis and the Kemp Hypothesis differ on. Because of their low signal, moving mammaliaforms from group 2 to group 3, or vice versa, has almost no effect on the group's overall K_{mult} value.

4.4.2 Evolutionary Rate Results for the Morpho-functional Hypotheses

Proximal humerus - There is no consistent trend in the fluctuation of group rate for the Five Group hypothesis. Rate is highest in mammaliaforms, and the transition from cynodont rate to mammaliaform rate is statistically significant ($p = 0.03$). This is also the case for the transition from mammaliaforms to mammals ($p = 0.04$), both cases showing that a meaningful increase and decrease in average rate occurred in mammaliaforms and mammals, respectively. The genera with the highest rates represent highly derived and unique taxa that would have undergone dramatic phenotypic change from their group's ancestral form. Specifically, *Fruitafossor* (mammaliaforms) (0.00019) has the highest rate of change in the proximal morphology, followed by the therapsid genus *Biarmosuchus* (0.00015). As for the historical hypotheses, none of the transitions in rate from group to group are statistically significant. This seems to be driven by the lower rates on average within each group, with the only large increases in rate being

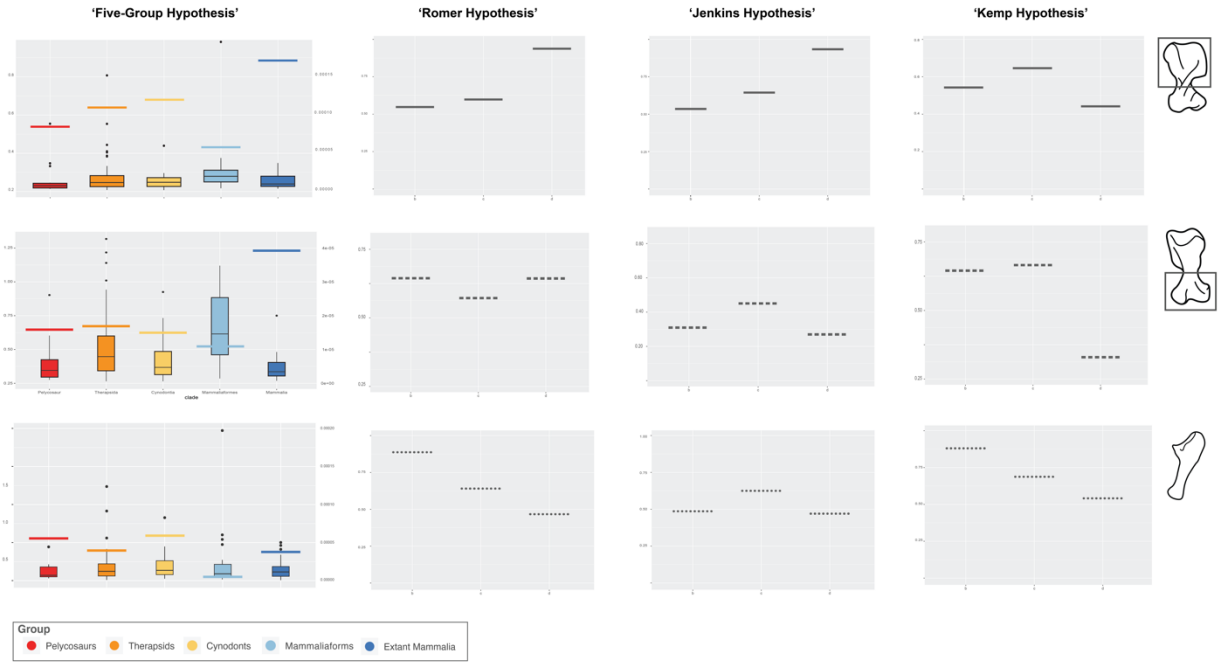

Figure 4.4 K_{mult} statistic for functional groups under all grouping hypotheses - Phylogenetic signal (horizontal lines) and evolutionary rates (box and whiskers) for The Five-Group Hypothesis, with colors by clade. K_{mult} values for the three main historical hypotheses.

driven, again, by individual highly derived taxa within the groups. However, these genera represent exceptions, and otherwise evolutionary rate does not appear to be changing much between phylogenetic groups as they are defined by the historical hypotheses.

Distal humerus - Evolutionary rate is more variable from group to group in distal morphology, although the magnitude of the rates is lower on average than for the proximal humerus. Mammaliaforms have the highest overall rate, but therapsids have the highest individual generic rates, which belong to members of the therapsid clade Therocephalia (*Cynariognathus*: 4.27e-5; *Ptomalestes*: 3.87e-5). The distal humerus also has more statistically significant fluctuations. The transition from pelycosaurs to therapsids is significant ($p = 0.015$), as is the transition from cynodonts to mammaliaforms ($p = 0.018$), and mammaliaforms to mammals ($p = 0.001$). However, it is important to note the difference in scale between the three functional units. The distal humerus as a whole has the lowest evolutionary rates of the three functional units, being an order of magnitude lower than the proximal rate and the ulnar rate.

The Jenkins Hypothesis has no statistically significant changes between the groups. However, both the Romer Hypothesis and the Kemp Hypothesis have a significant change from group 1 to group 2 ($p = 0.02$). In both of these hypotheses, group 1 is defined solely by pelycosaurs, with a transition happening at therapsids. That this result is recovered in both - hypotheses, despite differences in the overall composition of group 2, suggests that a critical change is taking place as synapsids transition from the pelycosaur to a therapsid morphology.

Ulna - Ulnar morphology has the highest rates of overall phenotypic change of all the functional units, complementing the results from Chapter 3 that found ulnar morphology to be highly variable across Synapsida. For the Five Group Hypothesis a statistically significant change occurs from pelycosaurs to therapsids ($p = 0.003$), and from mammaliaforms to mammals ($p =$

0.003). The Romer Hypothesis has a significant change from group 1 to group 2 ($p = 0.001$), and from group 2 to group 3 ($p = 0.007$), making this the only dataset of the whole analysis in which changes between each hypothesized group are statistically significant. The Jenkins Hypothesis and the Kemp Hypothesis also have significant changes, but in different places. With the Jenkins hypothesis its between groups 2 and 3 ($p = 0.013$), whereas it is between groups 1 and 2 for the Kemp hypothesis ($p = 0.003$).

4.5 DISCUSSION

4.5.1 Morpho-functional Hypotheses

The Five Group Hypothesis, the Romer Hypothesis, and the Jenkins Hypothesis all recover a pattern of phylogenetic signal increasing through time, with phylogenetic signal increasing progressively towards Brownian motion values with each clade approaching extant mammals. This shows that through synapsid evolutionary history there has been an overall trend towards dispersion in morphospace, which each successive group partitioning more variance between the groups than within them. This is especially true for the distal humeral morphology, which has the only value above 1.0. This is expressed by the extant mammalian sample, and implies that these animals are much more similar than would be expected, which is in contrast to the rest of the synapsid distal humeral sample. Despite this, the distal humerus overall shows a pattern of constraint across its evolutionary history, with an apparent maintenance of low K_{mult} values and low rates of phenotypic change.

These types of changes can imply potential shifts in underlying processes, often as it relates to constraint. Mammaliaforms are the primary group for which the overall pattern of phylogenetic signal is consistently broken, especially in the proximal humeral end, with the exception of *Fruitafossor*, which has arguably the most unique mammaliaform humerus (Luo and Wible 2005) and has the highest levels of phenotypic change for the entire proximal and ulnar sample (Figure 4.6). The mammaliaform proximal humerus has some of the highest rates

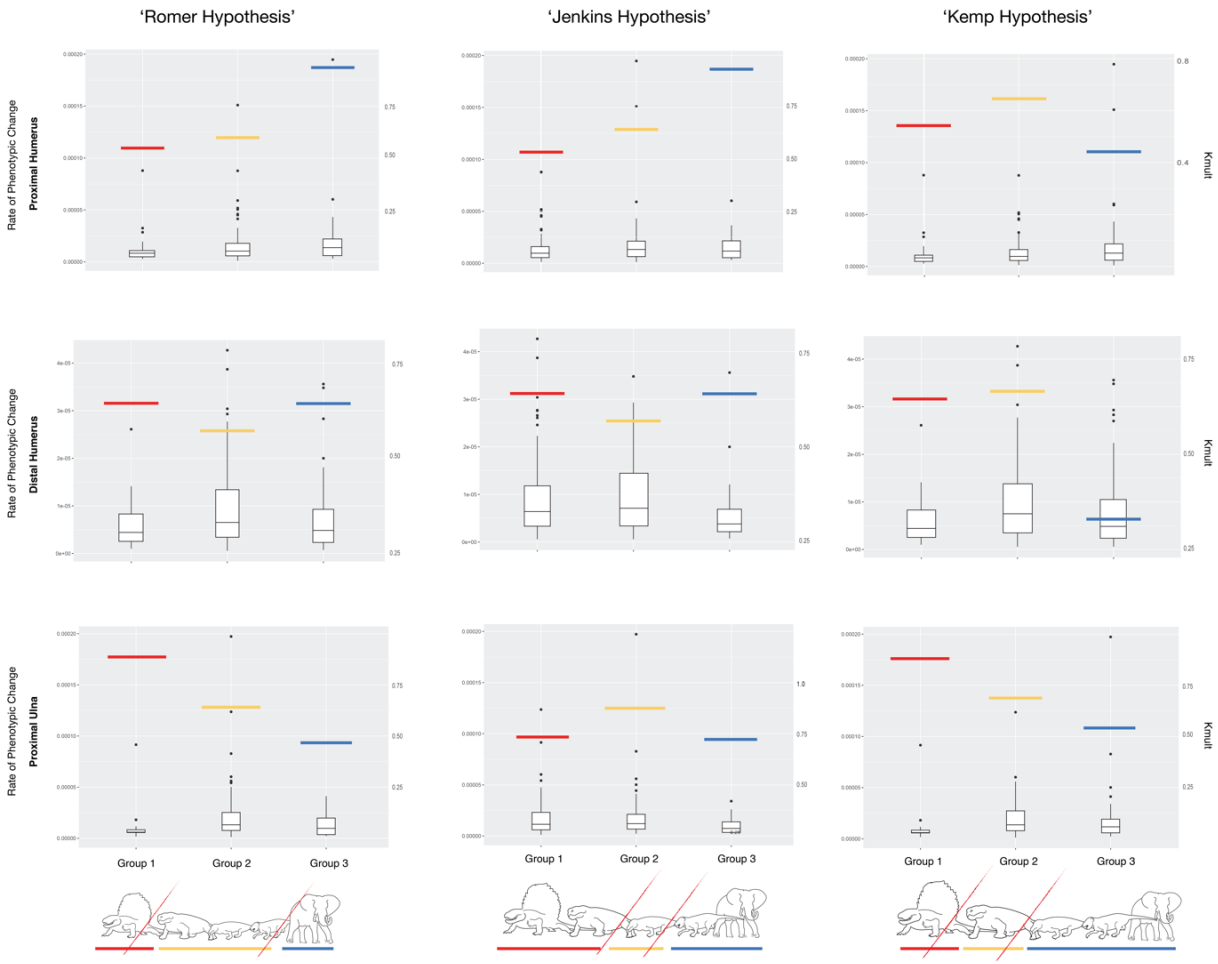

Figure 4.5 Evolutionary rate and phylogenetic signal for groups within each historical hypothesis - Each row is associated with a section of the forelimb (top: proximal humerus; middle: distal humerus; bottom: ulna). Solid lines represent K_{mult} value for each group. Boxplots are of the rate of phenotypic change for each genus represented in the defined group. Renderings at the bottom are a conceptualization of organisms in each historically hypotheses' groupings. Full generic sample in each group can be viewed in Table 4.2 and 4.3.

of phenotypic change, suggesting a critical evolutionary shift during the descent of mammaliaforms from cynodonts. More specifically, the combination of low phylogenetic signal with high evolutionary rates in mammaliaforms could imply convergence, wherein the variation across mammaliaforms is highly unstructured. Further, the lack of correlation between time-since-divergence within the mammaliaform tree with specific morphologies suggests a breakdown of possible constraint within this group that is allowing mammaliaforms to evolve highly variant shapes. This is consistent with the qualitative morphological comparison in more recent studies on mammaliaform fossils that have shown consistency in shape across the proximal part of the humerus in many different mammaliaform genera from across the tree (*Agilocodon*: (Q.-J. Meng et al. 2015); *Yanoconodon*; (M. Chen, Luo, and Wilson 2017); *Henkelotherium*: (Jäger, Luo, and Martin 2019)).

In contrast to the other two functional areas, ulnar signal has no apparent trend across the groups and instead fluctuates back and forth depending on the group. Pelycosaurs and cynodonts both have the highest phylogenetic signals and lowest rates of phenotypic change, while mammaliaforms and therapsids have the opposite pattern of lower K_{mult} and higher evolutionary rates. I would argue this is suggestive of morphological convergence in therapsids and mammaliaforms. The lack of consistent change through time, congruent with the dramatic increases in rates implies that there is a loss of structure in how variance is partitioned within these groups.

For the historical hypotheses, the critical distinction is that the functional groupings are fewer with each having more genera within them (Figure 4.5). This inherently lowers the specificity of the analyses, but does not prevent consideration of overall changes in phylogenetic signal and evolutionary rate. Differences between the three historical hypotheses can be

simplified as having to do with the placement of cynodonts and mammaliaforms. The grouping placement of cynodonts in particular is different in all three perspectives; this is critical in part because of the evolutionary pressures that appear to be acting on cynodonts specifically. Cynodonts consistently have high phylogenetic signal, coupled with low evolutionary rates (Figure 4.6), which is suggestive of overall constraint acting upon their evolutionary capabilities, and this finding proves to be easily detectable in the different functional grouping schemes. Similarly, the historical hypotheses show a similar pattern as the Five Group hypothesis for the proximal end, in which morphological variance is concentrated between groups instead of within them (higher phylogenetic signal). The inverse pattern is true for the ulna; phylogenetic signal decreases through time in most hypotheses. With the pattern of evolutionary rate, these results are suggestive of a switch from some sort of constrained or bounded process in the earlier parts of synapsid ulnar evolution, followed by a release where convergence in shape becomes increasingly common (decreasing phylogenetic signal) and each subsequent clade expands morphologically to accommodate new and increasingly diverse ecologies.

Leaving mammals by themselves as a morphotype, as is the case in the Romer, Kemp, and Five Group Hypotheses (Figure 4.4 & 4.5), produces arguably the most consistent results across the analysis, and supports the validity of Theria being considered independent of the rest of Synapsida in these types of analyses. Nonetheless, it does appear that the Five Group Hypothesis is an accurate representation of changes in phylogenetic signal through time. Adjusting to this more specific phylogenetic breakdown is an appropriate way to consider this large of an evolutionary clade. Furthermore, it appears that the Five Group Hypothesis provides a richer description of changes in phylogenetic signal and evolutionary rate that the historical hypotheses, whose smaller number of groups can obscure details that the Five Group Hypothesis

detects. Within an individual group, evolutionary rates can be either high or low, suggesting an organism-level lability wherein each element is fundamentally capable of changing its shape (in relation to the shape of its surrounding related taxa). However, the fact that rate levels are not observed to be constant within groups corroborates the idea that many of the changes being quantified in this chapter are happening at the within-group level, as opposed to at the level of the entire synapsid tree.

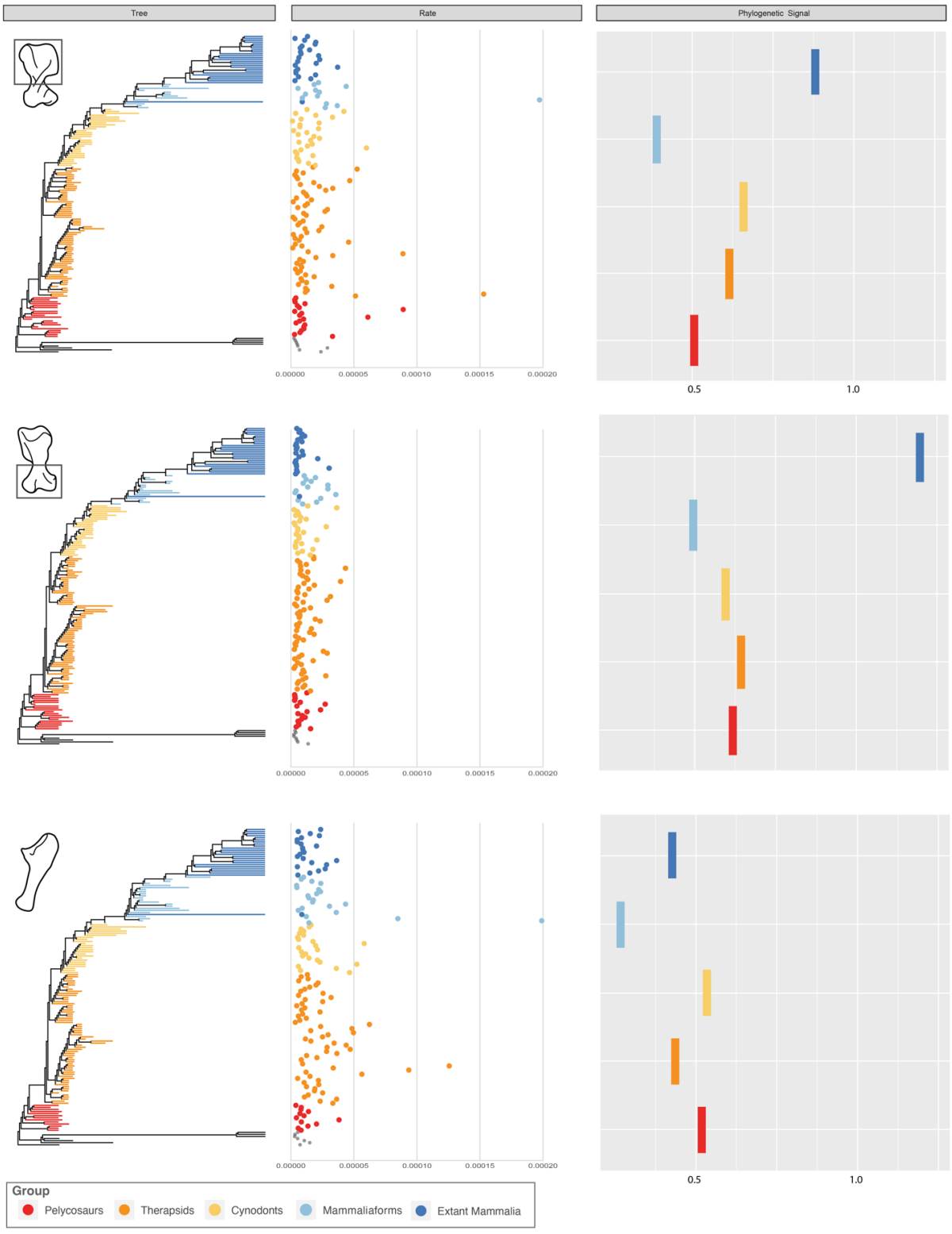

Figure 4.6 - Rate of phenotypic change across the forelimb - Associated trees and generic level rate of phenotypic change. Branch colors correspond to the Five Group Hypothesis.

4.5.2 Mosaic Evolution of the Synapsid Forelimb

A new observation of this study is that different areas of the forelimb are changing at different rates and seem to be acting under different types of selective pressure or evolutionary driver. This new insight comes from the new morphometrical methods that made it feasible for different parts of the forelimb to analyzed as separate data partitions, in contrast to the traditional qualitative analyses of the synapsid forelimb a single whole. Phylogenetic signal varies substantially across the three analyzed functional units (Figures 4.3- 4.6), which in turns reflects potentially different drivers for macroevolutionary changes in the limb. In all three sections of the forelimb, K_{mult} is below the expectation of Brownian motion, revealing that in all cases the elements are less similar than would be expected, and that variance across the sample is partitioned more heavily within groups than between them. The proximal humerus has the highest phylogenetic signal. As discussed in the introduction, this section of the forelimb is complex and relies on the inter-connection of many parts across the musculo-skeletal system (Lai, Biewener, and Pierce 2018; Fahn-Lai, Biewener, and Pierce 2020).

Of the three joints of the forelimb, the proximal humerus and its articulation with the glenoid apparatus undergoes arguably the most dramatic transformation of the three sections to evolve into the highly derived Therian shoulder girdle. This transformation would necessitate that proximal humeral morphology is expanding into new areas of morphospace across its evolutionary history (Jenkins and Weijs 1979; Luo 2015)(Chapter 3), and this corresponds to the higher observed levels of phylogenetic signal. Further, the proximal humerus most consistently

showed confirmation of the hypothesis, with each subsequent radiation of synapsids possessing increasing levels of phylogenetic signal. This suggests successive episodes of diversification at each phylogenetic interval. Distal humeral morphology as a whole is lower than the other two areas of the forelimb considered, providing further evidence that this functional unit is more conserved across synapsid evolutionary history. The K_{mult} value for the ulna is between the higher value of the proximal end and the lower value of the distal humerus. Importantly, the ulna appears to be undergoing the most change in terms of potentially underlying processes. With the transition to therapsids from pelycosaurs, phylogenetic signal drops and rate increases, implying the presence of convergence across therapsid ulna. However, with the emergence of cynodonts there appears to be a switch back to a system of constraint (higher K_{mult} and lower rates), which is then again released at the appearance of mammaliaforms. This implies a very dynamic evolutionary history for the ulna, and again suggests that there may have been a distinct type of evolutionary selective pressure being imparted on this area of the forelimb.

While the ulna does not have the highest phylogenetic signal of the forelimb, it does have the highest values for evolutionary rate, the other metric used here to consider the scale of change and placement of transitions (Figure 4.3 & 4.6). The ulna appears to have evolved more rapidly, conforming to mammalian morphologies through time, than the other functional units. The finding that the proximal humerus has been undergoing a rapid rate of phenotypic evolution across major the major synapsid grades is not as surprising because observationally it appears to be the part of the forelimb structure that is undergoing the most dramatic change through time (Jenkins and Weijs 1979; Sereno 2006). As discussed above, the pectoral girdle and its articulation with the humerus are arguably one of the most dramatic transformations that takes place in synapsid evolutionary history as it undergoes a radical reorganization. However, the

finding that the ulna is actually evolving somewhat faster than the proximal humerus is intriguing because the ulna's articulations at the elbow and the wrist are relatively simple, despite its shape (especially that of the olecranon process) being highly variable. The ulna has several critical muscle attachments that are undoubtedly influencing shape and morphology. These findings imply that some aspect of forelimb posture may have been accommodated in large part by changes in the ulna. As it is potentially related to posture, this might have to do with changes in the step cycle that are taking place as animals go from being highly sprawling (as it is in pelycosaurs) to being fully upright (as in eutherians). While the ulna is still a simple lever in pelycosaurs, the pelycosaur step cycle necessitates a swinging motion in conjunction with the twisting of the humerus, creating a complex and dynamic step series that requires a very specific set of morphologies for effective locomotion (Jenkins 1973; Hopson 1999; 2012; 2015). This is in contrast the therian mammalian system, in which the biomechanical role of the ulna as a lever has not changed but the step cycle is arguably simpler with a forward and aft movement than that of the swinging and rotating of early synapsids. It could be argued that this transformation, although already considered to be highly complex and enigmatic, is still even more dynamic than previously appreciated and is requiring changes across the forelimb in a way that has not been previously appreciated. Namely it is requiring different areas of individual elements to change in unique and diverse ways to accommodate the major musculoskeletal changes that are taking place as this evolutionary transformation is undertaken.

Further, work reveals a potential misinterpretation about the level at which researchers can make macroevolutionary statements for the synapsid forelimb evolutionary history. In the historical studies that focused on single isolated exemplary taxa without the diversity of the entire tree, the picture of ulna evolution was oversimplifies to the point at which trends are

actually lost. In contrast, when the morphological change of the ulna is considered in light of the total breath of diversity that is expressed across this 320 million year interval, it becomes apparent that this otherwise overlooked element likely played a critical role in the larger story of the evolution of the synapsid forelimb. It is understandable that previous researchers who worked on this topic simplified the overall process into a series of easily definable steps that could in turn contribute to the larger construct of a 'transition to mammals', such as a 'rule' or a 'law'. However, this runs increasingly counter to the way that researchers today are approaching this kind of studies, by taking into consideration the full breadth of diversity across this remarkable group of tetrapods.

4.6 CONCLUSION

The two metrics of phylogenetic signal and evolutionary rate are most powerful when considered in conjunction with one another. It is only by considering how these measurements change in light of each other that larger considerations of evolutionary processes can be attempted. Toward this goal, I made multiple phylogenetic frameworks within which to test how these metrics changed across the synapsid forelimb and throughout synapsid evolutionary history. I found that my novel contribution of a Five Group Hypothesis framework, wherein Synapsida is split into five paraphyletic groups or radiations, provides new insight into the synapsid evolutionary story, without incurring substantial error or noise. Within these five groups, mammaliaforms were consistently found to have the combination of low phylogenetic signal and high rate of phenotypic change, which strongly implies either convergence or a breakdown of constraint more broadly. This makes more sense in light of cynodonts, a group eventually replaced by mammaliaforms, that appear to be under strong constraint. This is also

evident in the historical hypotheses, in which cynodonts are one of the only groups of animals with alternative placements in forelimb evolutionary scenarios. Evolutionary constraint appears to be directly influencing how evolutionary rate and phylogenetic signal vary across these historical perspectives. Overall, adjusting to a more specific phylogenetic breakdown is an appropriate way to consider the evolutionary history of Synapsida, because it adds obvious nuance to these data.

The finding that different areas of the forelimb are changing at different rates and seem to be acting under different types of selective pressure is a new insight from this dissertation work, in large part because this work has considered the synapsid limb as multiple highly interconnected units (a proximal functional unit, a distal functional unit, and an ulna). This led to the finding that the ulna is apparently evolving faster than the humerus and its characters have a more dynamic evolutionary history, despite its relatively simple shape. When the morphological change of the synapsid forelimb is considered in light of the total diversity that is expressed across the 320 million year evolutionary history of Synapsida, it is increasingly evident that the story of the synapsid forelimb is only beginning to be fully understood.

REFERENCES

Abdala, Fernando. 2007. "Redescription of Platycraniellus Elegans (Therapsida, Cynodontia) from the Lower Triassic of South Africa, and the Cladistic Relationships of Eutheriodonts." *Palaeontology* 50 (3): 591–618.

Abdala, Fernando, Leandro C Gaetano, Roger M H Smith, and Bruce S Rubidge. 2019. "A New Large Cynodont from the Late Permian (Lopingian) of the South African Karoo Basin and Its Phylogenetic Significance." *Zoological Journal of the Linnean Society* 186 (4): 983–1005.

Adams, Dean C. 2014. "A Generalized K Statistic for Estimating Phylogenetic Signal from Shape and Other High-Dimensional Multivariate Data." *Systematic Biology* 63 (5): 685–97.

Adams, Dean C, Michael Collyer, Antigoni Kaliontzopoulou, and Emma Sherratt. 2016. "Geomorph: Software for Geometric Morphometric Analyses."

Adams, Dean C, and Erik Otárola-Castillo. 2013. "Geomorph: An R Package for the Collection and Analysis of Geometric Morphometric Shape Data." *Methods in Ecology and Evolution* 4 (4): 393–99.

Angielczyk, Kenneth D., and Christian F Kammerer. 2018. "Non-Mammalian Synapsids: The Deep Roots of the Mammalian Family Tree." *Handbook of Zoology: Mammalia: Mammalian Evolution, Diversity and Systematics, Eds Zachos FE, Asher RJ (De Gruyter, Berlin)*, 117–98.

Angielczyk, Kenneth D, P John Hancox, and Ali Nabavizadeh. 2017. "A Redescription of the Triassic Kannemeyeriiform Dicynodont Sangusaurus (Therapsida, Anomodontia), with an Analysis of Its Feeding System." *Journal of Vertebrate Paleontology* 37 (sup1): 189–227.

Angielczyk, Kenneth D, and Christian F Kammerer. 2017. "The Cranial Morphology, Phylogenetic Position and Biogeography of the Upper Permian Dicynodont Compsodon Helmoedi van Hoepen (Therapsida, Anomodontia)." *Papers in Palaeontology* 3 (4): 513–45. https://doi.org/10.1002/spp2.1087.

Angielczyk, Kenneth D, and Bruce S Rubidge. 2013. "Skeletal Morphology, Phylogenetic Relationships and Stratigraphic Range of Eosimops Newtoni Broom, 1921, a Pylaecephalid Dicynodont (Therapsida, Anomodontia) from the Middle Permian of South Africa." *Journal of Systematic Palaeontology* 11 (2): 191–231.

Archibald, J David, and Alexander O Averianov. 2006. "Late Cretaceous Asioryctitherian Eutherian Mammals from Uzbekistan and Phylogenetic Analysis of Asioryctitheria." *Acta Palaeontologica Polonica* 51 (2).

Augee, Michael L, Brett Gooden, and Anne Musser. 2006. *Echidna: Extraordinary Egg-Laying Mammal*. Colligwood: CSIRO publishing.

Barr, W Andrew. 2018. "Ecomorphology." In *Methods in Paleoecology*, 339–49. Springer.

Beck, Alison. 2004. "Locomotor Evolutuion of the No- Mammalian Synapsids." University of Chicago.

Benevento, Gemma Louise, Roger B J Benson, and Matt Friedman. 2019. "Patterns of

Mammalian Jaw Ecomorphological Disparity during the Mesozoic/Cenozoic Transition." *Proceedings of the Royal Society B* 286 (1902): 20190347.

Benson, Roger B J. 2012. "Interrelationships of Basal Synapsids: Cranial and Postcranial Morphological Partitions Suggest Different Topologies." *Journal of Systematic Palaeontology* 10 (4): 601–24. https://doi.org/10.1080/14772019.2011.631042.

Benton, Michael J, Philip C J Donoghue, Robert J Asher, Matt Friedman, Thomas J Near, and Jakob Vinther. 2015. "Constraints on the Timescale of Animal Evolutionary History." *Palaeontologia Electronica* 18 (1): 1–106.

Berman, David S, Amy C Henrici, Stuart S Sumida, and Thomas Martens. 2000. "Redescription of Seymouria Sanjuanensis (Seymouriamorpha) from the Lower Permian of Germany Based on Complete, Mature Specimens with a Discussion of Paleoecology of the Bromacker Locality Assemblage." *Journal of Vertebrate Paleontology* 20 (2): 253–68.

Berman, David S, Amy C Henrici, Stuart S Sumida, Thomas Martens, and Valerie Pelletier. 2014. "First European Record of a Varanodontine (Synapsida: Varanopidae): Member of a Unique Early Permian Upland Paleoecosystem, Tambach Basin, Central Germany." In *Early Evolutionary History of the Synapsida*, 69–86. Springer, Dordrecht. https://doi.org/10.1007/978-94-007-6841-3_5.

Blomberg, Simon P, Theodore Garland Jr, and Anthony R Ives. 2003. "Testing for Phylogenetic Signal in Comparative Data: Behavioral Traits Are More Labile." *Evolution* 57 (4): 717–45.

Bonaparte, José F. 2008. "On the Phylogenetic Relationships of Vincelestes Neuquenianus: Short Review." *Historical Biology* 20 (2): 81–86.

Botha-Brink, Jennifer, and Sean P Modesto. 2009. "Anatomy and Relationships of the Middle Permian Varanopid Heleosaurus Scholtzi Based on a Social Aggregation from the Karoo Basin of South Africa." *Journal of Vertebrate Paleontology* 29 (2): 389–400.

———. 2011. "A New Skeleton of the Therocephalian Synapsid Olivierosuchus Parringtoni from the Lower Triassic South African Karoo Basin." *Palaeontology* 54 (3): 591–606. https://doi.org/10.1111/j.1475-4983.2011.01048.x.

Brandt, Marc Van den, and Fernando Abdala. 2018. "Cranial Morphology and Phylogenetic Analysis of Cynosaurus Suppostus (Therapsida, Cynodontia) from the Upper Permian of the Karoo Basin, South Africa."

Brocklehurst, Neil. 2015. "The Early Evolution of Synapsida (Vertebrata, Amniota) and the Quality of Their Fossil Record."

Brocklehurst, Neil, Robert R Reisz, Vincent Fernandez, and Jörg Fröbisch. 2016. "A Re-Description of 'Mycterosaurus' Smithae, an Early Permian Eothyridid, and Its Impact on the Phylogeny of Pelycosaurian-Grade Synapsids." *PLoS One* 11 (6): e0156810.

Broom, Robert. 1911. "A Comparison of the Permian Reptiles of North America with Those of South Afrika." *Molecular and General Genetics MGG* 5 (1): 205–6.

Brusatte, Stephen L, Richard J Butler, Albert Prieto-Márquez, and Mark A Norell. 2012. "Dinosaur Morphological Diversity and the End-Cretaceous Extinction." *Nature Communications* 3: 804.

Burgess, S D, J D Muirhead, and S A Bowring. 2017. “Initial Pulse of Siberian Traps Sills as the Trigger of the End-Permian Mass Extinction.” *Nature Communications* 8.

Campione, Nicolás E, and Robert R Reisz. 2010. “Varanops Brevirostris (Eupelycosauria: Varanopidae) from the Lower Permian of Texas, with Discussion of Varanopid Morphology and Interrelationships.” *Journal of Vertebrate Paleontology* 30 (3): 724–46. https://doi.org/10.1080/02724631003762914.

Carroll, Robert L. 1988. “Vertebrate Paleontology and Evolution.”

Chen, Meng, Zhe-Xi Luo, and Gregory P Wilson. 2017. “The Postcranial Skeleton of Yanoconodon Allini from the Early Cretaceous of Hebei, China, and Its Implications for Locomotor Adaptation in Eutriconodontan Mammals.” *Journal of Vertebrate Paleontology* 37 (3): e1315425.

Chen, Meng, Caroline A E Strömberg, and Gregory P Wilson. 2019. “Assembly of Modern Mammal Community Structure Driven by Late Cretaceous Dental Evolution, Rise of Flowering Plants, and Dinosaur Demise.” *Proceedings of the National Academy of Sciences* 116 (20): 9931–40.

Chen, Meng, and Gregory P Wilson. 2015. “A Multivariate Approach to Infer Locomotor Modes in Mesozoic Mammals.” *Paleobiology* 41 (2): 280–312.

Chen, Zhong-Qiang, and Michael J Benton. 2012. “The Timing and Pattern of Biotic Recovery Following the End-Permian Mass Extinction.” *Nature Geoscience* 5 (6): 375–83. https://doi.org/10.1038/ngeo1475.

Claude, Julien. 2008. *Morphometrics with R*. Springer Science & Business Media.

Close, Roger A, Matt Friedman, Graeme T Lloyd, and Roger B J Benson. 2015. “Evidence for a Mid-Jurassic Adaptive Radiation in Mammals.” *Current Biology* 25 (16): 2137–42.

Cluver, M A. 1978. “The Skeleton of the Mammal-like Reptile Cistecephalus with Evidence for a Fossorial Mode of Life.” *Annals of the South African Museum* 76: 213–47.

Colbert, Edwin Harris. 1948. “The Mammal-like Reptile Lycaenops.” *Bulletin of the American Museum of Natural History* 89 (6).

Colbert, Edwin Harris, and Robert Broom. 1948. “The Mammal-like Reptile Lycaenops. Bulletin of the AMNH; v. 89, Article 6.”

Cox, C Barry. 1972. “A New Digging Dicynodont from the Upper Permian of Tanzania.” *Studies in Vertebrate Evolution. Oliver and Boyd, Edinburgh*, 173–89.

Erwin, Douglas H. 2007. “Disparity: Morphological Pattern and Developmental Context.” *Palaeontology* 50 (1): 57–73. https://doi.org/10.1111/j.1475-4983.2006.00614.x.

Fahn-Lai, Philip, Andrew A Biewener, and Stephanie E Pierce. 2020. “Broad Similarities in Shoulder Muscle Architecture and Organization across Two Amniotes: Implications for Reconstructing Non-Mammalian Synapsids.” *PeerJ* 8: e8556. https://doi.org/10.7717/peerj.8556.

Foote, Michael. 1993. “Discordance and Concordance between Morphological and Taxonomic Diversity.” *Paleobiology* 19 (2): 185–204. https://doi.org/10.2307/2400876.

———. 1997. “The Evolution of Morphological Diversity.” *Annual Review of Ecology and*

Systematics 28: 129–52.

Fourie, Heidi, and Bruce S Rubidge. 2007. “The Postcranial Skeletal Anatomy of the Therocephalian Regisaurus (Therapsida: Regisauridae) and Its Utilization for Biostratigraphic Correlation.”

———. 2009. “The Postcranial Skeleton of the Basal Therocephalian Glanosuchus Macrops (Scylacosauridae) and Comparison of Morphological and Phylogenetic Trends amongst the Theriodontia.”

Fröbisch, Jörg, and Robert R Reisz. 2009. “The Late Permian Herbivore Suminia and the Early Evolution of Arboreality in Terrestrial Vertebrate Ecosystems.” *Proceedings of the Royal Society of London B: Biological Sciences* 276 (1673).

Gaetano, Leandro C, and Guillermo W Rougier. 2011. “New Materials of Argentoconodon Fariasorum (Mammaliaformes, Triconodontidae) from the Jurassic of Argentina and Its Bearing on Triconodont Phylogeny.” *Journal of Vertebrate Paleontology* 31 (4): 829–43.

Gill, Pamela G, Mark A Purnell, Nick Crumpton, Kate Robson Brown, Neil J Gostling, Marco Stampanoni, and Emily J Rayfield. 2014. “Dietary Specializations and Diversity in Feeding Ecology of the Earliest Stem Mammals.” *Nature* 512 (7514): 303–5.

Gower, John C. 1975. “Generalized Procrustes Analysis.” *Psychometrika* 40 (1): 33–51. https://doi.org/10.1007/BF02291478.

Gregory, William King, and Robert Broom. 1926. *The Skeleton of Moschops Capensis Broom: A Dinocephalian Reptile from the Permian of South Africa*. order of the Trustees, the American Museum of Natural History.

Grossnickle, David M. 2017. “The Evolutionary Origin of Jaw Yaw in Mammals.” *Scientific Reports* 7: 45094.

———. 2019. “Jaw Morphologies Provide Novel Insight on the Ecological Radiation of Early Therian Mammals.” In *JOURNAL OF MORPHOLOGY*, 280:S66–S66. WILEY 111 RIVER ST, HOBOKEN 07030-5774, NJ USA.

Grossnickle, David M, Stephanie M Smith, and Gregory P Wilson. 2019. “Untangling the Multiple Ecological Radiations of Early Mammals.” *Trends in Ecology & Evolution* 34 (10): 936–49.

Grunert, Henrik Richard, Neil Brocklehurst, and Jörg Fröbisch. 2019. “Diversity and Disparity of Therocephalia: Macroevolutionary Patterns through Two Mass Extinctions.” *Scientific Reports* 9 (1): 1–11.

Guignard, Morgan L, Agustin G Martinelli, and Marina B Soares. 2019. “Postcranial Anatomy of Riograndia Guaibensis (Cynodontia: Ictidosauria).” *Geobios* 53: 9–21.

Hildebrand, Milton. 1985. “Digging of Quadrupeds.” In *Functional Vertebrate Morphology*, 89–109. Cambridge: Harvard University Press.

Hildebrand, Milton, Dennis M Bramble, Karel F Liem, and David B Wake. 1985. “Walking and Running.” In *Functional Vertebrate Morphology*, 38–57. Harvard University Press.

Holmes, Robert. 1977. “The Osteology and Musculature of the Pectoral Limb of Small Captorhinids.” *Journal of Morphology* 152 (1): 101–40.

Hopkins, Melanie J, and Andrew B Smith. 2015. “Dynamic Evolutionary Change in Post-Paleozoic Echinoids and the Importance of Scale When Interpreting Changes in Rates of Evolution.” *Proceedings of the National Academy of Sciences* 112 (12): 3758–63.

Hopson, James A. 1994. “Synapsid Evolution and the Radiation of Non-Eutherian Mammals.” *Short Courses in Paleontology* 7: 190–219.

———. 1999. “Locomotion : A Case Study of Dimetrodon.”

———. 2012. “The Role of Foraging Mode in the Origin of Therapsids: Implications for the Origin of Mammalian Endothermy.” *Fieldiana Life and Earth Sciences* 5 (October): 126–48. https://doi.org/10.3158/2158-5520-5.1.126.

———. 2015. “Fossils, Trackways, and Transitions in Locomotion: A Case Study of Dimetrodon.” In *Great Transformations in Vertebrate Evolution*, 125–41. Chicago: University of Chicago Press.

Hopson, James A, and H R Barghusen. 1986. “An Analysis of Therapsid Relationships.” *The Ecology and Biology of Mammal-like Reptiles*, 83–106.

Horovitz, Inés. 2003. “Postcranial Skeleton of Ukhaatherium Nessovi (Eutheria, Mammalia) from the Late Cretaceous of Mongolia.” *Journal of Vertebrate Paleontology* 23 (4): 857–68.

Hotton, Nicholas, Everett C Olson, and Richard Beerbower. 1997. “Amniote Origins and the Discovery of Herbivory.” *Amniote Origins*, 207–64.

Hughes, Martin, Sylvain Gerber, and Matthew Albion Wills. 2013. “Clades Reach Highest Morphological Disparity Early in Their Evolution.” *Proceedings of the National Academy of Sciences of the United States of America* 110 (34): 13875–79. https://doi.org/10.1073/pnas.1302642110.

Hurum, Jørn H, and Zofia Kielan-Jaworowska. 2008. “Postcranial Skeleton of a Cretaceous Multituberculate Mammal Catopsbaatar.” *Acta Palaeontologica Polonica* 53 (4): 545–66.

Huttenlocker, Adam K, David M Grossnickle, James I Kirkland, Julia A Schultz, and Zhe-Xi Luo. 2018. “Late-Surviving Stem Mammal Links the Lowermost Cretaceous of North America and Gondwana.” *Nature* 558 (7708): 108–12.

Huttenlocker, Adam K, and Christian A Sidor. 2016. “The First Karenitid (Therapsida, Therocephalia) from the Upper Permian of Gondwana and the Biogeography of Permo-Triassic Therocephalians.” *Journal of Vertebrate Paleontology* 36 (4): e1111897.

Huttenlocker, Adam K, and Roger M H Smith. 2017. “New Whaitsioids (Therapsida: Therocephalia) from the Teekloof Formation of South Africa and Therocephalian Diversity during the End-Guadalupian Extinction.” *PeerJ* 5: e3868.

Jablonski, David. 2017. “Approaches to Macroevolution: 1. General Concepts and Origin of Variation.” *Evolutionary Biology* 44 (4): 427–50. https://doi.org/10.1007/s11692-017-9420-0.

Jäger, K R K, Zhe-Xi Luo, and Thomas Martin. 2019. “Postcranial Skeleton of Henkelotherium Guimarotae (Cladotheria, Mammalia) and Locomotor Adaptation.” *Journal of Mammalian Evolution*, 1–24.

Jenkins Jr, Farish A. 1970. “Limb Movements in a Monotreme (Tachyglossus Aculeatus): A

Cineradiographic Analysis." *Science* 168 (3938): 1473–75.

———. 1971a. "Part One: Postcranial Axial Skeleton." In *The Postcranial Skeleton of African Cynodonts*, 36th ed., 1–91. New Haven: Peabody Museum of Natural HIstory.

———. 1971b. "The Postcranial Skeleton of African Cynodonts." *Bulletin of the Peabody Museum of Natural History* 36: 1–216.

———. 1973. "The Functional Anatomy and Evolution of the Mammalian Humero-ulnar Articulation." *Developmental Dynamics* 137 (3): 281–97. https://doi.org/10.1002/aja.1001370304.

———. 1974. "The Movement of the Shoulder in Claviculate and Aclaviculate Mammals." *Journal of Morphology* 144 (1): 71–83.

Jenkins Jr, Farish A, and Francis Rex Parrington. 1976. "The Postcranial Skeletons of the Triassic Mammals Eozostrodon, Megazostrodon and Erythrotherium." *Philosophical Transactions of the Royal Society of London. B, Biological Sciences* 273 (926): 387–431.

Jenkins Jr, Farish A, and Charles R Schaff. 1988. "The Early Cretaceous Mammal Gobiconodon (Mammalia, Triconodonta) from the Cloverly Formation in Montana." *Journal of Vertebrate Paleontology* 8 (1): 1–24.

Jenkins Jr, Farish A, and W A Weijs. 1979. "The Functional Anatomy of the Shoulder in the Virginia Opossum (Didelphis Virginiana)." *Journal of Zoology* 188 (3): 379–410.

Ji, Qiang, Zhe-Xi Luo, Chong-Xi Yuan, and Alan R Tabrum. 2006. "A Swimming Mammaliaform from the Middle Jurassic and Ecomorphological Diversification of Early Mammals." *Science (New York, N.Y.)* 311 (5764): 1123–27. https://doi.org/10.1126/science.1123026.

Jones, Katrina E, Kenneth D Angielczyk, P David Polly, Jason J Head, V Fernandez, Jacqueline K Lungmus, Sarah Tulga, and Stephanie E Pierce. 2018. "Fossils Reveal the Complex Evolutionary History of the Mammalian Regionalized Spine." *Science* 361 (6408): 1249 LP – 1252. https://doi.org/10.1126/science.aar3126.

Jones, Katrina E, Sarah Gonzalez, Kenneth D Angielczyk, and Stephanie E Pierce. 2020. "Regionalization of the Axial Skeleton Predates Functional Adaptation in the Forerunners of Mammals." *Nature Ecology & Evolution* 4 (3): 470–78.

Jun, Liu, Marina Bento Soares, and Miriam Reichel. 2008. "Massetognathus (Cynodontia, Traversodontidae) from the Santa Maria Formation of Brazil." *Revista Brasileira de Paleontologia. Vol. 11, n. 1 (Jan./Abr. 2008), p. 27-36*.

Kamilar, Jason M, and Natalie Cooper. 2013. "Phylogenetic Signal in Primate Behaviour, Ecology and Life History." *Philosophical Transactions of the Royal Society B: Biological Sciences* 368 (1618): 20120341.

Kammerer, Christian F. 2011. "Systematics of the Anteosauria (Therapsida: Dinocephalia)." *Journal of Systematic Palaeontology* 9 (2): 261–304.

———. 2014. "Theriodontia: Introduction." In *Early Evolutionary History of the Synapsids*, edited by Christian F Kammerer, Kenneth D Angielczyk, and Jorg Frobisch, 174–87. Springer.

———. 2018. “The First Skeletal Evidence of a Dicynodont from the Lower Elliot Formation of South Africa.”

———. 2019. “Revision of the Tanzanian Dicynodont Dicynodon Huenei (Therapsida: Anomodontia) from the Permian Usili Formation.” *PeerJ* 2019 (8). https://doi.org/10.7717/peerj.7420.

Kammerer, Christian F, and Kenneth D Angielczyk. 2009. “A Proposed Higher Taxonomy of Anomodont Therapsids.” *Zootaxa* 2018: 1–24.

Kammerer, Christian F, Saswati Bandyopadhyay, and Sanghamitra Ray. 2016. “A New Taxon of Cistecephalid Dicynodont from the Upper Permian Kundaram Formation of India.” *Papers in Palaeontology* 2 (4): 569–84.

Kammerer, Christian F, John J Flynn, Lovasoa Ranivoharimanana, and André R Wyss. 2008. “New Material of Menadon Besairiei (Cynodontia: Traversodontidae) from the Triassic of Madagascar.” *Journal of Vertebrate Paleontology* 28 (2): 445–62.

Kammerer, Christian F, and Vladimir Masyutin. 2018. “Gorgonopsian Therapsids (Nochnitsa Gen. Nov. and Viatkogorgon) from the Permian Kotelnich Locality of Russia.” *PeerJ* 6: e4954.

Kemp. 2009. “Stance and Gait in the Hindlimb of a Therocephalian Mammal-like Reptile.” *Journal of Zoology* 186 (2): 143–61. https://doi.org/10.1111/j.1469-7998.1978.tb03362.x.

Kemp, Thomas Stainforth. 1978. “Stance and Gait in the Hindlimb of a Therocephalian Mammal-like Reptile.” *Journal of Zoology* 186 (2): 143–61. https://doi.org/10.1111/j.1469-7998.1978.tb03362.x.

———. 1980. “The Primitive Cynodont Procynosuchus: Structure, Function and Evolution of the Postcranial Skeleton.” *Philosophical Transactions of the Royal Society B: Biological Sciences* 288 (1027): 217–58. https://doi.org/10.1098/rstb.1980.0001.

———. 1982. *Mammal-like Reptiles and the Origin of Mammals*. Academic Pr.

———. 1986. “The Skeleton of a Baurioid Therocephalian Therapsid from the Lower Triassic (Lystrosaurus Zone) of South Africa.” *Journal of Vertebrate Paleontology* 6 (3): 215–32. http://www.jstor.org/stable/4523096.

———. 2005. *The Origin and Evolution of Mammals*. Oxford University Press on Demand.

———. 2006. “The Origin and Early Radiation of the Therapsid Mammal-like Reptiles: A Palaeobiological Hypothesis.” *Journal of Evolutionary Biology* 19 (4): 1231–47. https://doi.org/10.1111/j.1420-9101.2005.01076.x.

———. 2012. “The Origin and Radiation of Therapsids.” In *Forerunners of Mammals*, edited by Anusuya Chinsamy-Turan, 3–32. Indiana University Press.

Kendall, David G. 1977. “The Diffusion of Shape.” *Advances in Applied Probability* 9 (3): 428–30.

Kilbourne, Brandon M. 2017. “Selective Regimes and Functional Anatomy in the Mustelid Forelimb: Diversification toward Specializations for Climbing, Digging, and Swimming.” *Ecology and Evolution* 7 (21): 8852–63.

Kilbourne, Brandon M, and John R Hutchinson. 2019. “Morphological Diversification of Biomechanical Traits: Mustelid Locomotor Specializations and the Macroevolution of Long Bone Cross-Sectional Morphology.” *BMC Evolutionary Biology* 19 (1): 1–16.

King, Gillian M. 1981. *The Postcranial Skeleton of Robertia Broomiana, an Early Dicynodont (Reptilia, Therapsida) from the South African Karoo*. South African Museum.

Knope, M L, N A Heim, L O Frishkoff, and J L Payne. 2015. “Limited Role of Functional Differentiation in Early Diversification of Animals.” *Nature Communications* 6 (January): 6455. https://doi.org/10.1038/ncomms7455.

Laaß, Michael. 2015. “Bone-Conduction Hearing and Seismic Sensitivity of the Late Permian Anomodont Kawingasaurus Fossilis.” *Journal of Morphology* 276 (2): 121–43. https://doi.org/10.1002/jmor.20325.

Lai, Phil H, Andrew A Biewener, and Stephanie E Pierce. 2018. “Three-Dimensional Mobility and Muscle Attachments in the Pectoral Limb of the Triassic Cynodont Massetognathus Pascuali (Romer, 1967).” *Journal of Anatomy* 232 (3): 383–406. https://doi.org/10.1111/joa.12766.

Laurin, Michel, and Robert R Reisz. 1990. “Tetraceratops Is the Oldest Known Therapsid.” *Nature* 345 (6272): 249–50.

Liu, Jun, and Fernando Abdala. 2014. “Phylogeny and Taxonomy of the Traversodontidae.” In *Early Evolutionary History of the Synapsida*, 255–79. Springer.

Liu, Jun, Bruce Rubidge, and Jinling Li. 2009. “New Basal Synapsid Supports Laurasian Origin for Therapsids.” *Acta Palaeontologica Polonica* 54 (3): 393–400.

Liu, Jun, Bruce S Rubidge, and Jinling Li. 2010. “A New Specimen of Biseridens Qilianicus Indicates Its Phylogenetic Position as the Most Basal Anomodont.” *Proceedings of the Royal Society of London B: Biological Sciences* 277 (1679): 285–92.

Liu, Jun, Vincent P Schneider, and Paul E Olsen. 2017. “The Postcranial Skeleton of Boreogomphodon (Cynodontia: Traversodontidae) from the Upper Triassic of North Carolina, USA and the Comparison with Other Traversodontids.” *PeerJ* 5: e3521.

Lloyd, Graeme T. 2008. “Generalized Differencing of Time Series.” 2008. http://www.graemetlloyd.com/methgd.html.

———. 2015. “Claddis: An R Package for Performing Disparity and Rate Analysis on Cladistic-Type Data Sets.” *Online at GitHub. See Https://Github. Com/Graemetlloyd/Claddis*.

Lungmus, Jacqueline K, and Kenneth D Angielczyk. 2019. “Antiquity of Forelimb Ecomorphological Diversity in the Mammalian Stem Lineage (Synapsida).” *Proceedings of the National Academy of Sciences* 116 (14): 6903–7.

Luo, Zhe-Xi. 2015. “Origin of the Mammalian Shoulder.” *Great Transformations in Vertebrate Evolution*, 167.

Luo, Zhe-Xi, Zofia Kielan-Jaworowska, and Richard L Cifelli. 2002. “In Quest for a Phylogeny of Mesozoic Mammals.” *Acta Palaeontologica Polonica* 47 (1).

Luo, Zhe-Xi, Qing-Jin Meng, David M Grossnickle, Di Liu, April I Neander, Yu-Guang Zhang, and Qiang Ji. 2017. “New Evidence for Mammaliaform Ear Evolution and Feeding

Adaptation in a Jurassic Ecosystem." *Nature* 548 (7667): 326–29.

Luo, Zhe-Xi, and John R Wible. 2005. "A Late Jurassic Digging Mammal and Early Mammalian Diversification." *Science* 308 (5718): 103–7.

Mann, Arjan, Bryan M Gee, Jason D Pardo, David Marjanović, Gabrielle R Adams, Ami S Calthorpe, Hillary C Maddin, and Jason S Anderson. n.d. "Reassessment of Historic 'Microsaurs' from Joggins, Nova Scotia, Reveals Hidden Diversity in the Earliest Amniote Ecosystem." *Papers in Palaeontology*.

Martin, Thomas. 2005. "Postcranial Anatomy of Haldanodon Exspectatus (Mammalia, Docodonta) from the Late Jurassic (Kimmeridgian) of Portugal and Its Bearing for Mammalian Evolution." *Zoological Journal of the Linnean Society* 145 (2): 219–48.

———. 2013. "Mammalian Postcranial Bones from the Late Jurassic of Portugal and Their Implications for Forelimb Evolution." *Journal of Vertebrate Paleontology* 33 (6): 1432–41.

Martinelli, Agustín G, Marina Bento Soares, and Cibele Schwanke. 2016. "Two New Cynodonts (Therapsida) from the Middle-Early Late Triassic of Brazil and Comments on South American Probainognathians." *PloS One* 11 (10): e0162945.

Meng, Jin, Yaoming Hu, Yuanqing Wang, Xiaolin Wang, and Chuankui Li. 2006. "A Mesozoic Gliding Mammal from Northeastern China." *Nature* 444 (7121): 889–93. https://doi.org/10.1038/nature05234.

Meng, Qing-Jin, David M Grossnickle, Di Liu, Yu-Guang Zhang, April I Neander, Qiang Ji, and Zhe-Xi Luo. 2017. "New Gliding Mammaliaforms from the Jurassic." *Nature* 548 (7667): 291.

Meng, Qing-Jin, Qiang Ji, Yu-Guang Zhang, Di Liu, David M Grossnickle, and Zhe-Xi Luo. 2015. "An Arboreal Docodont from the Jurassic and Mammaliaform Ecological Diversification." *Science* 347 (6223): 764–68.

Mitchell, Jonathan S. 2015. "Extant-only Comparative Methods Fail to Recover the Disparity Preserved in the Bird Fossil Record." *Evolution* 69 (9): 2414–24.

Moyne, Sébastien, and Pascal Neige. 2007. "The Space-Time Relationship of Taxonomic Diversity and Morphological Disparity in the Middle Jurassic Ammonite Radiation." *Palaeogeography, Palaeoclimatology, Palaeoecology* 248 (1–2): 82–95. https://doi.org/10.1016/j.palaeo.2006.11.011.

Müller, Johannes, and Robert R Reisz. 2006. "The Phylogeny of Early Eureptiles: Comparing Parsimony and Bayesian Approaches in the Investigation of a Basal Fossil Clade." *Systematic Biology* 55 (3): 503–11.

Nasterlack, Tobias, Aurore Canoville, and Anusuya Chinsamy. 2012. "New Insights into the Biology of the Permian Genus Cistecephalus (Therapsida, Dicynodontia)." *Journal of Vertebrate Paleontology* 32 (6): 1396–1410. https://doi.org/10.1080/02724634.2012.697410.

Oliveira, Edison V. 2006. "Reevaluation of Therioherpeton Cargnini Bonaparte & Barberena, 1975 (Probainognathia, Therioherpetidae) from the Upper Triassic of Brazil." *Geodiversitas* 28 (3): 447–65.

Pavanatto, Ane Elise Branco, Rodrigo Temp Müller, Átila Augusto Stock Da-Rosa, and Sérgio Dias-da-Silva. 2016. "New Information on the Postcranial Skeleton of Massetognathus Ochagaviae Barberena, 1981 (Eucynodontia, Traversodontidae), from the Middle Triassic of Southern Brazil." *Historical Biology* 28 (7): 978–89.

Polly, P David. 2007. "Limbs in Mammalian Evolution." *Fins into Limbs: Evolution, Development and Transformation*, 245–68.

Regnault, Sophie, and Stephanie E Pierce. 2018. "Pectoral Girdle and Forelimb Musculoskeletal Function in the Echidna (Tachyglossus Aculeatus): Insights into Mammalian Locomotor Evolution." *Royal Society Open Science* 5 (11): 181400.

Reisz, Robert R. 2006. "Origin of Dental Occlusion in Tetrapods: Signal for Terrestrial Vertebrate Evolution?" *Journal of Experimental Zoology Part B: Molecular and Developmental Evolution* 306 (3): 261–77.

Reisz, Robert R, and David S Berman. 1986. "Ianthasaurus Hardestii n.Sp., a Primitive Edaphosaur (Reptilia, Pelycosauria) from the Upper Pennsylvanian Rock Lake Shale near Garnett, Kansas." *Canadian Journal of Earth Sciences* 23 (1): 77–91. https://doi.org/10.1139/e86-008.

Reisz, Robert R, and Michel Laurin. 2004. "A Reevaluation of the Enigmatic Permian Synapsid Watongia and of Its Stratigraphic Significance." *Canadian Journal of Earth Sciences* 41 (4): 377–86.

Reisz, Robert R, Hillary C Maddin, Jörg Fröbisch, and Jocelyn Falconnet. 2011. "A New Large Caseid (Synapsida, Caseasauria) from the Permian of Rodez (France), Including a Reappraisal of 'Casea' Rutena Sigogneau-Russell & Russell, 1974." *Geodiversitas* 33 (2): 227–46.

Reisz, Robert R, H Wilson, and D Scott. 1997. "Varanopseid Synapsid Skeletal Elements from Richards Spur, a Lower Permian Fissure Fill near Fort Sill, Oklahoma." *Oklahoma Geology Notes* 57 (5): 160–70.

Revell, Liam J. 2010. "Phylogenetic Signal and Linear Regression on Species Data." *Methods in Ecology and Evolution* 1 (4): 319–29. https://doi.org/10.1111/j.2041-210x.2010.00044.x.

Revell, Liam J, Luke J Harmon, and David C Collar. 2008. "Phylogenetic Signal, Evolutionary Process, and Rate." *Systematic Biology* 57 (4): 591–601.

Revelle, William. 2011. "An Overview of the Psych Package." *Department of Psychology Northwest UniversityPsychol Northwest Univ* 3: 1–25.

Rodrigues, Pablo Gusmão, Agustín G Martinelli, Cesar Leandro Schultz, Ian J Corfe, Pamela G Gill, Marina B Soares, and Emily J Rayfield. 2019. "Digital Cranial Endocast of Riograndia Guaibensis (Late Triassic, Brazil) Sheds Light on the Evolution of the Brain in Non-Mammalian Cynodonts." *Historical Biology* 31 (9): 1195–1212.

Rohlf, F James. 1999. "Shape Statistics: Procrustes Superimpositions and Tangent Spaces." *Journal of Classification* 16 (2): 197–223.

———. 2010. "TpsDig, Version 2.12. Stony Brook, NY: Department of Ecology and Evolution, State University of New York at Stony Brook."

Rohlf, F James, and Dennis Slice. 1990. “Extensions of the Procrustes Method for the Optimal Superimposition of Landmarks.” *Systematic Zoology* 39 (1): 40. https://doi.org/10.2307/2992207.

Romano, Marco. 2017. “Long Bone Scaling of Caseid Synapsids: A Combined Morphometric and Cladistic Approach.” *Lethaia*.

Romer, Alfred Sherwood. 1922. “The Locomotor Apparatus of Some Primitive and Mammal-like Reptiles.” *Bulletin of the American Museum of Natural History* 46 (10): 517–606.

Romer, Alfred Sherwood, and L. W. Price. 1940. *28 : Review of the Pelycosauria*. *Geological Society of America Special Papers*. Vol. 28. Geological Society of America Special Papers. Geological Society of America. https://doi.org/10.1130/SPE28.

Rougier, Guillermo W. 1993. “Vincelestes Neuquenianus Bonaparte (Mammalia, Theria), Un Primitivo Mamífero Del Cretácico Inferior de La Cuenca Neuquina.” Universidad Nacional de Buenos Aires Buenos Aires.

Rubidge, Bruce S, and Juri Van den Heever. 1997. “Morphology and Systematic Position of the Dinocephalian Styracocephalus Platyrhynchus.” *Lethaia* 30 (2): 157–68.

Ruta, Marcello, Kenneth D Angielczyk, Jörg Fröbisch, and Michael J Benton. 2013. “Decoupling of Morphological Disparity and Taxic Diversity during the Adaptive Radiation of Anomodont Therapsids.” *Proceedings. Biological Sciences / The Royal Society* 280 (1768): 20131071. https://doi.org/10.1098/rspb.2013.1071.

Ruta, Marcello, Jennifer Botha-Brink, Stephen A Mitchell, and Michael J Benton. 2013. “The Radiation of Cynodonts and the Ground Plan of Mammalian Morphological Diversity.” *Proceedings. Biological Sciences / The Royal Society* 280 (1769): 20131865. https://doi.org/10.1098/rspb.2013.1865.

Sansalone, Gabriele, Paolo Colangelo, Anna Loy, Pasquale Raia, Stephen Wroe, and Paolo Piras. 2019. “Impact of Transition to a Subterranean Lifestyle on Morphological Disparity and Integration in Talpid Moles (Mammalia, Talpidae).” *BMC Evolutionary Biology* 19 (1): 1–15. https://doi.org/10.1186/s12862-019-1506-0.

Sereno, Paul. 2006. “Shoulder Girdle and Forelimb in a Cretaceous Multituberculate: Form, Functional Evolution, and a Proposal for Basal Mammalian Taxonomy.” *Amniote Paleobiology: Perspectives on the Evolution of Mammals, Birds, and Reptiles. University of Chicago Press, Chicago*, 315–70.

Sidor, Christian A, and James A Hopson. 1998. “Ghost Lineages and" Mammalness": Assessing the Temporal Pattern of Character Acquisition in the Synapsida.” *Paleobiology*, 254–73.

Slater, Graham J. 2013. “Phylogenetic Evidence for a Shift in the Mode of Mammalian Body Size Evolution at the Cretaceous-Palaeogene Boundary.” Edited by Luke Harman. *Methods in Ecology and Evolution* 4 (8): 734–44. https://doi.org/10.1111/2041-210X.12084.

Slater, Graham J, and Luke J Harmon. 2013. “Unifying Fossils and Phylogenies for Comparative Analyses of Diversification and Trait Evolution.” Edited by Robert Freckleton. *Methods in Ecology and Evolution* 4 (8): 699–702. https://doi.org/10.1111/2041-210X.12091.

Spindler, Frederik, D Scott, and Robert R Reisz. 2015. “New Information on the Cranial and Postcranial Anatomy of the Early Synapsid Ianthodon Schultzei (Sphenacomorpha:

Sphenacodontia), and Its Evolutionary Significance." *Fossil Record* 18 (1): 17–30. https://doi.org/10.5194/fr-18-17-2015.

Spindler, Frederik, Ralf Werneburg, Joerg W Schneider, Ludwig Luthardt, Volker Annacker, and Ronny Rößler. 2018. *First Arboreal "pelycosaurs" (Synapsida: Varanopidae) from the Early Permian Chemnitz Fossil Lagerstätte, SE Germany, with a Review of Varanopid Phylogeny*. *PalZ*. Vol. 92. Springer Berlin Heidelberg. https://doi.org/10.1007/s12542-018-0405-9.

Stöver, Ben C, and Kai F Müller. 2010. "TreeGraph 2: Combining and Visualizing Evidence from Different Phylogenetic Analyses." *BMC Bioinformatics* 11 (1): 7.

Sues, Hans-Dieter. 1986. "Locomotion and Body Form in Early Therapsids (Dinocephalia, Gorgonopsia, and Therocephalia)." *The Ecology and Biology of Mammal-like Reptiles. Smithsonian Institution Press, Washington, DC*, 61–70.

Sues, Hans-Dieter, and Robert R Reisz. 1998. "Origins and Early Evolution of Herbivory in Tetrapods." *Trends in Ecology & Evolution* 13 (4): 141–45.

Sulej, Tomasz, and Grzegorz Niedźwiedzki. 2019. "An Elephant-Sized Late Triassic Synapsid with Erect Limbs." *Science* 363 (6422): 78–80.

Sumida, Stuart S. 1989. "The Appendicular Skeleton of the Early Permian Genus Labidosaurus (Reptilia, Captorhinomorpha, Captorhinidae) and the Hind Limb Musculature of Captorhinid Reptiles." *Journal of Vertebrate Paleontology* 9 (3): 295–313.

"The Paleobiological Database." n.d. Accessed January 1, 2018. www.paleobiodb.org.

Upham, Nathan S, Jacob A Esselstyn, and Walter Jetz. 2019. "Inferring the Mammal Tree: Species-Level Sets of Phylogenies for Questions in Ecology, Evolution, and Conservation." *PLoS Biology* 17 (12): e3000494.

Vizcaíno, S F, and N Milne. 2002. "Structure and Function in Armadillo Limbs (Mammalia: Xenarthra: Dasypodidae)." *Journal of Zoology* 257 (1): 117–27. https://doi.org/10.1017/S0952836902000717.

Wainwright, Peter C. 1991. "Ecomorphology: Experimental Functional Anatomy for Ecological Problems1." *American Zoologist* 31 (4): 680–93. https://doi.org/10.1093/icb/31.4.680.

Watson, D M. 1917. "The Evolution of the Tetrapod Shoulder Girdle and Fore-Limb." *Journal of Anatomy* 52 (Pt 1): 1–63.

Wickham, Hadley. 2016. *Ggplot2: Elegant Graphics for Data Analysis*. springer.

Wills, Matthew A, Derek E G Briggs, and Richard A Fortey. 1994. "Disparity as an Evolutionary Index: A Comparison of Cambrian and Recent Arthropods." *Paleobiology* 20 (2): 93–130.

Wilson, Gregory P. 2013. "Mammals across the K/Pg Boundary in Northeastern Montana, U.S.A.: Dental Morphology and Body-Size Patterns Reveal Extinction Selectivity and Immigrant-Fueled Ecospace Filling." *Paleobiology* 39 (3): 429–69. https://doi.org/10.1666/12041.

Zelditch, Miriam Leah, Donald L Swiderski, and H David Sheets. 2012. *Geometric Morphometrics for Biologists: A Primer*. Academic Press.

APPENDIX A - Museum abbreviations associated with specimen numbers throughout

AMNH - American Museum of Natural History, New York, USA

BMNH – Beijing Museum of Natural History, Beijing, China

BP – Evolutionary Studies Institute, University of the Witwatersrand, Johannesburg, South Africa

CNHM - Cleveland Museum of Natural History, Cleveland, OH, USA

CMZ - University Museum of Zoology, Cambridge, UK

FMNH - Field Museum of Natural History, Chicago, IL, USA

GPIT - Paläontologische Sammlung, Eberhard Karls Universität Tübingen, Tübingen, Germany

IVPP - Institute of Paleoanthropology and Paleontology, Beijing, China

KUVP - University of Kansas Natural History Museum, Lawrence, KA, USA

MCP - Museu de Ciências e Tecnologia, Pontifícia Universidade Católica do Rio Grande do Sul, Porto Allegre, Brazil

MCN - Museu de Ciências Naturais, Fundação Zoobotânica do Rio Grande do Sul, Porto Allegre, Brazil

MCZ - Museum of Comparative Zoology, Cambridge, MA, USA

MNG - Museum der Natur, Gotha, Germany

MNHN - Muséum national d'Histoire naturelle, Paris, France

NHCC - National Heritage Conservation Commission, Lusaka, Zambia

NHMUK - Natural History Museum, London, UK

NMB - Natural History Museum of Basel, Basel, Germany

NMT - National Museum of Tanzania, Dar es Salaam, Tanzania

NMQR - National Museum, Bloemfontein, South Africa

OUMNH - University of Oklahoma Sam Noble Museum, Norman, OK, USA

PIN - Paleontological Institute of the Russian Academy of Sciences, Moscow, Russia

PVL - Instituto Miguel Lillo, Tucumán, Argentina

SAM – Iziko South African Museum, Cape Town, South Africa

TMM - Texas Memorial Museum, Austin, TX, USA

UCMP - University of California Museum of Paleontology, Berkeley, CA, USA

UFRGS – Universidade Federal do Rio Grande del Sul, Porto Allegre, Brazil

USNM - National Museum of Natural History (Smithsonian Institution), Washington D.C., USA

APPENDIX B - Specimen numbers, classifications, and section of humerus used for analyses of Chapter 2

specimen	clade	family	genus	part of humerus
AMNH_21017	Pelycosaur	Edaphosauridae	*Lupeosaurus*	Proximal & Distal
AMNH_21027	Pelycosaur	Edaphosauridae	*Lupeosaurus*	Distal
AMNH_21049	Pelycosaur	Sphenacodontidae	*Dimetrodon*	Proximal & Distal
AMNH_21116	Pelycosaur	Sphenacodontidae	*Dimetrodon*	Proximal & Distal
AMNH_21116	Pelycosaur	Sphenacodontidae	*Dimetrodon*	Distal
AMNH_21122	Pelycosaur	Sphenacodontidae	*Dimetrodon*	Proximal & Distal
AMNH_21125	Pelycosaur	Sphenacodontidae	*Dimetrodon*	Proximal
AMNH_21148	Pelycosaur	Sphenacodontidae	*Dimetrodon*	Distal
AMNH_21222	Pelycosaur	Sphenacodontidae	*Dimetrodon*	Proximal & Distal
AMNH_21226	Pelycosaur	Sphenacodontidae	*Dimetrodon*	Distal
AMNH_21227	Pelycosaur	Sphenacodontidae	*Dimetrodon*	Proximal & Distal
AMNH_21288	Pelycosaur	Sphenacodontidae	*Dimetrodon*	Proximal & Distal
AMNH_21293	Pelycosaur	Sphenacodontidae	*Dimetrodon*	Proximal & Distal
AMNH_21334	Pelycosaur	Sphenacodontidae	*Dimetrodon*	Distal
AMNH_21346	Pelycosaur	Sphenacodontidae	*Dimetrodon*	Distal
AMNH_21360	Pelycosaur	Sphenacodontidae	*Dimetrodon*	Proximal & Distal
AMNH_2458	Pelycosaur	Sphenacodontidae	*Dimetrodon*	Distal
AMNH_24591	Pelycosaur	Ophiacodontidae	*Ophiacodon*	Distal
AMNH_24739	Pelycosaur	Edaphosauridae	*Edaphosaurus*	Distal
AMNH_2731	Therapsida	Anomodontia	*Lystrosaurus*	Proximal
AMNH_2731	Therapsid	Anomodontia	*Lystrosaurus*	Distal
AMNH_33894	Therapsid	Cynodontia	*Tapinocephalus*	Proximal
AMNH_4006	Pelycosaur	Edaphosauridae	*Lupeosaurus*	Proximal

AMNH_4007	Pelycosaur	Sphenacodontidae	*Secodontosaurus*	Proximal
AMNH_4007_02	Pelycosaur	Ophiacodontidae	*Ophiacodon*	Distal
AMNH_4007_02	Pelycosaur	Sphenacodontidae	*Secodontosaurus*	Proximal
AMNH_4037A	Pelycosaur	Sphenacodontidae	*Dimetrodon*	Proximal & Distal
AMNH_4054	Pelycosaur	Sphenacodontidae	*Dimetrodon*	Proximal
AMNH_4066_01	Pelycosaur	Sphenacodontidae	*Dimetrodon*	Proximal & Distal
AMNH_4066_02	Pelycosaur	Sphenacodontidae	*Dimetrodon*	Distal
AMNH_4073	Pelycosaur	Sphenacodontidae	*Dimetrodon*	Proximal
AMNH_4075	Pelycosaur	Sphenacodontidae	*Dimetrodon*	Proximal
AMNH_4104_01	Pelycosaur	Sphenacodontidae	*Dimetrodon*	Distal
AMNH_4104_02	Pelycosaur	Sphenacodontidae	*Dimetrodon*	Distal
AMNH_4127	Pelycosaur	Sphenacodontidae	*Dimetrodon*	Distal
AMNH_4141	Pelycosaur	Ophiacodontidae	*Ophiacodon*	Proximal & Distal
AMNH_4145	Pelycosaur	Sphenacodontidae	*Dimetrodon*	Proximal
AMNH_4148	Pelycosaur	Sphenacodontidae	*Dimetrodon*	Proximal & Distal
AMNH_4152	Pelycosaur	Sphenacodontidae	*Dimetrodon*	Proximal & Distal
AMNH_4290	Pelycosaur	Sphenacodontidae	*Dimetrodon*	Proximal & Distal
AMNH_4625	Pelycosaur	Sphenacodontidae	*Dimetrodon*	Distal
AMNH_4627	Pelycosaur	Sphenacodontidae	*Dimetrodon*	Distal
AMNH_4777	Pelycosaur	Ophiacodontidae	*Ophiacodon*	Proximal & Distal
AMNH_5300	Therapsid	Anomodontia	*Oudenodon*	Distal
AMNH_5322	Therapsid	Dinocephalia	*Moschops*	Distal
AMNH_5511	Therapsida	Dinocephalia	*Moschops*	Proximal & Distal

AMNH_5553	Therapsid	Dinocephalia	*Moschops*	Distal
AMNH_5603	Therapsida	Anomodontia	*Endothiodon*	Proximal & Distal
AMNH_5609	Therapsid	Anomodontia	*Diictodon*	Distal
AMNH_7128	Pelycosaur	Edaphosauridae	*Edaphosaurus*	Proximal & Distal
BMNH_3740	Therapsida	Anomodontia	*Kannemeyeria*	Proximal
BMNH_3758	Therapsida	Anomodontia	*Kannemeyeria*	Proximal & Distal
BMNH_4044	Therapsida	Anomodontia	*Endothiodon*	Proximal & Distal
BMNH_4067	Therapsida	Anomodontia	*Oudenodon*	Proximal
BMNH_4067	Therapsida	Anomodontia	*Oudenodon*	Proximal
BMNH_9089	Therapsid	Anomodontia	*Zambiasaurus*	Distal
BMNH_9140	Therapsid	Anomodontia	*Zambiasaurus*	Distal
BP_749	Therapsid	Anomodontia	*Oudenodon*	Distal
BPI_3973	Therapsida	Therocephalia	*Ictidosuchops*	Proximal
BPI_4086	Therapsida	Anomodontia	*Cistecephalus*	Proximal
BSPG_AS-XXV-148_Stahleckeria_potens_hum_L_ventral.png'	Therapsida	Anomodontia	*Stahleckeria*	Distal
Cambridge_T837_Regisauridae_hum_L_all views.jpg'	Therapsida	Anomodontia	*Regisaurus*	Distal
CB_28_Odontocyclops_hum_L_dorsal.jpg'	Pelycosaur	Varanopidae	*Odontocyclops*	Distal
FMNH_PR_272	Pelycosaur	Caseidae	*Cotylorhynchus*	Distal
FMNH_UC_1136	Pelycosaur	Sphenacodontidae	*Dimetrodon*	Proximal & Distal
FMNH_UC_1147	Pelycosaur	Sphenacodontidae	*Dimetrodon*	Proximal & Distal

FMNH_UC_1156	Pelycosaur	Ophiacodontidae	*Ophiacodon*	Distal
FMNH_UC_1165_A	Pelycosaur	Sphenacodontidae	*Dimetrodon*	Proximal
FMNH_UC_1165_B	Pelycosaur	Sphenacodontidae	*Dimetrodon*	Distal
FMNH_UC_1165_D	Pelycosaur	Sphenacodontidae	*Dimetrodon*	Distal
FMNH_UC_1165_G	Pelycosaur	Sphenacodontidae	*Dimetrodon*	Proximal
FMNH_UC_1165_H	Pelycosaur	Sphenacodontidae	*Dimetrodon*	Distal
FMNH_UC_1165_I	Pelycosaur	Sphenacodontidae	*Dimetrodon*	Distal
FMNH_UC_1304	Pelycosaur	Sphenacodontidae	*Dimetrodon*	Proximal
FMNH_UC_143	Pelycosaur	Ophiacodontidae	*Ophiacodon*	Proximal & Distal
FMNH_UC_149	Pelycosaur	Sphenacodontidae	*Dimetrodon*	Proximal & Distal
FMNH_UC_1532	Therapsida	Anomodontia	*Aulacephalodon*	Proximal & Distal
FMNH_UC_157_A	Pelycosaur	Ophiacodontidae	*Ophiacodon*	Distal
FMNH_UC_157_B	Pelycosaur	Ophiacodontidae	*Ophiacodon*	Proximal & Distal
FMNH_UC_240	Pelycosaur	Ophiacodontidae	*Ophiacodon*	Proximal & Distal
FMNH_UC_241	Pelycosaur	Ophiacodontidae	*Ophiacodon*	Distal
FMNH_UC_247	Pelycosaur	Sphenacodontidae	*Dimetrodon*	Distal
FMNH_UC_248	Pelycosaur	Sphenacodontidae	*Dimetrodon*	Proximal & Distal
FMNH_UC_3	Pelycosaur	Ophiacodontidae	*Ophiacodon*	Distal
FMNH_UC_32	Pelycosaur	Sphenacodontidae	*Dimetrodon*	Distal
FMNH_UC_35	Pelycosaur	Sphenacodontidae	*Sphenacodon*	Proximal & Distal
FMNH_UC_414	Pelycosaur	Sphenacodontidae	*Dimetrodon*	Distal

FMNH_UC_421	Pelycosaur	Sphenacodontidae	*Dimetrodon*	Proximal & Distal
FMNH_UC_458	Pelycosaur	Ophiacodontidae	*Ophiacodon*	Proximal & Distal
FMNH_UC_459	Pelycosaur	Ophiacodontidae	*Ophiacodon*	Proximal
FMNH_UC_531	Pelycosaur	Sphenacodontidae	*Dimetrodon*	Proximal & Distal
FMNH_UC_538	Pelycosaur	Sphenacodontidae	*Dimetrodon*	Distal
FMNH_UC_545	Pelycosaur	Sphenacodontidae	*Dimetrodon*	Proximal & Distal
FMNH_UC_549	Pelycosaur	Sphenacodontidae	*Dimetrodon*	Proximal & Distal
FMNH_UC_552	Pelycosaur	Sphenacodontidae	*Dimetrodon*	Distal
FMNH_UC_644	Pelycosaur	Varanopidae	*Varanops*	Proximal & Distal
FMNH_UC_646	Pelycosaur	Ophiacodontidae	*Ophiacodon*	Proximal & Distal
FMNH_UC_6543	Pelycosaur	Ophiacodontidae	*Clepysdrops*	Distal
FMNH_UC_6553	Pelycosaur	Ophiacodontidae	*Clepsydrops*	Proximal
FMNH_UC_6575	Pelycosaur	Ophiacodontidae	*Clepsydrops*	Proximal & Distal
FMNH_UC_671	Pelycosaur	Ophiacodontidae	*Ophiacodon*	Proximal & Distal
FMNH_UC_682	Pelycosaur	Sphenacodontidae	*Dimetrodon*	Proximal & Distal
FMNH_UC_736	Pelycosaur	Sphenacodontidae	*Dimetrodon*	Distal
FMNH_UC_75	Pelycosaur	Sphenacodontidae	*Dimetrodon*	Distal
FMNH_UC_756_A	Pelycosaur	Sphenacodontidae	*Dimetrodon*	Proximal & Distal
FMNH_UC_79	Pelycosaur	Sphenacodontidae	*Dimetrodon*	Proximal & Distal
FMNH_UC_802_A	Pelycosaur	Sphenacodontidae	*Dimetrodon*	Distal
FMNH_UC_802_B	Pelycosaur	Sphenacodontidae	*Dimetrodon*	Proximal
FMNH_UC_802_C	Pelycosaur	Sphenacodontidae	*Dimetrodon*	Proximal & Distal
FMNH_UC_802_D	Pelycosaur	Sphenacodontidae	*Dimetrodon*	Proximal & Distal

FMNH_UC_802_E	Pelycosaur	Sphenacodontidae	*Dimetrodon*	Proximal
FMNH_UC_802_F	Pelycosaur	Sphenacodontidae	*Dimetrodon*	Proximal & Distal
FMNH_UC_816_A	Pelycosaur	Sphenacodontidae	*Dimetrodon*	Proximal & Distal
FMNH_UC_816_D	Pelycosaur	Sphenacodontidae	*Dimetrodon*	Distal
FMNH_UC_816_E	Pelycosaur	Sphenacodontidae	*Dimetrodon*	Distal
FMNH_UC_816_F	Pelycosaur	Sphenacodontidae	*Dimetrodon*	Proximal & Distal
FMNH_UC_816_G	Pelycosaur	Sphenacodontidae	*Dimetrodon*	Proximal
FMNH_UC_841	Pelycosaur	Sphenacodontidae	*Dimetrodon*	Proximal & Distal
FMNH_UC_843	Pelycosaur	Sphenacodontidae	*Dimetrodon*	Proximal & Distal
FMNH_UC_844	Pelycosaur	Sphenacodontidae	*Dimetrodon*	Proximal & Distal
FMNH_UC_860	Pelycosaur	Sphenacodontidae	*Dimetrodon*	Proximal & Distal
FMNH_UC_exhibits_Dimetrodon	Pelycosaur	Sphenacodontidae	*Secodontosaurus*	Distal
FMNH_UR_12	Therapsida	Dinocephalia	*Jonkeria*	Proximal & Distal
FMNH_UR_149	Pelycosaur	Caseidae	*Angelosaurus*	Proximal & Distal
FMNH_UR_156	Therapsid	Cynodontia	*Thrinaxodon*	Distal
FMNH_UR_2438	Therapsida	Dinocephalia	*Jonkeria*	Proximal & Distal
FMNH_UR_2444	Therapsida	Dinocephalia	*Jonkeria*	Proximal
FMNH_UR_2584	Therapsida	Anomodontia	*Aulacephalodon*	Proximal
FMNH_UR_259	Pelycosaur	Caseidae	*Angelosaurus*	Proximal

FMNH_UR_2590	Therapsida	Anomodontia	*Oudenodon*	Proximal & Distal
FMNH_UR_2597	Therapsida	Anomodontia	*Oudenodon*	Proximal & Distal
FMNH_UR_2598	Therapsid	Anomodontia	*Oudenodon*	Distal
FMNH_UR_2706	Therapsida	Anomodontia	*Lystrosaurus*	Proximal & Distal
FMNH_UR_288	Pelycosaur	Edaphosauridae	*Edaphosaurus*	Distal
FMNH_UR_315	Pelycosaur	Sphenacodontidae	*Dimetrodon*	Distal
FMNH_UR_316	Pelycosaur	Edaphosauridae	*Edaphosaurus*	Proximal
FMNH_UR_364	Therapsida	Anomodontia	*Lystrosaurus*	Proximal
FMNH_UR_364	Therapsida	Anomodontia	*Lystrosaurus*	Proximal
FMNH_UR_364_02	Therapsida	Anomodontia	*Lystrosaurus*	Proximal & Distal
FMNH_UR_365	Therapsida	Anomodontia	*Lystrosaurus*	Proximal & Distal
FMNH_UR_367	Therapsida	Dinocephalia	*Moschops*	Proximal
FMNH_UR_488	Pelycosaur	Caseidae	*Cotylorhynchus*	Proximal & Distal
FMNH_UR_488	Pelycosaur	Caseidae	*Cotylorhynchus*	Proximal & Distal
FMNH_UR_581	Pelycosaur	Caseidae	*Cotylorhynchus*	Distal
FMNH_UR_622	Pelycosaur	Caseidae	*Cotylorhynchus*	Proximal & Distal
FMNH_UR_632	Pelycosaur	Ophiacodontidae	*Ophiacodon*	Proximal & Distal
FMNH_UR_635	Pelycosaur	Ophiacodontidae	*Ophiacodon*	Distal
FMNH_UR_656	Pelycosaur	Ophiacodontidae	*Ophiacodon*	Proximal & Distal
FMNH_UR_695	Pelycosaur	Ophiacodontidae	*Varanasaurus*	Distal
FMNH_UR_695	Pelycosaur	Varanopidae	*Varanops*	Proximal & Distal
FMNH_UR_734	Pelycosaur	Edaphosauridae	*Edaphosaurus*	Proximal & Distal
FMNH_UR_736	Pelycosaur	Sphenacodontidae	*Dimetrodon*	Proximal
FMNH_UR_822	Pelycosaur	Caseidae	*Cotylorynchus*	Distal
FMNH_UR_879	Pelycosaur	Caseidae	*Cotylorhynchus*	Proximal & Distal

FMNH_UR_907	Pelycosaur	Caseidae	*Angelosaurus*	Proximal & Distal
FMNH_UR_970	Pelycosaur	Caseidae	*Angelosaurus*	Proximal & Distal
GPIT_30	Therapsida	Anomodontia	*Rhachiocephalus*	Proximal & Distal
GPIT_7113	Therapsida	Gorgonopsidae	*Sauroctonus*	Proximal
GPIT_K55	Therapsida	Anomodontia	*Kawingasaurus*	Proximal & Distal
GSP_15	Therapsida	Anomodontia	*Dolichuranus*	Proximal
GSP_15_Dolichuranus_hum_R_post.jpg'	Therapsida	Cynodontia	*Dolichuranus*	Distal
IVP2415	Therapsida	Anomodontia	*Shansiodon*	Proximal & Distal
IVPP_RV_35012	Therapsida	Anomodontia	*Lystrosaurus*	Proximal & Distal
IVPP_unnumbered_Dicynodontia	Therapsida	Anomodontia	*Lystrosaurus*	Proximal
IVPP_V4458	Therapsida	Anomodontia	*Xiukannemeyeria*	Proximal
IVPP_V4458_03	Therapsid	Anomodontia	*Xiyukannemeryia*	Distal
IVPP_V4458_05	Therapsid	Anomodontia	*Xiyukannemeryia*	Distal
IVPP_V4458_06	Therapsid	Anomodontia	*Zambiasaurus*	Distal
IVPP_V4695	Therapsida	Anomodontia	*Kunpania*	Proximal
IVPP_V4792	Therapsida	Therocephalia	*Ordosiodon*	Proximal & Distal
IVPP_V972	Therapsida	Anomodontia	*Sinokannemeyeria*	Proximal & Distal
IVPP_V979_Parakannemeyeria_youngi_hum_R_dorsal.jpg	Therapsida	Therocephalia	*Parakannemeyeria*	Distal
KUVP_4854	Pelycosaur	Sphenacodontidae	*Dimetrodon*	Distal
KUVP_68481	Pelycosaur	Sphenacodontidae	*Dimetrodon*	Proximal & Distal

KUVP_69035	Pelycosaur	Edaphosauridae	*Ianthosaurus*	Proximal & Distal
KUVP_707	Pelycosaur	Sphenacodontidae	*Dimetrodon*	Proximal & Distal
KUVP_739	Pelycosaur	Sphenacodontidae	*Dimetrodon*	Proximal & Distal
KUVP_9746	Pelycosaur	Sphenacodontidae	*Dimetrodon*	Proximal & Distal
MCZ_1121	Pelycosaur	Ophiacodontidae	*Ophiacodon*	Proximal & Distal
MCZ_1283	Pelycosaur	Sphenacodontidae	*Dimetrodon*	Proximal & Distal
MCZ_1283	Pelycosaur	Sphenacodontidae	*Dimetrodon*	Proximal
MCZ_1325	Pelycosaur	Sphenacodontidae	*Dimetrodon*	Proximal & Distal
MCZ_1338	Pelycosaur	Sphenacodontidae	*Dimetrodon*	Proximal & Distal
MCZ_1340	Pelycosaur	Sphenacodontidae	*Dimetrodon*	Distal
MCZ_1361	Pelycosaur	Sphenacodontidae	*Dimetrodon*	Proximal & Distal
MCZ_1365	Pelycosaur	Sphenacodontidae	*Dimetrodon*	Proximal & Distal
MCZ_1366	Pelycosaur	Ophiacodontidae	*Ophiacodon*	Distal
MCZ_1368	Pelycosaur	Edaphosauridae	*Lupeosaurus*	Proximal & Distal
MCZ_1368	Pelycosaur	Sphenacodontidae	*Dimetrodon*	Proximal
MCZ_1395	Pelycosaur	Sphenacodontidae	*Dimetrodon*	Distal
MCZ_1426	Pelycosaur	Ophiacodontidae	*Ophiacodon*	Proximal & Distal
MCZ_1435	Pelycosaur	Ophiacodontidae	*Ophiacodon*	Proximal
MCZ_1486	Pelycosaur	Ophiacodontidae	*Ophiacodon*	Proximal & Distal
MCZ_1537	Pelycosaur	Sphenacodontidae	*Dimetrodon*	Proximal & Distal
MCZ_1542	Pelycosaur	Sphenacodontidae	*Dimetrodon*	Distal
MCZ_1572	Pelycosaur	Sphenacodontidae	*Dimetrodon*	Proximal
MCZ_1650	Pelycosaur	Eothyrididae	*Baldwinonus*	Proximal
MCZ_1670	Therapsida	Anomodontia	*Dinodontosaurus*	Proximal & Distal
MCZ_1755	Pelycosaur	Edaphosauridae	*Edaphosaurus*	Proximal
MCZ_1915	Pelycosaur	Ophiacodontidae	*Ophiacodon*	Proximal
MCZ_1915	Pelycosaur	Ophiacodontidae	*Ophiacodon*	Distal
MCZ_1917	Pelycosaur	Sphenacodontidae	*Dimetrodon*	Proximal & Distal

MCZ_1917_B	Pelycosaur	Sphenacodontidae	*Dimetrodon*	Proximal & Distal
MCZ_1926	Pelycosaur	Varanopidae	*Varanops*	Proximal & Distal
MCZ_1930	Pelycosaur	Sphenacodontidae	*Dimetrodon*	Distal
MCZ_1972	Pelycosaur	Sphenacodontidae	*Dimetrodon*	Proximal
MCZ_2819	Pelycosaur	Ophiacodontidae	*Ophiacodon*	Proximal & Distal
MCZ_2832	Pelycosaur	Sphenacodontidae	*Dimetrodon*	Distal
MCZ_2832_B	Pelycosaur	Sphenacodontidae	*Dimetrodon*	Proximal & Distal
MCZ_2845	Pelycosaur	Sphenacodontidae	*Dimetrodon*	Proximal
MCZ_2847	Pelycosaur	Sphenacodontidae	*Dimetrodon*	Proximal
MCZ_2855	Pelycosaur	Edaphosauridae	*Edaphosaurus*	Proximal
MCZ_2875	Pelycosaur	Sphenacodontidae	*Dimetrodon*	Proximal
MCZ_2875	Pelycosaur	Sphenacodontidae	*Dimetrodon*	Distal
MCZ_2926	Pelycosaur	Ophiacodontidae	*Ophiacodon*	Distal
MCZ_2931	Pelycosaur	Sphenacodontidae	*Dimetrodon*	Distal
MCZ_2944	Pelycosaur	Sphenacodontidae	*Secodontosaurus*	Proximal & Distal
MCZ_3119	Therapsid	Anomodontia	*Kannemeyeria*	Distal
MCZ_3150	Pelycosaur	Varanopidae	*Ruthiromia*	Proximal
MCZ_3222	Pelycosaur	Sphenacodontidae	*Dimetrodon*	Proximal & Distal
MCZ_3246	Pelycosaur	Sphenacodontidae	*Dimetrodon*	Proximal & Distal
MCZ_3306	Pelycosaur	Edaphosauridae	*Edaphosaurus*	Proximal
MCZ_3417	Pelycosaur	Edaphosauridae	*Edaphosaurus*	Proximal & Distal
MCZ_3418	Pelycosaur	Edaphosauridae	*Edaphosaurus*	Proximal & Distal
MCZ_3419	Pelycosaur	Edaphosauridae	*Edaphosaurus*	Distal
MCZ_3426	Pelycosaur	Sphenacodontidae	*Dimetrodon*	Proximal
MCZ_3454	Therapsida	Anomodontia	*Dinodontosaurus*	Proximal & Distal
MCZ_3454	Therapsida	Anomodontia	*Dinodontosaurus*	Proximal & Distal

MCZ_3455	Therapsid	Anomodontia	*Endothiodon*	Distal
MCZ_3615	Therapsida	Cynodontia	*Chiniquodon*	Proximal & Distal
MCZ_3615_B	Therapsida	Cynodontia	*Chiniquodon*	Proximal & Distal
MCZ_3691	Therapsida	Cynodontia	*Massetognathus*	Proximal & Distal
MCZ_3812	Therapsida	Cynodontia	*Massetognathus*	Proximal & Distal
MCZ_4002	Therapsida	Cynodontia	*Chiniquodon*	Proximal & Distal
MCZ_4079	Pelycosaur	Ophiacodontidae	*Archeothyris*	Proximal
MCZ_4099	Therapsida	Cynodontia	*Chiniquodon*	Proximal
MCZ_4318	Pelycosaur	Edaphosauridae	*Edaphosaurus*	Proximal & Distal
MCZ_4318_B	Pelycosaur	Edaphosauridae	*Edaphosaurus*	Proximal
MCZ_4319	Pelycosaur	Edaphosauridae	*Edaphosaurus*	Proximal & Distal
MCZ_4470	Therapsid	Cynodontia	*Exaeretodon*	Distal
MCZ_4503	Therapsid	Cynodontia	*Exaeretodon*	Distal
MCZ_4503	Therapsida	Cynodontia	*Exaeretodon*	Proximal
MCZ_4816	Pelycosaur	Ophiacodontidae	*Ophiacodon*	Proximal & Distal
MCZ_4906	Pelycosaur	Sphenacodontidae	*Sphenacodon*	Proximal & Distal
MCZ_5018	Pelycosaur	Sphenacodontidae	*Secodontosaurus*	Proximal & Distal
MCZ_5018_04	Pelycosaur	Sphenacodontidae	*Secodontosaurus*	Distal
MCZ_5018_06-07	Pelycosaur	Sphenacodontidae	*Secodontosaurus*	Distal
MCZ_5018_C	Pelycosaur	Sphenacodontidae	*Secodontosaurus*	Proximal & Distal
MCZ_5018_D	Pelycosaur	Sphenacodontidae	*Secodontosaurus*	Proximal & Distal
MCZ_5018_G	Pelycosaur	Sphenacodontidae	*Secodontosaurus*	Proximal & Distal
MCZ_5019_B	Pelycosaur	Sphenacodontidae	*Secodontosaurus*	Proximal & Distal

MCZ_5020	Pelycosaur	Sphenacodontidae	*Secodontosaurus*	Proximal & Distal
MCZ_5020_B	Pelycosaur	Sphenacodontidae	*Secodontosaurus*	Proximal & Distal
MCZ_5020_C	Pelycosaur	Sphenacodontidae	*Secodontosaurus*	Proximal
MCZ_5021	Pelycosaur	Edaphosauridae	*Edaphosaurus*	Proximal & Distal
MCZ_5026	Pelycosaur	Ophiacodontidae	*Ophiacodon*	Proximal
MCZ_5037	Pelycosaur	Sphenacodontidae	*Dimetrodon*	Proximal & Distal
MCZ_5038	Pelycosaur	Sphenacodontidae	*Dimetrodon*	Distal
MCZ_5039	Pelycosaur	Sphenacodontidae	*Dimetrodon*	Proximal & Distal
MCZ_5041	Pelycosaur	Sphenacodontidae	*Dimetrodon*	Proximal & Distal
MCZ_5043	Pelycosaur	Sphenacodontidae	*Dimetrodon*	Proximal & Distal
MCZ_5043_B	Pelycosaur	Sphenacodontidae	*Dimetrodon*	Proximal & Distal
MCZ_5044	Pelycosaur	Sphenacodontidae	*Dimetrodon*	Distal
MCZ_5047	Pelycosaur	Ophiacodontidae	*Ophiacodon*	Proximal & Distal
MCZ_5049	Pelycosaur	Ophiacodontidae	*Ophiacodon*	Proximal
MCZ_5083	Pelycosaur	Sphenacodontidae	*Dimetrodon*	Proximal
MCZ_5423	Pelycosaur	Sphenacodontidae	*Dimetrodon*	Proximal & Distal
MCZ_5517	Pelycosaur	Ophiacodontidae	*Ophiacodon*	Proximal
MCZ_5661	Pelycosaur	Ophiacodontidae	*Ophiacodon*	Proximal & Distal
MCZ_5682	Pelycosaur	Sphenacodontidae	*Dimetrodon*	Proximal
MCZ_5721	Pelycosaur	Sphenacodontidae	*Dimetrodon*	Proximal & Distal
MCZ_5779	Pelycosaur	Sphenacodontidae	*Dimetrodon*	Proximal & Distal
MCZ_5836	Pelycosaur	Sphenacodontidae	*Dimetrodon*	Proximal
MCZ_5839	Pelycosaur	Sphenacodontidae	*Dimetrodon*	Distal
MCZ_5892	Pelycosaur	Ophiacodontidae	*Ophiacodon*	Distal
MCZ_5935	Pelycosaur	Ophiacodontidae	*Ophiacodon*	Proximal & Distal
MCZ_6097	Pelycosaur	Sphenacodontidae	*Dimetrodon*	Proximal & Distal

MCZ_6218	Pelycosaur	Sphenacodontidae	*Dimetrodon*	Distal
MCZ_6220	Pelycosaur	Sphenacodontidae	*Dimetrodon*	Proximal
MCZ_6289	Pelycosaur	Ophiacodontidae	*Ophiacodon*	Proximal
MCZ_6289	Pelycosaur	Ophiacodontidae	*Ophiacodon*	Proximal
MCZ_6289_B	Pelycosaur	Ophiacodontidae	*Ophiacodon*	Proximal
MCZ_6905	Pelycosaur	Sphenacodontidae	*Dimetrodon*	Proximal
MCZ_6960	Pelycosaur	Ophiacodontidae	*Ophiacodon*	Proximal
MCZ_7004	Pelycosaur	Sphenacodontidae	*Dimetrodon*	Distal
MCZ_7012	Pelycosaur	Sphenacodontidae	*Secodontosaurus*	Proximal & Distal
MCZ_7013	Pelycosaur	Sphenacodontidae	*Secodontosaurus*	Proximal & Distal
MCZ_7014	Pelycosaur	Sphenacodontidae	*Secodontosaurus*	Proximal & Distal
MCZ_7035	Pelycosaur	Sphenacodontidae	*Dimetrodon*	Distal
MCZ_7074	Pelycosaur	Sphenacodontidae	*Dimetrodon*	Proximal & Distal
MCZ_8710	Pelycosaur	Sphenacodontidae	*Dimetrodon*	Proximal & Distal
MCZ_8771	Pelycosaur	Sphenacodontidae	*Dimetrodon*	Proximal
MLP_65-VI-18-1_Pascaulgnathus_polanskii_hum_L_ventral.png'	Therapsida	Anomodontia	*Pascualgnathus*	Distal
MNG_10596	Pelycosaur	Varanopidae	*Tambicarnifex*	Proximal & Distal
NCSM_20698_Boreogomphodon_hum_LR_ventral.png'	Therapsida	Cynodontia	*Boreogomphodon*	Distal
NHCCLB_211	Therapsida	Anomodontia	*Dicynodontoides*	Proximal
NHCCLB_222	Therapsida	Anomodontia	*Dicynodontoides*	Proximal
NHCCLB_277	Therapsida	Cynodontia	*Abdalodon*	Proximal

NHCCLB_335	Therapsida	Gorgonopsidae	*Aelurosaurus*	Proximal
NHCCLB_350	Therapsida	Gorgonopsidae	*Aelurognathus*	Proximal & Distal
NHCCLB_366	Therapsida	Anomodontia	*Cistecephalidae. nov.gen1*	Proximal & Distal
NHCCLB_820	Therapsida	Anomodontia	*Cistecephalidae. nov.gen2*	Proximal
NHMUK_R9140	Therapsid	Anomodontia	*Aleodon*	Distal
NHMW_1876-VII-B-123_Pentasaurus_goggani_hum_L_ventral-dorsal.png'	Therapsida	Cynodontia	*Pentasaurus*	Distal
NMB_C2693	Therapsida	Cynodontia	*Diademodon*	Proximal & Distal
NMBQR_3351	Therapsida	Therocephalia	*Moschorhinus*	Proximal
NMMNH_P_43121	Pelycosaur	Ophiacodontidae	*Ophiacodon*	Proximal
NMMNH_P_43122	Pelycosaur	Ophiacodontidae	*Ophiacodon*	Distal
NMNH_12691	Therapsid	Anomodontia	*Lystrosaurus*	Distal
NMNH_22814	Therapsid	Anomodontia	*Oudenodon*	Distal
NMNH_23345	Therapsida	Anomodontia	*Eosimops*	Proximal & Distal
NMNH_24635	Therapsid	Anomodontia	*Diictodon*	Distal
NMNH_24645	Therapsida	Anomodontia	*Daptocephalus*	Proximal
NMNH_24645_Daptocephalus_leon_hum_L_dorsal.jpg'	Therapsida	Gorgonopsia	*Daptocephalus*	Distal
NMNH_25176	Therapsid	Anomodontia	*Dicynodontoides*	Distal
NMNH_407847	Pelycosaur	Sphenacodontidae	*Dimetrodon*	Distal
NMNH_407947	Pelycosaur	Sphenacodontidae	*Dimetrodon*	Proximal

NMNH_407947_01	Pelycosaur	Sphenacodontidae	*Dimetrodon*	Proximal & Distal
NMNH_407947_02	Pelycosaur	Sphenacodontidae	*Dimetrodon*	Distal
NMNH_407947_03	Pelycosaur	Sphenacodontidae	*Dimetrodon*	Proximal & Distal
NMNH_407947_04	Pelycosaur	Sphenacodontidae	*Dimetrodon*	Proximal & Distal
NMNH_407947_05-06	Pelycosaur	Sphenacodontidae	*Dimetrodon*	Proximal & Distal
NMNH_407947_05-06	Pelycosaur	Sphenacodontidae	*Dimetrodon*	Distal
NMNH_407947_07-08	Pelycosaur	Sphenacodontidae	*Dimetrodon*	Proximal & Distal
NMNH_407947_07-08	Pelycosaur	Sphenacodontidae	*Dimetrodon*	Distal
NMNH_407947_09-10	Pelycosaur	Sphenacodontidae	*Dimetrodon*	Proximal & Distal
NMNH_407947_09-10	Pelycosaur	Sphenacodontidae	*Dimetrodon*	Distal
NMNH_407947_11-12	Pelycosaur	Sphenacodontidae	*Dimetrodon*	Proximal & Distal
NMNH_407947_11-12	Pelycosaur	Sphenacodontidae	*Dimetrodon*	Distal
NMNH_407947_13	Pelycosaur	Sphenacodontidae	*Dimetrodon*	Proximal & Distal
NMNH_407947_14	Pelycosaur	Sphenacodontidae	*Dimetrodon*	Proximal & Distal
NMNH_407947_15	Pelycosaur	Sphenacodontidae	*Dimetrodon*	Distal
NMNH_407947_16	Pelycosaur	Sphenacodontidae	*Dimetrodon*	Distal

NMNH_410251_Cynario_hum_R_dorsal.jpg'	Therapsida	Anomodontia	*Cynariognathus*	Distal
NMNH_6723	Pelycosaur	Sphenacodontidae	*Dimetrodon*	Proximal & Distal
NMNH_PAL_407688	Pelycosaur	Sphenacodontidae	*Dimetrodon*	Proximal
NMNH_PAL_407867	Pelycosaur	Sphenacodontidae	*Dimetrodon*	Proximal
NMQR_1478	Therapsida	Anomodontia	*Aulacephalodon*	Proximal
NMQR_3153	Therapsida	Anomodontia	*Eodicynodon*	Proximal
NMTRB_0001	Therapsid	Anomodontia	*Dicynodontoides*	Distal
NMTRB_156	Therapsida	Anomodontia	*Cryptodontia.nov.gen*	Proximal
NMTRB_156_hum_R_dorsal.jpg'	Therapsida	Anomodontia	*Cryptodontia_nov.gen*	Distal
NMTRB_2	Therapsid	Anomodontia	*Dicynodontoides*	Distal
NMTRB_207	Therapsida	Anomodontia	*Oudenodon*	Proximal & Distal
NMTRB_236	Therapsid	Anomodontia	*Dicynodontoides*	Distal
NMTRB_27	Therapsida	Anomodontia	*Oudenodon*	Proximal & Distal
NMTRB_29	Therapsida	Anomodontia	*Dicynodontoides*	Proximal & Distal
NMTRB_30	Therapsida	Anomodontia	*Oudenodon*	Proximal
NMTRB_329	Therapsid	Anomodontia	*Dicynodon*	Distal
NMTRB_375	Therapsida	Cynodontia	*Aleodon*	Proximal & Distal
NMTRB_376	Therapsida	Cynodontia	*Aleodon*	Proximal & Distal
NMTRB_399	Therapsida	Cynodontia	*Chiniquodon*	Proximal & Distal
NMTRB_402	Therapsida	Anomodontia	*Dicynodontoides*	Proximal & Distal

NMTRB_408	Therapsid	Cynodontia	*Aleodon*	Distal
NMTRB_409	Therapsid	Cynodontia	*Chiniquodon*	Distal
NMTRB_414	Therapsida	Cynodontia	*Chiniquodon*	Proximal
NMTRB_44	Therapsid	Anomodontia	*Dicynodontoides*	Distal
NMTRB_459	Therapsida	Cynodontia	*Cynognathus*	Proximal
NMTRB_459_Cynognathus_hum_R_ant.jpg'	Therapsida	Therocephalia	*Cynognathus*	Distal
NMTRB_544	Therapsid	Anomodontia	*Diictodon*	Distal
NMTRB_615	Therapsida	Anomodontia	*Dolichuranus*	Proximal
NMTRB_672	Therapsida	Anomodontia	*Dolichuranus*	Proximal
OMMNH_EdaphosaurusMount	Pelycosaur	Edaphosauridae	*Edaphosaurus*	Proximal & Distal
OMNH_04188	Pelycosaur	Caseidae	*Cotylorhynchus*	Proximal & Distal
OMNH_1727	Pelycosaur	Sphenacodontidae	*Dimetrodon*	Proximal
OMNH_52368_Mycterosaurus_longiceps_ILL_hum_L_ventral.jpg'	Therapsida	Cynodontia	*Mycterosaurus*	Distal
OMNH_55203	Pelycosaur	Ophiacodontidae	*Ophiacodon*	Proximal & Distal
OMNH_55204	Pelycosaur	Ophiacodontidae	*Ophiacodon*	Distal
OMNH_55207	Pelycosaur	Ophiacodontidae	*Ophiacodon*	Proximal
OMNH_590	Pelycosaur	Sphenacodontidae	*Dimetrodon*	Proximal & Distal
OMNH_631	Pelycosaur	Caseidae	*Cotylorhynchus*	Proximal & Distal
OMNH_CotylorhynchusMount	Pelycosaur	Caseidae	*Cotylorhynchus*	Proximal & Distal
OMNH_WallMount	Pelycosaur	Caseidae	*Cotylorynchus*	Distal
OUM_14	Therapsida	Anomodontia	*Dicynodon*	Proximal

OUMNH_TSK_121	Therapsida	Cynodontia	*Luangwa*	Proximal & Distal
PIN_1536_Vivaxosaurus_hum_R_ant.jpg'	Pelycosaur	Caseidae	*Vivaxosaurus*	Distal
PIN_2212-116	Therapsida	Anomodontia	*Suminia*	Proximal & Distal
PIN_2212-116	Therapsida	Anomodontia	*Suminia*	Proximal & Distal
PIN_3447	Therapsid	Anomodontia	*Lystrosaurus*	Distal
PVL_2467	Therapsida	Cynodontia	*Exaeretodon*	Proximal & Distal
PVL_3807	Therapsid	Anomodontia	*Ischigualastia*	Distal
PVL_3807	Therapsida	Anomodontia	*Ischiagualastia*	Proximal
PVL_3894	Therapsida	Cynodontia	*Andescynodon*	Proximal & Distal
R567_GSO	Therapsida	Cynodontia	*Titanogomphodon*	Proximal
SAM_PK_10009	Therapsida	Anomodontia	*Emydops*	Proximal & Distal
SAM_PK_10016	Therapsida	Anomodontia	*Aulacephalodon*	Proximal
SAM_PK_10017	Therapsida	Cynodontia	*Thrinaxodon*	Proximal & Distal
SAM_PK_10102	Therapsid	Anomodontia	*Tropidostoma*	Distal
SAM_PK_10161	Therapsida	Anomodontia	*Pristerodon*	Proximal
SAM_PK_10220	Therapsida	Anomodontia	*Oudenodon*	Proximal
SAM_PK_10221	Therapsida	Anomodontia	*Lystrosaurus*	Proximal
SAM_PK_10465	Therapsida	Cynodontia	*Galesaurus*	Proximal & Distal
SAM_PK_10466	Therapsid	Anomodontia	*Lystrosaurus*	Distal
SAM_PK_10467	Therapsida	Anomodontia	*Lystrosaurus*	Proximal
SAM_PK_10636	Therapsid	Anomodontia	*Dinodontosaurus*	Distal
SAM_PK_10645	Therapsid	Anomodontia	*Xiyukannemeryia*	Distal
SAM_PK_10645	Therapsida	Anomodontia	*Tropidostoma*	Proximal
SAM_PK_10906	Therapsida	Anomodontia	*Dolichuranus*	Proximal

SAM_PK_11114	Therapsida	Anomodontia	*Oudenodon*	Proximal & Distal
SAM_PK_11258	Therapsida	Anomodontia	*Diictodon*	Proximal
SAM_PK_11271	Therapsida	Anomodontia	*Endothiodon*	Proximal
SAM_PK_11885	Therapsida	Anomodontia	*Robertia*	Proximal & Distal
SAM_PK_2771	Therapsid	Anomodontia	*Kannemeyeria*	Distal
SAM_PK_4807	Therapsid	Anomodontia	*Oudenodon*	Distal
SAM_PK_4807	Therapsida	Anomodontia	*Oudenodon*	Proximal
SAM_PK_6222	Therapsid	Anomodontia	*Oudenodon*	Distal
SAM_PK_7607	Therapsida	Anomodontia	*Brachyprosopus*	Proximal
SAM_PK_7852	Therapsida	Anomodontia	*Rhachiocephalus*	Proximal & Distal
SAM_PK_8017	Therapsida	Anomodontia	*Lystrosaurus*	Proximal
SAM_PK_8305_Heleosaurus_hum-ulna-rad_dorsal.JPG'	Therapsida	Therocephalia	*Heleosaurus*	Distal
SAM_PK_8561	Therapsida	Anomodontia	*Diictodon*	Proximal
SAM_PK_8659_Ictidosuchops_hum_L_dorsal.JPG'	Pelycosaur	Edaphosauridae	*Ictidosuchops*	Distal
SAM_PK_9958	Therapsida	Anomodontia	*Lystrosaurus*	Proximal & Distal
SAM_PK_unnumbered	Therapsida	Anomodontia	*Oudenodon*	Proximal
SAMPK_1395	Therapsida	Cynodontia	*Thrinaxodon*	Proximal
SAMPK_7809_Glanoschus_macrops_hum_L_dorsal.jpg'	Therapsida	Cynodontia	*Glanosuchus*	Distal
T_Th_BP_3973	Therapsida	Therocephalia	*Regisaurus*	Proximal
T_Th_UMZC_T837	Therapsida	Therocephalia	*Regisaurus*	Proximal

TMM_30966_339	Pelycosaur	Sphenacodontidae	*Dimetrodon*	Distal
TMM_30966_50	Pelycosaur	Sphenacodontidae	*Dimetrodon*	Proximal & Distal
TMM_30966-214	Pelycosaur	Sphenacodontidae	*Dimetrodon*	Proximal & Distal
TMM_30966-377	Pelycosaur	Sphenacodontidae	*Dimetrodon*	Proximal & Distal
TMM_30966-438	Pelycosaur	Sphenacodontidae	*Dimetrodon*	Proximal & Distal
TMM_30966-470	Pelycosaur	Sphenacodontidae	*Dimetrodon*	Proximal
TMM_30966-499	Pelycosaur	Sphenacodontidae	*Dimetrodon*	Proximal & Distal
TMM_31222-16	Pelycosaur	Ophiacodontidae	*Ophiacodon*	Distal
TMM_31222-16	Pelycosaur	Sphenacodontidae	*Dimetrodon*	Proximal & Distal
TMM_31225-24	Pelycosaur	Edaphosauridae	*Edaphosaurus*	Proximal
TMM_31225-70	Pelycosaur	Edaphosauridae	*Edaphosaurus*	Proximal
TMM_42552-1_Cynosaurus_longiceps_hum_R_dorsal.jpg	Therapsida	Cynodontia	*Cynosaurus*	Distal
TMM_43628	Pelycosaur	Varanopidae	*Varanops*	Proximal & Distal
UC_512	Pelycosaur	Ophiacodontidae	*Varanosaurus*	Proximal
UC_652	Pelycosaur	Caseidae	*Trichasaurus*	Proximal & Distal
UC_656	Pelycosaur	Caseidae	*Casea*	Proximal & Distal
UCMP_143278	Pelycosaur	Varanopidae	*Watongia*	Proximal & Distal
UCMP_25361	Therapsid	Anomodontia	*Rhaciocephalus*	Distal
UCMP_2834	Pelycosaur	Sphenacodontidae	*Sphenacodon*	Proximal
UCMP_3431	Pelycosaur	Sphenacodontidae	*Sphenacodon*	Distal
UCMP_40076	Pelycosaur	Sphenacodontidae	*Sphenacodon*	Proximal & Distal
UCMP_42400	Therapsid	Anomodontia	*Aulacephalodon*	Distal

UCMP_42400	Therapsida	Anomodontia	*Pristerodon*	Proximal
UCMP_42444	Therapsida	Dinocephalia	*Tapinocephalus*	Proximal
UCMP_42749	Therapsida	Cynodontia	*Cynognathus*	Proximal
UCMP_42870	Therapsida	Anomodontia	*Lystrosaurus*	Proximal & Distal
UCMP_5219	Pelycosaur	Sphenacodontidae	*Sphenacodon*	Proximal
UCMP_65341	Therapsida	Anomodontia	*Lystrosaurus*	Proximal
UCMP_76019	Therapsida	Anomodontia	*Lystrosaurus*	Proximal
UCMP_78395	Therapsida	Therocephalia	*Tetracynodon*	Proximal & Distal
UCMP_83534	Pelycosaur	Sphenacodontidae	*Sphenacodon*	Proximal & Distal
UCMP_83535	Pelycosaur	Sphenacodontidae	*Sphenacodon*	Proximal & Distal
UCMP_83536	Pelycosaur	Sphenacodontidae	*Sphenacodon*	Proximal
UCMP_83537	Pelycosaur	Sphenacodontidae	*Sphenacodon*	Proximal
UCMP_83543	Pelycosaur	Sphenacodontidae	*Sphenacodon*	Distal
UCMP_83544	Pelycosaur	Sphenacodontidae	*Sphenacodon*	Distal
UCMP_83544	Pelycosaur	Sphenacodontidae	*Sphenacodon*	Distal
UCMP_83546	Pelycosaur	Sphenacodontidae	*Sphenacodon*	Proximal & Distal
UCMP_83546	Pelycosaur	Sphenacodontidae	*Sphenacodon*	Distal
UCMP_83546	Pelycosaur	Sphenacodontidae	*Sphenacodon*	Proximal & Distal
UCMP_83546	Pelycosaur	Sphenacodontidae	*Sphenacodon*	Distal
UCMP_A269-25361	Therapsid	Anomodontia	*Placerias*	Distal
UCMP_V36113-38373	Therapsid	Anomodontia	*Lystrosaurus*	Distal
UCMP_V5219	Pelycosaur	Sphenacodontidae	*Dimetrodon*	Distal
UCMP_V99058	Pelycosaur	Sphenacodontidae	*Dimetrodon*	Proximal
UMZC_883	Therapsida	Gorgonopsidae	*Gorgonopsia*	Proximal
UMZC_987	Therapsid	Anomodontia	*Dicynodon*	Distal
UR_485	Therapsida	Dinocephalia	*Tappenosaurus*	Proximal & Distal
USNM_15562	Pelycosaur	Ophiacodontidae	*Dimetrodon*	Distal

USNM_24645	Therapsida	Anomodontia	*Daptocephalus*	Proximal
USNM_452057	Therapsida	Anomodontia	*Diictodon*	Proximal
USNM_617068	Therapsida	Anomodontia	*Diictodon*	Proximal
USNM_6722	Pelycosaur	Sphenacodontidae	*Dimetrodon*	Distal
USNM_8659	Pelycosaur	Sphenacodontidae	*Dimetrodon*	Distal
USNM_8659	Pelycosaur	Sphenacodontidae	*Dimetrodon*	Proximal
USNM_PAL_407685	Pelycosaur	Ophiacodontidae	*Ophiacodon*	Proximal
USNM_PAL_407688	Pelycosaur	Sphenacodontidae	*Dimetrodon*	Distal
Z04_Compsodon_hum_R_dorsal.jpg'	Therapsida	Anomodontia	*Compsodon*	Distal
Z257	Therapsid	Anomodontia	*Suminia*	Distal

APPENDIX C -Extant mammalian sample and ecological categorizations used in Chapter 3

#	Genus	Group	Family	Common name	Ecological categorization
1	*Bison*	Mammalia	Artiodactyla	Bison	cursorial
2	*Canis*	Mammalia	Carnivora	Wolf	cursorial
3	*Chaetophractus*	Mammalia	Cingulata	Hairy armadillo	semifossorial
4	*Chlamyphoridae*	Mammalia	Cingulata	Giant armadillo	semifossorial
5	*Condylura*	Mammalia	Eulipotyphla	Star-nosed mole	fossorial
6	*Conepatus*	Mammalia	Carnivora	Hog-nosed skunk	terrestrial
7	*Dasypus*	Mammalia	Cingulata	9-banded armadillo	semifossorial
8	*Geomys*	Mammalia	Rodentia	Pocket gopher	fossorial
9	*Hylobates*	Mammalia	Primates	Gibbon	arboreal
10	*Hippopotamus*	Mammalia	Artiodactyla	Hippopotamus	graviportal
11	*Martes*	Mammalia	Carnivora	Marten	arboreal
12	*Mephitis*	Mammalia	Carnivora	Striped skunk	terrestrial
13	*Neofelis*	Mammalia	Carnivora	Clouded leopard	arboreal
14	*Orycteropus*	Mammalia	Tubulidentata	Aardvark	semifossorial
15	*Potos*	Mammalia	Carnivora	Kinkajou	arboreal
16	*Procyon*	Mammalia	Carnivora	Raccoon	terrestrial
17	*Rhinocerotidae*	Mammalia	Perissodactyla	Rhinoceros	graviportal
18	*Scalopus*	Mammalia	Eulipotyphla	Eastern mole	fossorial
19	*Spilogale*	Mammalia	Carnivora	Spotted skunk	terrestrial
20	*Sus*	Mammalia	Artiodactyla	Pig	terrestrial
21	*Tachyglossus*	Mammalia	Monotremata	Echidna	terrestrial
22	*Tapirus*	Mammalia	Perissodactyla	Tapir	terrestrial

23	*Taxidea*	Mammalia	Carnivora	Badger	semifossorial
24	*Vulpes*	Mammalia	Carnivora	Fox	cursorial
25	*Heliophobius*	Mammalia	Rodentia	Silvery mole-rat	fossorial
26	*Cryptomys*	Mammalia	Rodentia	African mole-rat	fossorial

APPENDIX D - Proximal humerus generic sample and occurrence dates used in Chapter 3 and Chapter 4

genus	FAD	LAD	genus	FAD	LAD
Abdalodon	259.9	254.14	*Luangwa*	247.2	237
Aelurognathus	259.1	254.14	*Lumkuia*	247.2	242.2
Aelurosaurus	265.1	254.17	*Lupeosaurus*	290.1	272.95
Akidolestes	129.4	125	*Lystrosaurus*	254.14	247.2
Aleodon	247.2	227	*Maiopatagium*	163.5	157.3
Andescynodon	247.2	242	*Martes*	22.4	0
Angelosaurus	272.95	268.8	*Massetognathus*	242	227
Anteosaurus	265.1	259.9	*Megazostrodon*	201.3	190.8
Archaeothyris	311.45	306.95	*Mephitis*	8.78	0
Arctognathus	259.9	254.17	*Mirotenthes*	259.9	254.17
Aulacephalodon	259.1	251.9	*Morganucodon*	208.5	164.7
Baldwinonus	303.4	290.1	*Moschops*	265.1	259.1
Cryptodontia_nov.gen	259.9	252.17	*Moschorhinus*	259.9	251.2
Bauriidae	252	252	*Nemegtbaatar*	83.5	72.1
Biarmosuchus	279.5	265	*Neofelis*	54.96	0
Bienotherium	201.3	190.8	*Nochnitsa*	265	252.3
Bison	26	0	*Olivierosuchus*	252.1	247.2
Brachyprosopus	265.1	259.9	*Ophiacodon*	303.7	272.95
Brasilodon	228	208.5	*Ordosiodon*	247.2	242
Cacops	279.3	272.3	*Orycteropus*	100.79	0
Canis	12.6	0	*Oudenodon*	259.1	251.9
Captorhinus	290.1	254.17	*Pachygenelus*	201.3	196.5
Casea	283.5	272.95	*Potos*	22.7	0
Castorocauda	164.7	161.2	*Pristerodon*	265.1	254.17

Chaetophractus	37.73	0	*Pristerognathus*	265.1	259.9
Chiniquodon	247.2	227	*Procolophon*	265	201.3
Chlamyphoridae	69	0	*Procynosuchus*	259.9	247.2
Choerosaurus	272.3	254.17	*Procyon*	22.7	0
Cistecephalidae_nov.gen_1	259.1	254.14	*Prozostrodon*	232	221.5
Cistecephalus	259.9	254.17	*Ptomalestes*	265.1	259.9
Clepsydrops	314.6	268	*Regisaurus*	251.9	251.2
Condylura	40.4	0	*Repenomamus*	125.45	122.46
Conepatus	11.36	0	*Rhachiocephalus*	259.1	251.9
Cotylorhynchus	283.5	268.8	*Rhinocerotidae*	40.8	0
Cricodon	247.2	242	*Riograndia*	228	208.5
Cryptomys	20.89	0	*Robertia*	265.1	259.1
Cyclura	33.9	0	*Ruthiromia*	303.4	298.9
Cynognathus	251.2	237	*Santacruzodon*	237	228
Cynosaurus	259.9	254.17	*Sauroctonus*	259.9	254.17
Daptocephalus	259.9	252.17	*Scaloposaurus*	259.9	247.2
Dasypus	37.73	0	*Scalopus*	40.4	0
Diademodon	251.2	237	*Scylacosauridae*	268.8	259.9
Dicynodon	259.1	251.9	*Scymnosaurus*	265.1	259.9
Dicynodontoides	265.1	251.9	*Secodontosaurus*	290.1	272.95
Diictodon	265.1	251.9	*Shansiodon*	247.2	242
Dimetrodon	290.1	272.95	*Sinokannemeyeria*	247.2	242
Dinodontosaurus	242	237	*Sphenacodon*	303.7	283.5
Dipsosaurus	33.9	0	*Spilogale*	8.78	0
Dolichuranus	251.2	242	*Struthiocephalus*	265.1	259.9
Edaphosaurus	303.7	272.95	*Suminia*	265.1	254.14
Emydops	265.1	251.9	*Sus*	63.5	0
Endothiodon	265.1	254.14	*Tachyglossus*	179.19	0

Eodicynodon	268.8	265.1	*Tambacarnifex*	290.1	279.3
Eosimops	265.1	259.1	*Tapinocaninus*	279.3	272.3
Eozostrodon	208.5	201.3	*Tapinocephalus*	265.1	259.1
Exaeretodon	237	227	*Tapirus*	40.8	0
Fruitafossor	157.3	152.1	*Tappenosaurus*	279.3	268.8
Galesaurus	251.9	251.2	*Taxidea*	22.4	0
Geomys	77.19	0	*Tetracynodon*	251.9	251.2
Glanosuchus	268.8	259.9	*Theriognathus*	259.9	242
Gobiconodon	139.8	100.5	*Therocephalia*	268	252
Gorgonops	265.1	254.17	*Thrinaxodon*	251.9	251.2
Gorgonopsia	272.3	254	*Tiarajudens*	272.3	259.9
Haldanodon	157.3	152.1	*Titanogomphodon*	247.2	237
Heleosaurus	265.1	259.1	*Titanosuchus*	265.1	259.9
Heliophobius	20.89	0	*Trichasaurus*	283.5	272.95
Hippopotamus	56.32	0	*Trirachodon*	252.17	242
Hipposaurus	265.1	259.9	*Tritylodon*	228	190.8
Hylobates	90.89	0	*Tropidostoma*	259.1	254.14
Ianthasaurus	307	303.7	*Trucidocynodon*	237	228
Ictidosuchops	259.1	251.2	*Varanops*	290.1	272.95
Iguana	33.9	0	*Varanosaurus*	283.5	272.95
Irajatherium	228	208.5	*Varanus*	23	0
Ischigualastia	237	227	*Vincelestes*	129.4	122.46
Jonkeria	265.1	259.1	*Vulpes*	12.6	0
Kannemeyeria	251.2	242	*Watongia*	272.95	268.8
Kawingasaurus	254.14	251.9	*Xianshou*	163.5	157.3
Kayentatherium	199.3	182.7	*Xiukannemeyeria*	251.2	242
Kembawacela	259.1	254.14	*Yanoconodon*	129.4	122.46
Kunpania	259.9	252.17	*ZAM_Cynodontia*	245	235

Labidosaurus	279.3	272.3	*Zinnosaurus*	249	249
Liaoconodon	125	113	*Zorillodontops*	247.2	247.2
Lisowicia	211	211			

APPENDIX E - Distal Humerus generic sample and occurrence dates used in Chapter 3 and Chapter 4

genus	FAD	LAD	genus	FAD	LAD
Aelurognathus	259.1	254.14	*Lystrosaurus*	254.14	247.2
Akidolestes	129.4	125	*Maiopatagium*	163.5	157.3
Aleodon	247.2	227	*Martes*	22.4	0
Andescynodon	247.2	242	*Massetognathus*	242	227
Angelosaurus	272.95	268.8	*Megazostrodon*	201.3	190.8
Anteosaurus	265.1	259.9	*Mephitis*	8.78	0
Arctognathus	259.9	254.17	*Mirotenthes*	259.9	254.17
Aulacephalodon	259.1	251.9	*Moschops*	265.1	259.1
Batagonda	259.9	252.17	*Moschorhinus*	259.9	251.2
Biarmosuchus	279.5	265	*Mycterosaurus*	283.5	272.95
Bienotherium	201.3	190.8	*Neofelis*	54.96	0
Bison	26	0	*Odontocyclops*	259.1	254.14
Boreogomphodon	237	227	*Olivierosuchus*	252.1	247.2
Brachyprosopus	265.1	259.9	*Ophiacodon*	303.7	272.95
Brasilodon	228	208.5	*Ordosiodon*	247.2	242
Cacops	279.3	272.3	*Orycteropus*	100.79	0
Canis	12.6	0	*Oudenodon*	259.1	251.9
Captorhinus	290.1	254.17	*Pachygenelus*	201.3	196.5
Casea	283.5	272.95	*Parakannemeyeria*	247.2	242
Castorocauda	164.7	161.2	*Pascualgnathus*	237	227
Chaetophractus	37.73	0	*Pentasaurus*	228	201.3
Chiniquodon	247.2	227	*Placerias*	237	208.5
Chlamyphoridae	69	0	*Platycraniellus*	252.17	247.2
Cistecephalidae_nov.gen_1	259.1	254.14	*Potos*	22.7	0
Cistecephalus	259.9	254.17	*Pristerodon*	265.1	254.17

Clepsydrops	314.6	268	*Pristerognathus*	265.1	259.9
Compsodon	259.1	251.9	*Procolophon*	265	201.3
Condylura	40.4	0	*Procynosuchus*	259.9	247.2
Conepatus	11.36	0	*Procyon*	22.7	0
Cotylorhynchus	283.5	268.8	*Prozostrodon*	232	221.5
Cricodon	247.2	242	*Ptomalestes*	265.1	259.9
Cryptomys	20.89	0	*Regisaurus*	251.9	251.2
Cyclura	33.9	0	*Rhachiocephalus*	259.1	251.9
Cynariognathus	265.1	259.9	*Rhinocerotidae*	40.8	0
Cynognathus	251.2	237	*Riograndia*	228	208.5
Cyonosaurus	259.9	252.1	*Robertia*	265.1	259.1
Daptocephalus	259.9	252.17	*Rugosodon*	163.5	157.3
Dasypus	37.73	0	*Ruthenosaurus*	295.5	254.17
Delphinognathus	265.1	259.9	*Santacruzodon*	237	228
Diademodon	251.2	237	*Scaloposaurus*	259.9	247.2
Dicynodon	259.1	251.9	*Scalopus*	40.4	0
Dicynodontoides	265.1	251.9	*Scylacops*	259.9	254.17
Diictodon	265.1	251.9	*Scylacosauridae*	268.8	259.9
Dimetrodon	290.1	272.95	*Scymnosaurus*	265.1	259.9
Dinodontosaurus	242	237	*Secodontosaurus*	290.1	272.95
Dipsosaurus	33.9	0	*Shansiodon*	247.2	242
Dolichuranus	251.2	242	*Shenshou*	163.5	157.3
Dryolestes	157.3	145	*Sinokannemeyeria*	247.2	242
Edaphosaurus	303.7	272.95	*Sphenacodon*	303.7	283.5
Emydops	265.1	251.9	*Spilogale*	8.78	0
Endothiodon	265.1	254.14	*Stahleckeria*	242	237
Eosimops	265.1	259.1	*Suminia*	265.1	254.14
Exaeretodon	237	227	*Sus*	63.5	0

Fruitafossor	157.3	152.1	*Tachyglossus*	179.19	0
Galesaurus	251.9	251.2	*Tambacarnifex*	290.1	279.3
Geomys	77.19	0	*Tapinocaninus*	279.3	272.3
Glanosuchus	268.8	259.9	*Tapinocephalid*	279.3	254.17
Gorgonops	265.1	254.17	*Tapinocephalus*	265.1	259.1
Gorgonopsia	272.3	254	*Tapirus*	40.8	0
Haldanodon	157.3	152.1	*Taxidea*	22.4	0
Heleosaurus	265.1	259.1	*Tetracynodon*	251.9	251.2
Heliophobius	20.89	0	*Theriognathus*	259.9	242
Henkelotherium	157.3	152.1	*Therioherpeton*	237	208.5
Hippopotamus	56.32	0	*Therioides*	265.1	259.9
Hipposaurus	265.1	259.9	*Therocephalia*	268	252
Hylobates	90.89	0	*Thrinaxodon*	251.9	251.2
Ianthasaurus	307	303.7	*Titanosuchus*	265.1	259.9
Ictidodraco	257.4	254.4	*Trichasaurus*	283.5	272.95
Ictidosuchops	259.1	251.2	*Trirachodon*	252.17	242
Iguana	33.9	0	*Tritylodon*	228	190.8
Ictidosuchops	259.1	251.2	*Tropidostoma*	259.1	254.14
Iguana	33.9	0	*Trucidocynodon*	237	228
Irajatherium	228	208.5	*Varanasaurus*	283.5	272.95
Ischigualastia	237	227	*Varanops*	290.1	272.95
Jonkeria	265.1	259.1	*Varanus*	23	0
Kannemeyeria	251.2	242	*Vincelestes*	129.4	122.46
Kawingasaurus	254.14	251.9	*Vivaxosaurus*	259.1	251.9
Kayentatherium	199.3	182.7	*Volaticotherium*	164.7	161.1
Kembawacela	259.1	254.14	*Vulpes*	12.6	0
Labidosaurus	279.3	272.3	*Watongia*	272.95	268.8
Liaoconodon	125	113	*Xiukannemeyeria*	251.2	242

Lisowicia	211	211	*Yanoconodon*	129.4	122.46
Luangwa	247.2	237	*Zambiasaurus*	247.2	237
Lupeosaurus	290.1	272.95	*Zhangheotherium*	129.4	122.46
Lycosuchus	265.1	259.9	*Zinnosaurus*	249	249

APPENDIX F - Ulna generic sample and occurrence dates used in Chapter 3 and Chapter 4

genus	FAD	LAD	genus	FAD	LAD
Aelurognathus	259.1	254.14	*Mephitis*	8.78	0
Agilodocodon	164.7	161.2	*Mirotenthes*	259.9	254.17
Akidolestes	129.4	125	*Moschops*	265.1	259.1
Andescynodon	247.2	242	*Neofelis*	54.96	0
Angonisaurus	247.2	242	*Oligokyphus*	208.5	182.7
Arctognathus	259.9	254.17	*Olivierosuchus*	252.1	247.2
Aulacephalodon	259.1	251.9	*Ophiacodon*	303.7	272.95
Batagonda	259.9	252.17	*Orycteropus*	100.79	0
Biarmosuchus	279.5	265	*Oudenodon*	259.1	251.9
Bienotheroides	163.5	157.3	*Pachygenelus*	201.3	196.5
Bison	26	0	*Parakannemeyeria*	247.2	242
Boreogomphodon	237	227	*Pascualgnathus*	237	227
Brasilodon	228	208.5	*Pentasaurus*	228	201.3
Canis	12.6	0	*Potos*	22.7	0
Captorhinus	290.1	254.17	*Procolophon*	265	201.3
Casea	283.5	272.95	*Procynosuchus*	259.9	247.2
Catopsbaatar	164.7	161.2	*Procyon*	22.7	0
Ch_Cynodontia	165.5	157.3	*Protuberum*	242	237
Chaetophractus	37.73	0	*Ptomalestes*	265.1	259.9
Chiniquodon	247.2	227	*Regisaurus*	251.9	251.2
Chlamyphoridae	69	0	*Repenomamus*	125.45	122.46
Cistecephalidae_nov.gen_1	259.1	254.14	*Rhinocerotidae*	40.8	0
Cistecephalus	259.9	254.17	*Robertia*	265.1	259.1
Clepsydrops	314.6	268	*Rugosodon*	163.5	157.3
Compsodon	259.1	251.9	*Sauroctonus*	259.9	254.17

Condylura	40.4	0	*Scalenodon*	247.2	237
Conepatus	11.36	0	*Scaloposauridae*	259.9	247.2
Cotylorhynchus	283.5	268.8	*Scaloposaurus*	259.9	247.2
Cyclura	33.9	0	*Scalopus*	40.4	0
Cynariognathus	265.1	259.9	*Scymnosaurus*	265.1	259.9
Cynognathus	251.2	237	*Secodontosaurus*	290.1	272.95
Cyonosaurus	259.9	252.1	*Seymouria*	290.1	272.3
Dasypus	37.73	0	*Shaanbeikannemeyeria*	247.2	242
Diademodon	251.2	237	*Shansiodon*	247.2	242
Dicynodon	259.1	251.9	*Shenshou*	163.5	157.3
Diictodon	265.1	251.9	*Sinobaatar*	129.4	100.5
Dimetrodon	290.1	272.95	*Sinokannemeyeria*	247.2	242
Dinodontosaurus	242	237	*Sphenacodon*	303.7	283.5
Dolichuranus	251.2	242	*Spilogale*	8.78	0
Edaphosaurus	303.7	272.95	*Stahleckeria*	242	237
Emydops	265.1	251.9	*Stereophallodon*	296.4	268
Endothiodon	265.1	254.14	*Struthiocephalus*	265.1	259.9
Eomaia	129.4	125	*Sus*	63.5	0
Eosimops	265.1	259.1	*Tachyglossus*	179.19	0
Eriphostoma	265.1	254.1	*Tapinocaninus*	279.3	272.3
Erythrotherium	210	210	*Tapinocephalus*	265.1	259.1
Exaeretodon	237	227	*Tapirus*	40.8	0
Fruitafossor	157.3	152.1	*Tappenosaurus*	279.3	268.8
Galesaurus	251.9	251.2	*Taxidea*	22.4	0
Geomys	77.19	0	*Tetracynodon*	251.9	251.2
Gobiconodon	139.8	100.5	*Theriognathus*	259.9	242
Gorgonops	265.1	254.17	*Therocephalia*	268	252
Gorgonopsia	272.3	254	*Thrinaxodon*	251.9	251.2

Haldanodon	157.3	152.1	*Tiarajudens*	272.3	259.9
Heleosaurus	265.1	259.1	*Titanogomphodon*	247.2	237
Henkelotherium	157.3	152.1	*Titanosuchidae*	265.1	259.9
Hippopotamus	56.32	0	*Titanosuchus*	265.1	259.9
Hipposaurus	265.1	259.9	*TNZ_Cynodontia*	245	235
Hylobates	90.89	0	*TNZ_Gorgonopsia*	260	254
Ictidodraco	257.4	254.4	*Traversodontidae_nov.gen_1*	245	235
Ictidosuchops	259.1	251.2	*Trichasaurus*	283.5	272.95
Iguana	33.9	0	*Triconodon*	145	140.2
Ischigualastia	237	227	*Tritylodon*	228	190.8
Jonkeria	265.1	259.1	*Tropidostoma*	259.1	254.14
Kannemeyeria	251.2	242	*Trucidocynodon*	237	228
Kawingasaurus	254.14	251.9	*Ukhaatherium*	83.5	72.1
Kayentatherium	199.3	182.7	*Varanops*	290.1	272.95
Kembawacela	259.1	254.14	*Varanus*	23	0
Labidosaurus	279.3	272.3	*Vincelestes*	129.4	122.46
Liaoconodon	125	113	*Volaticotherium*	164.7	161.1
Lisowicia	211	211	*Vulpes*	12.6	0
Lycosuchus	265.1	259.9	*Xianshou*	163.5	157.3
Lystrosaurus	254.14	247.2	*Xiukannemeyeria*	251.2	242
Maiopatagium	163.5	157.3	*Yanoconodon*	129.4	122.46
Martes	22.4	0	*ZAM_Gorgonopsia*	260	254
Massetognathus	242	227	*Zinnosaurus*	249	249
Menadon	237	228			